MARIA THEREZA DE MORAES GOMES ROSA

APLICAÇÃO E POTENCIAL DAS TECNOLOGIAS DE MICRONIZAÇÃO E EMULSIFICAÇÃO PARA O PROCESSAMENTO DE PRODUTOS ALIMENTÍCIOS E FARMACÊUTICOS.

Campinas
2015

UNIVERSIDADE ESTADUAL DE CAMPINAS
FACULDADE DE ENGENHARIA DE ALIMENTOS

MARIA THEREZA DE MORAES GOMES ROSA

APLICAÇÃO E POTENCIAL DAS TECNOLOGIAS DE MICRONIZAÇÃO E EMULSIFICAÇÃO PARA O PROCESSAMENTO DE PRODUTOS ALIMENTÍCIOS E FARMACÊUTICOS.

APPLICATIONS AND POTENTIAL OF MICRONIZATION AND EMULSIFICATION TECHNOLOGIES IN FOOD AND PHARMACEUTICAL PROCESSING.

Tese apresentada ao Programa de Pós-Graduação em Engenharia de Alimentos da Faculdade de Engenharia de Alimentos da Universidade Estadual de Campinas como parte dos requisitos exigidos para a obtenção do título de Doutora em Engenharia de Alimentos.

Thesis presented to the Food Engineering Postgraduation Programme of the School of Food Engineering of the University of Campinas in partial fulfillment of the requirements for the degree of Ph.D. in Food Engineering.

Orientadora: Profª. Drª. Maria Angela de Almeida Meireles
Co-orientador: Dr. Diego Tresinari dos Santos

ESTE EXEMPLAR CORRESPONDE À VERSÃO FINAL DA TESE DEFENDIDA PELA ALUNA MARIA THEREZA DE MORAES GOMES ROSA E ORIENTADA PELA PROF^{A}. DR^{A}. MARIA ANGELA DE ALMEIDA MEIRELES.

_____
Assinatura do orientador

Campinas
2015

Ficha catalográfica
Universidade Estadual de Campinas
Biblioteca da Faculdade de Engenharia de Alimentos
Claudia Aparecida Romano - CRB 8/5816

Rosa, Maria Thereza de Moraes Gomes, 1986-
R71a Aplicação e potencial das tecnologias de micronização e emulsificação para o processamento de produtos alimentícios e farmacêuticos / Maria Thereza de Moraes Gomes Rosa. – Campinas, SP : [s.n.], 2015.

Orientador: Maria Angela de Almeida Meireles.
Coorientador: Diego Tresinari dos Santos.
Tese (doutorado) – Universidade Estadual de Campinas, Faculdade de Engenharia de Alimentos.

1. Micropartículas. 2. Fluido supercrítico. 3. Emulsões. 4. Tocotrienol. 5. Ultrassom. I. Meireles, Maria Angela de Almeida. II. Santos, Diego Tresinari dos. III. Universidade Estadual de Campinas. Faculdade de Engenharia de Alimentos. IV. Título.

Informações para Biblioteca Digital

Título em outro idioma: Applications and potential of micronization and emulsification technologies in food and pharmaceutical processing.
Palavras-chave em inglês:
Microparticles
Supercritical fluid
Emulsions
Tocotrienol
Ultrasound
Área de concentração: Engenharia de Alimentos
Titulação: Doutora em Engenharia de Alimentos
Banca examinadora:
Maria Angela de Almeida Meireles [Orientador]
Diego Alvarenga Botrel
Luiz Henrique Fasolin
Pedro Esteves Duarte Augusto
Rodrigo Nunes Cavalcanti
Data de defesa: 31-03-2015
Programa de Pós-Graduação: Engenharia de Alimentos

BANCA EXAMINADORA

_____

Profa. Dra. Maria Angela de Almeida Meireles
DEA/FEA/UNICAMP
Orientadora

_____

Prof. Dr. Diego Alvarenga Botrel
Universidade Federal de Lavras
Titular

_____

Dr. Luiz Henrique Fasolin
DEA/FEA/UNICAMP
Titular

_____

Prof. Dr. Pedro Esteves Duarte Augusto
ESALQ/USP
Titular

_____

Dr. Rodrigo Nunes Cavalcanti
DEA/FEA/UNICAMP
Titular

_____

Profa. Dra. Daniela Helena Pelegrine Guimarães
Escola de Engenharia de Lorena/USP
Suplente

_____

Prof. Dr. Fernando Antonio Cabral
DEA/FEA/UNICAMP
Suplente

_____

Dra. Isabel Cristina do Nascimento Debien
DEA/FEA/UNICAMP
Suplente

TESE DE DOUTORADO

Autora: Maria Thereza de Moraes Gomes Rosa
Título: Aplicação e potencial das tecnologias de micronização e emulsificação para o processamento de produtos alimentícios e farmacêuticos.
Orientadora: Profa. Dra. Maria Angela de Almeida Meireles
Co-orientador: Dr. Diego Tresinari dos Santos

RESUMO

O presente trabalho de doutorado está dividido em dois temas principais, um sobre o uso da tecnologia supercrítica para a formação de partículas e outro sobre o uso do ultrassom para a formulação de emulsões.

A revisão da literatura sobre o estado da arte do emprego do CO_2 supercrítico para formação de micro e nanopartículas e encapsulação mostrou as potencialidades do uso desta tecnologia. A unidade usada para os experimentos de micronização via tecnologia supercrítica foi desenvolvida pelo grupo de pesquisa e validada utilizando uma substância modelo, o sal de ibuprofeno sódico. Esse fármaco foi selecionado devido às informações sobre o sistema CO_2-Ibuprofeno encontradas na literatura. O efeito das condições operacionais (temperatura, pressão, vazão da solução, vazão do CO_2, tipo de injetor e concentração de ibuprofeno sódico na solução etanólica) no rendimento de precipitação, teor de solvente residual, morfologia das partículas e consumo energético por unidade de produto processado foi investigado utilizando o método *split-plot*. Sal de ibuprofeno sódico foi micronizado com sucesso via Antissolvente Supercrítico (SAS) utilizando a unidade construída. A vazão de CO_2 influenciou estatisticamente no rendimento de precipitação, enquanto que, não houve influência das condições operacionais no teor de solvente residual das partículas micronizadas. Com a apropriada seleção das condições operacionais, foi possível a obtenção de partículas de ibuprofeno sódico com morfologia de folha, sendo ideal para os processos de compressão do fármaco, com baixo teor de solvente residual e alto rendimento de precipitação.

Neste trabalho também foi explorado o uso do ultrassom para a formulação de emulsões, contendo extrato rico em δ-tocotrienol, com o intuito de aumentar o valor agregado deste extrato obtido das sementes de urucum por extração supercrítica com dióxido de carbono. As sementes de urucum já são valiosas pela característica de produzir

pigmentos, a bixina e a norbixina. Contudo, essas sementes também vêm adquirindo notoriedade por conter outras substâncias de importância para a saúde do homem, como tocoferóis, tocotrienóis e geranil geraniol. Devido à importância desses compostos bioativos, que apresentam propriedades antioxidade, hidratante e fotoprotetora, este estudo visou o desenvolvimento de métodos para formação de emulsões permitindo a proteção desses compostos instáveis às condições adversas, aumentando assim o valor agregado dos extratos obtidos das sementes de urucum. Extrato de raiz de ginseng brasileiro, rico em saponinas, foi utilizado como biossurfactante. Adicionalmente, emulsões foram obtidas utilizando um homogeneizador tipo dispersor de fase múltipla na mesma densidade energética que foi aplicada no ultrassom. A influência do processo de emulsificação, densidade energética, concentração do biosurfactante, tipo de óleo e de biosurfactante no tamanho de gota e estabilidade da emulsão foi investigada. Os resultados indicaram que o extrato rico em saponinas pode ser uma boa opção para formulação de emulsões para aplicação em produtos alimentícios. Miniemulsões, com tamanho de gota variando entre 0,35 e 0,83 μm, foram obtidas, sendo que os menores tamanhos de gota foram observados empregando o extrato de raiz de ginseng e o ultrassom. O processo de emulsificação influenciou estatisticamente a estabilidade das emulsões.

Palavras chave: Micropartículas, fluido supercrítico, emulsão, δ-tocotrienol, ultrassom.

DOCTORAL THESIS

Author: Maria Thereza de Moraes Gomes Rosa
Title: Applications and potential of micronization and emulsification technologies in food and pharmaceutical processing.
Supervisor: Dra. Maria Angela de Almeida Meireles
Cosupervisor: Dr. Diego Tresinari dos Santos

ABSTRACT

The presented doctoral work is divided into two main themes under which one is about the use of supercritical technology for particle formation and the another one about the use of ultrasound for emulsion formulation.

A literature review about the state of the art in using supercritical CO_2 for micro and nanoparticles formation and encapsulation showed the potential of this technology. A homemade experimental apparatuses constructed by our research group and used for micro and nanoparticles formation has been validated using a model substance, the ibuprofen sodium salt. This drug was selected due to the literature information of the CO_2-Ibuprofen system. The effect of operational conditions (temperature, pressure, CO_2 flow rate, solution flow rate, injector and concentration of ibuprofen sodium in the ethanol solution) on the precipitation yield, energy consumption per unit of manufactured product, residual solvent content and particle morphology have been investigated using split-plot designs. Ibuprofen sodium salt was successfully micronized by Antisolvent Supercritical (SAS) using the constructed unit. The CO_2 flow rate influenced the precipitation yield at statistically significant levels meanwhile none operating parameters did influence the residual solvent content in the micronized particles. Selecting appropriate process conditions, it has been shown to facilitate the production of homogeneous sheet-like microparticles of ibuprofen particles, the best for tableting purposes, with low residual solvent and high precipitation yield.

In this work, the use of ultrasound has been also explored for fabricating microemulsion of δ-tocotrienol-rich oil in order to add value to these extracts obtained from annatto seeds using supercritical extraction (SFE). The main pigments of annatto seeds are bixin and norbixin, wich are valuable natural colorants. However, these seeds have acquired notoriety by containing other important substances for human health, such as

tocopherols, tocotrienols and geranylgeraniol. Due to the bioactive compounds importance, which have moisturizers, sunscreens and antioxidant properties, this study aimed to develop methods for emulsion formulation enabling the protection of these unstable compounds to adverse conditions, thus increasing the value of extracts from annatto seeds. Saponin-rich extract from Brazilian ginseng roots was used as biosurfactant. Additionally, emulsion was generated through mechanical stirring by dispax Reactor at the same energy density than ultrasound. The influence of the emulsification process, energy density, oil type, biosurfactant type and biosurfactant concentration on the size and stability of the resulting droplets was investigated. The results indicated that saponin-rich extract might be an attractive biosurfactant choice for emulsion formulations for use in food and beverage products. Mini-emulsions were obtained in this work; their droplet sizes ranged from 0.35 to 0.83 μm, saponin-rich extract and ultrasound gave the smallest droplet size. The emulsification process significantly affected the emulsion stability values.

Keywords: Microparticles, supercritical fluid, emulsion, δ-tocotrienol, ultrasound.

SUMÁRIO

*Ao meu marido, meu companheiro e meu melhor amigo **Jean Cláudio**, por todo o amor, carinho e cuidado. Pela nossa história, nossas conquistas e nossas viagens. Por ser tão bom comigo, cuidar tão bem de mim, realizar todos os meus sonhos e me fazer mais feliz do que eu jamais imaginei ser um dia. E, acima de tudo, por me fazer querer ser uma pessoa melhor a cada dia que passa. Eu te amo!*

AGRADECIMENTOS

Primeiramente a Deus, meu maior mestre, que sempre me levanta em todas as vezes que a vida me faz cair. Obrigada por reconhecer o meu valor, meu Pai!

À minha querida orientadora M. Angela, por ser o meu maior exemplo de força, dedicação e determinação. Eu sinto um orgulho enorme de ter tido o privilégio e a honra de trabalharmos juntas. Agradeço por me ajudar a crescer profissionalmente quanto pessoalmente. Será sempre a minha inspiração durante a minha vida acadêmica!

Aos meus pais, Giovani e Cláudia, minha avó Thereza, meus irmãos Camila, Renan e João Victor e meu marido Jean, por me fazerem sonhar, sentir melhor, crescer, rir, acreditar, querer mudar, ir em frente e compartilhar. Como é gratificante ser FAMÍLIA!

À Universidade Estadual de Campinas (UNICAMP), pelo conceituado curso de doutorado em Engenharia de Alimentos e por oferecer toda a estrutura necessária para a realização deste trabalho.

Ao CNPq e à CAPES, pelas bolsas concedidas de doutorado e doutorado sanduíche, respectivamente.

À Profª Marleny Saldaña, por ter me recebido e me auxiliado tão bem durante o período de doutorado sanduíche na Universidade de Alberta, e aos que me foram companheiros e fizeram da minha estadia no Canadá maravilhosa e inesquecível.

Aos membros da banca pelas valiosas contribuições na redação final deste trabalho.

Aos velhos e novos amigos: Kaliana, Renato, Kelly, Luana, Mariana, Susana, Bebel, Renata, Liara, Moysés, Julio e Giovani, por todos os momentos compartilhados. Em especial ao meu grande e querido amigo Éric Keven, que aguentou muita lamúria, mas que sempre me mostrou o lado bom de todas as coisas. As amizades que levo comigo me fazem acreditar que tudo que vivi valeu a pena! Obrigada pessoal!

Aos demais colegas da UNICAMP pelo convívio durante este período do doutorado.

Ao técnico do LASEFI, Ariovaldo, pela amizade, paciência que sempre teve comigo e por todo auxílio durante os problemas enfrentados com as unidades.

Aos funcionários da FEA, em especial aos secretários, por serem sempre solícitos.

A todos que contribuíram direta ou indiretamente para a realização deste trabalho, meu muito obrigada!

LISTA DE FIGURAS

LISTA DE TABELAS

ABREVIATURAS E SIGLAS

ASES	Aerosol solvent extraction system
BGR	Brazilian ginseng roots
CA	Cholesterol acetate
CAN-BD	Carbon dioxide-assisted nebulisation with a bubble dryer
COM	Cost of manufacturing
CMC	Critical micellar concentration
CSE	Conventional solvent evaporation
DR	Dispax reactor
DSC	Differential scanning calorimetry
ED	Energy density
FID	Flame ionization detection
GAS	Gas antisolvent
GC	Gas chromatography
GF	Griseofulvin
HLB	Hydrophilic-Lipophilic Balance
IN	Indomethacin
KP	Ketoprofen
MA	Megestrol acetate
NAP	Nominal applied powers
NSAID	Nonsteroidal anti-inflamatory drug
OSA	N-octenyl succinic anhydride
O/W	Oil-in-water
PCA	Precipitation by compressed antisolvent
pDNA	Plasmid DNA
PEG	Polyethylene glycol
PGSS	Particles from gas-saturated solutions
PHWE	Pressurised hot water extraction
PLGA	Poly-lactic-co-glycolic acid
POE	Polyethylene oxide
PVA	Polyvinyl alcohol

PVP	Polyvinyl pyrrolidone
RESOLV	Rapid expansion of a supercritical solution into a liquid solvent
RESS	Rapid expansion of supercritical solutions
SAA	Supercritical-assisted atomisation
SAS	Supercritical antisolvent
SEA	Supercritical enhanced atomization
SEDS	Solution enhanced dispersion by supercritical fluids
SEM	Scanning electron microscopy
SFE	Supercritical fluid extraction
SFEE	Supercritical Fluid Extraction of Emulsions
US	Ultrasound
VLE	Vapour-liquid equilibrium
WEPO	Water extraction and particle formation on-line

CAPÍTULO 1 – ASPECTOS GERAIS

1 INTRODUÇÃO

Este trabalho apresenta um estudo dos processos de formação de micro e nanopartículas de fármacos e emulsificação dos compostos bioativos das sementes de urucum. Condições e métodos de formação das nanoemulsões, incluindo o método de emulsificação com ultrassom e condições de formação dos microfármacos utilizando CO_2 supercrítico como antissolvente foram utilizados.

O estudo foi realizado no LASEFI (Laboratório de Tecnologia Supercrítica: Extração, Fracionamento e Identificação de extratos vegetais) da Faculdade da Engenharia de Alimentos da UNICAMP, dando continuidade aos estudos realizados por Santos (2011) e Albuquerque (2013). Santos (2011) implantou uma unidade multipropósito para o desenvolvimento de processos com fluidos pressurizados para a extração, micronização e encapsulação de diversas substâncias. A unidade foi batizada de ARADIME, por ter sido elaborada pelos profissionais ARiovaldo Astini, DIego Tresinari dos Santos e Maria Angela de Almeida MEireles, e dela originou a unidade utilizada neste estudo para os processos de formação de micro e nanopartículas usando CO_2 supercrítico. Já Albuquerque (2013) visou à obtenção de óleo rico em antioxidantes das sementes de urucum usando o processo de extração com a tecnologia supercrítica. Esse óleo foi utilizado como matéria-prima para os experimentos de emulsificação.

O fármaco Ibuprofeno na forma de sal de sódio foi utilizado como sistema modelo durante o desenvolvimento experimental empregando a tecnologia *Supercritical antisolvent (SAS) precipitation*. Ibuprofeno é um anti-inflamatório não esteroidal (AINES) utilizado no combate de inflamações, dor e febre e está entre os fármacos mais consumidos no mundo. Sal de ibuprofeno sódico foi o fármaco selecionado para os experimentos de micronização devido às informações sobre o sistema CO_2-Ibuprofeno encontradas na literatura.

A tecnologia SAS *precipitation* consiste em extrair o solvente orgânico de uma solução contendo o soluto de interesse que será micronizado pelo CO_2 supercrítico. O emprego desta técnica apresenta muitas vantagens principalmente devido aos fatores ambientais e de qualidade envolvidos. Pois, trata-se de um processo não confere toxidade ao produto final, não necessita de pós-processamento das partículas para a eliminação do solvente, previne reações de oxidação devido à ausência de luz e oxigênio e não provoca a degradação térmica das partículas por permitir o emprego de baixas temperaturas. Além disso, esta técnica permite o controle do

tamanho e distribuição das partículas, a modificação do hábito cristalino e morfologia, e a obtenção de altos rendimentos e eficiência de encapsulamento.

As sementes de urucum foram selecionadas como matéria-prima por ser um ingrediente natural e pelas propriedades funcionais dos seus extratos. O urucum é bastante conhecido pelo uso de seus colorantes naturais, a bixina e a norbixina, para conferir cor em produtos elaborados pelas indústrias de alimentos, de cosméticos e de fármacos (Smith, 2006). Além disso, possui uma fração lipídica rica em tocotrienóis e geranil geraniol, que podem ser usados como suplemento nutricional em alimentos e bebidas funcionais (Tan, 2005; Albuquerque e Meireles, 2012). Devido à importância desses compostos bioativos, que são instáveis e que apresentam propriedades antioxidante, hidratante e fotoprotetora, este estudo visou o desenvolvimento de métodos para a formulação de emulsões. A emulsificação resulta em uma maior biodisponibilidade e permite a proteção desses compostos instáveis às condições adversas, aumentando assim o valor agregado dos extratos obtidos das sementes de urucum.

A emulsificação tem um papel importante na indústria de alimentos, principalmente na formação da consistência e textura, bem como na dispersão de fase e na solubilização de aromas. Este processo é definido como a operação em que dois líquidos imiscíveis são intimamente misturados, em que um deles (a fase dispersa) encontra-se na forma de gotas ou glóbulos dispersos no seio do outro líquido (a fase contínua), formando uma mistura estável. Os surfactantes são utilizados na formulação de emulsões como emulsionantes. Em países industrializados existe uma tendência da substituição dos surfactantes sintéticos pelos naturais, os biossurfactantes (Nitschke e Pastore, 2002). Este trabalho também propõe o uso de uma nova fonte de saponinas (composto com propriedades tenso-ativas) consideradas como biossurfactantes.

Para a formação de emulsões, é necessário o fornecimento de energia ao sistema. Essa energia pode ser fornecida por meio de diversos mecanismos, como por exemplo, agitação mecânica e ultrassom. Neste estudo, a técnica de ultrassom foi investigada para a formulação das emulsões. O ultrassom é produzido a partir de um transdutor, que converte a energia elétrica em energia mecânica sonora com frequências ultrassônicas. Através do sistema de sondas, o sinal acústico é amplificado e dirigido diretamente ao fluido através de uma haste metálica. A emulsificação através do ultrassom ocorre devido ao efeito da cavitação, o qual envolve a formação, crescimento e colapso implosivo de bolhas em um fluido. Quando a

cavitação ocorre próxima da interface de dois fluidos imiscíveis, a bolha sofre grande deformação, fazendo com que jatos de líquido oriundos da implosão da bolha sejam projetados para a outra fase. Este efeito faz com que pequenas gotículas de um fluido fiquem suspensas no outro fluido, formando uma emulsão (Duarte, 2009).

2 REVISÃO BIBLIOGRÁFICA GERAL

2.1 Sementes de urucum

As sementes de urucum são valiosas por produzirem pigmentos muito utilizados como corante natural nas indústrias alimentícia, farmacêutica e cosmética. Os extratos obtidos a partir das sementes são utilizados como corante alimentar (colorau) e usados em cosméticos como bronzeadores. As sementes do urucum contêm: 40 - 45% de celulose, 3,5 - 5,2% de açúcares, 0,3 - 0,9% de óleo essencial, 3% de óleo fixo, 4,5 - 5,5% de pigmentos, 13 - 16% de proteínas, além de α- e β-caroteno, taninos, saponinas e outros constituintes (Anselmo *et al.*, 2008).

Os pigmentos do urucum, pertencentes à classe dos carotenóides, são extraídos da camada externa das sementes, consistindo basicamente de cis-bixina, que representa mais de 80% dos carotenóides totais presentes. Da bixina são obtidos os demais pigmentos do urucum, como a norbixina (Oliveira, 2005). A Figura 1.1 apresenta a estrutura química dos principais colorantes presentes nas sementes de urucum: a bixina e norbixina.

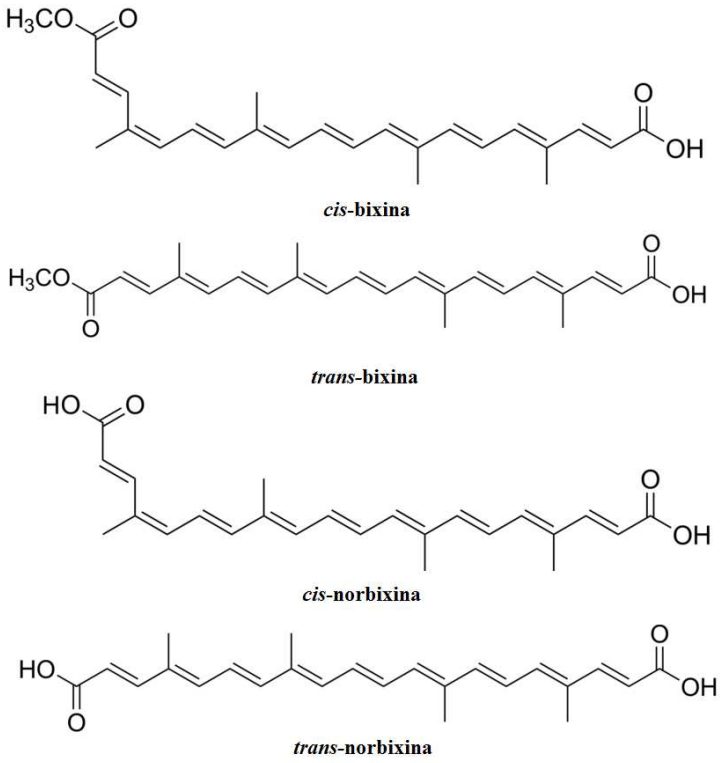

Figura 2.1: Estrutura química dos isômeros de bixina e norbixina (Albuquerque, 2013).

Muitos isoprenóides têm sido identificados nas sementes de urucum incluindo geranil-geraniol, farnesilacetona, octadecanoato de geranilgeranil, formiato de geranilgeranila e δ-tocotrienol. O constituinte oleoso majoritário das sementes é o geranil-geraniol representando 1% das sementes secas (Barbosa-Filho, 2006). Mas estudos têm mostrado que a grande peculiaridade das sementes de urucum é o teor de δ-tocotrienol. Frega *et al.* (1998) identificaram na fração lipídica da semente de urucum, extraída com hexano, a presença de tocotrienóis. Enquanto o óleo possui quantidades pequenas de tocoferol, o mesmo apresenta concentrações maiores de δ-tocotrienóis, além de traços de β-tocotrienol, destacando-se a elevada concentração do δ-tocotrienol, ao redor de 0,14 % de sementes secas na fração lipídica. Segundo os autores, a concentração encontrada é maior do que aquelas normalmente encontradas em qualquer outra espécie vegetal.

Os tocoferóis e os tocotrienóis são antioxidantes lipídicos e compõem um grupo de compostos que apresentam atividade vitamínica E. São derivados da estrutura 6-hidroxicromanol e possuem diferentes atividades biológicas próprias. Os oitos homólogos

existentes na natureza são α-, β-, γ- e δ-tocoferol, caracterizados por uma cadeia lateral saturada consistindo de três unidades isoprenóides, e os α-, β-, γ- e δ-tocotrienóis que possuem duplas ligações nas posições 3,7 e 11 da cadeia isoprenóide lateral (Abidi, 2000). Os isômeros se diferem com a posição e número dos grupos metila no anel cromanol, como demonstrado na Figura 1.2.

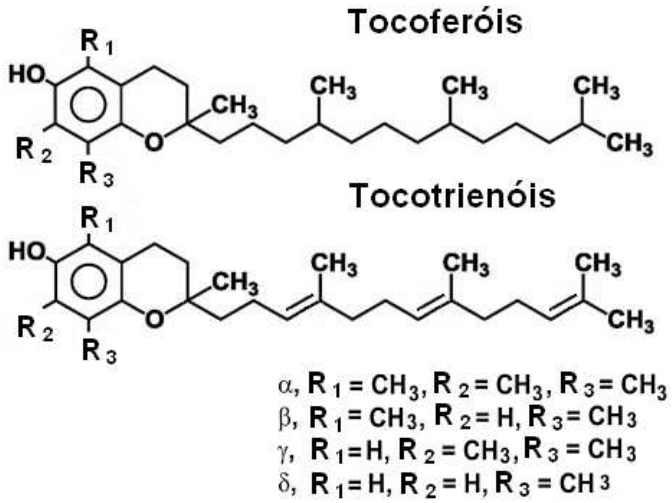

Figura 2.2: Fórmulas estruturais dos tocoferóis e tocotrienóis (Modificado de Papas (2006)).

Tocoferóis estão presentes em óleos vegetais e partes verdes de plantas superiores. Em contraste, tocotrienóis são encontrados na fração germe de várias sementes e cereais. Geralmente a presença de δ-tocotrienol na natureza é rara, sendo encontrado somente em alguns vegetais. Os óleos de palma, de farelo de arroz e de urucum são descritos pelo autor Tan (2011) como as mais ricas fontes naturais de tocotrienóis. A proporção de tocoferóis:tocotrienóis encontrada no óleo de farelo de arroz, de palma e de urucum é 50:50, 25:75 e 0,1:99,9, respectivamente. Além de conter traços de tocoferóis, o óleo de urucum contém 90% de δ-tocotrienol e 10% de γ-tocotrienol.

A atividade antioxidante dos tocotrienóis é relatada como mais efetiva quando comparada a dos tocoferóis. Tocotrienóis também apresentam efeitos na redução do colesterol e na inibição do crescimento das células cancerígenas (Aggarwal *et al.*, 2010). Todavia a presença de tocoferóis interfere nas funções dos tocotrienóis, como na redução do colesterol (Qureshi *et al.*, 1996) e também na sua absorção (Tan, 2005). Portanto, a

quase ausência de tocoferóis no urucum o torna a melhor fonte de tocotrienóis segundo Tan (2011).

2.2 Métodos de formação de micro e nanopatículas e encapsulação baseados na utilização de fluidos supercríticos

A produção de partículas em escala micro e nanométrica com as propriedades específicas e um controle preciso do tamanho e morfologia das mesmas é o objetivo de muitas indústrias. Com a redução do tamanho, as partículas apresentam um aumento da taxa de dissolução devido ao significativo aumento na área superficial e a estabilidade da suspensão é também aumentada. Diversas técnicas podem ser empregadas para produção de micro e nanopartículas. Contudo as técnicas convencionais, como spray dryer, liofilização, coacervação, polimerização interfacial, dentre outras, apresentam diversas desvantagens, como o uso excessivo de solvente, degradação térmica e química do soluto, alto teor de solvente residual e dificuldade de controlar a distribuição do tamanho das partículas durante o processamento (He *et al.*, 2004). Entretanto, o fluido supercrítico para formação de micro e nanopartículas tem sido empregado com o intuito de eliminar essas desvantagens. Além disso, o fluido supercrítico pode ser empregado para a encapsulação do soluto. Encapsulação é definida como uma tecnologia de armazenamento de materiais sólidos, líquidos ou gasosos em matrizes que podem liberar o seu conteúdo sob determinadas condições específicas (Desai e Jin Park, 2005).

Os processos que empregam fluido supercrítico para formação de micro e nanopartículas e encapsulação são classificados de acordo com a função do fluido supercrítico no processo. Maiores detalhes sobre esses processos podem ser encontrados nos Capítulos 2 e 3. A técnica que emprega fluidos pressurizados como antissolvente é conhecida por diversos acrônimos, como GAS (gas antisolvent), PCA (precipitation by compressed antisolvent), ASES (aerosol solvent extraction system), SEDS (solution enhanced dispersion by supercritical fluids), and SAS (Supercritical Antisolvent) (Reverchon, 1999). Esses processos são basicamente os mesmos, com pequenas modificações no injetor do solvente e do antissolvente usado, podendo o processo ser co- ou contra-corrente, em batelada ou contínuo (Tabernero *et al.*, 2012).

2.3 Antissolvente supercrítico (SAS)

O processo SAS, que emprega o fluido supercrítico como antissolvente, é baseado no uso de dois fluidos, solvente orgânico e antissolvente (sendo o mais empregado o CO_2 supercrítico), que são completamente miscíveis. O soluto de interesse, que será micronizado ou encapsulado, deverá ser solúvel no solvente orgânico e insolúvel no CO_2 supercrítico. Nesta técnica, a solução contendo o soluto e o antissolvente são alimentados separadamente e continuamente na câmara de precipitação. No capítulo 4 deste trabalho está apresentado na Figura 4.1 o fluxograma desse processo. Quando a solução contendo o soluto é colocada em contato com o antissolvente ocorre a nucleação e a formação dos cristais do sistema soluto/solvente orgânico/antissolvente que são governadas por dois mecanismos: difusão do antissolvente na fase orgânica e evaporação do solvente orgânico pelo antisolvente. O fenômeno de difusão aumenta o volume do solvente orgânico, reduzindo sua densidade, causando um decréscimo no seu poder de solvatação. Dessa forma, a solubilidade do soluto no solvente orgânico é drasticamente reduzida, levando à supersaturação do soluto e à sua precipitação na forma de micro ou nanopartículas, através da eliminação do solvente orgânico pelo fluido supercrítico (antissolvente) (Subra e Jestin, 1999; Kalani *et al.*, 2011). Este processo geralmente opera com pressões moderadas (9–15 MPa). Quando o objetivo é encapsular, a solução é preparada usando o soluto de interesse, o material de encapsulação (biopolímero, ciclodextrina, etc) e um solvente orgânico capaz de dissolver ambos os compostos (Santos, 2011). Este processo permite um fácil controle da formação de partículas através de pequenas variações nas condições de operação (pressão, temperatura, vazão, concentração, etc.) (Mattea *et al.*, 2008).

As principais vantagens deste processo são: (i) possibilidade de obter uma estreita distribuição do tamanho das partículas controlando as condições operacionais; (ii) facilidade de remoção do antissolvente (CO_2 supercrítico) pela redução da pressão; (iii) o processo pode ser operado à temperatura ambiente, evitando assim a degradação térmica das partículas; (iv) é possível obter partículas com alta pureza polimórfica, com aumento da taxa de dissolução e com teor de solvente residual aceitável; (v) este processo é adaptado para operação contínua, sendo importante para produção em larga escala; (vi) o processo ocorre num sistema fechado, que vastamente reduz o risco de contaminação; (vii) eso de

menores quantidades de solvente orgânico que os processos convencionais, além disso, permite a reciclagem do solvente orgânico e do CO_2, uma vez que é um processo independente em única etapa (Yeo e Kiran, 2005; York, 2005; Majerik *et al.*, 2007; Kalani *et al.*, 2011).

2.4 Formação de emulsão através do ultrassom

Emulsões são sistemas termodinamicamente instáveis devido ao contato desfavorável entre as moléculas de água e de óleo. Assim, há uma tendência à separação das fases a fim de minimizar a área interfacial e energia livre de Gibbs do sistema. Essa instabilidade pode se manifestar através de diferentes mecanismos, como a floculação, cremagem, acomodação de Ostwald, coalescência e inversão de fases (Mcclements, 2004).

A técnica ultrassom é aplicada na preparação de emulsões como uma alternativa aos processos de emulsificação. No Apêndice deste trabalho está apresentado na Figura A.5 um equipamento comum de ultrassom utilizado para o preparo de emulsões, que consiste em um gerador de energia, um transdutor e uma sonda ou probe. O gerador produz energia elétrica de alta frequência, e o transdutor, por sua vez, converte essa energia elétrica em energia mecânica, que são amplificadas e propagadas através de um sonotrodo na forma de ondas acústicas (Abbas *et al.*, 2013).

As ondas de ultrassom são capazes de gerar cavitação. Através desse fenômeno, a aplicação da energia de ultrassom fornece ambiente favorável para a emulsificação. Cavitação é um fenômeno físico baseado no processo de criar, aumentar e implodir bolhas de vapor e gases em um líquido. As ondas de ultrassom resultam em um ciclo de compressão-expansão. Durante a etapa de compressão, as ondas fornecem uma pressão positiva no líquido, enquanto que a expansão resulta em vácuo (pressão negativa) e assim gerando as microbolhas ou cavidades, que tendem a implodir, resultando na formação de uma emulsão (Anton *et al.*, 2008).

3 OBJETIVOS

3.1 GERAL

Avaliar o processo de formação de micro ou nanopartículas de fármacos empregando a tecnologia supercrítica e avaliar a formulação de emulsões ricas em compostos bioativos das sementes de urucum empregando o ultrassom.

3.2 ESPECÍFICOS

- ✓ Analisar o estado da arte da formação de micro e nanopartículas utilizando fluido supercrítico.
- ✓ Validar a unidade SAS/SFEE usando o processo SAS (Supercritical antisolvent) precipitation utilizando como substância modelo o sal de ibuprofeno sódico.
- ✓ Comparar as micropartículas de sal de ibuprofeno sódico obtidas por SAS precipitation com as obtidas por método convencional (Evaporação convencional do solvente por rotaevaporador).
- ✓ Emulsionar óleo de semente de urucum rico em δ-tocotrienóis utilizando extrato de raíz de ginseng como surfactantes e homogeneizadores do tipo Dispersor de fase múltipla e ultrassom.
- ✓ Comparar as emulsões preparadas com óleo de semente de urucum e extrato de raiz de ginseng com as emulsões preparadas com um óleo e um biossurfactante modelo: óleo de soja e saponina comercial, respectivamente.

4 ESTRUTURA DA TESE

A presente tese está dividida em 6 capítulos, compostos por artigos científicos e capítulos de livros publicados e que ainda serão publicados. O **Capítulo 1 – ASPECTOS GERAIS**, como já visto, apresenta de forma sucinta o tema principal deste trabalho, os objetivos pretendidos e as etapas envolvidas para a realização do projeto de pesquisa de doutorado. A estrutura deste trabalho está apresentada na Figura 1.3, que esquematiza as atividades realizadas durante o período do doutorado.

O **Capítulo 2 -** ***TRENDS IN PARTICLE FORMATION OF BIOACTIVE COMPOUNDS USING SUPERCRITICAL FLUIDS AND NANOEMULSIONS*** contextualiza o estado da arte dos métodos de formação de micro e nanopartículas e encapsulação que empregam fluido supercrítico. Neste trabalho de revisão, os princípios da formação de partículas e encapsulação e as diversas técnicas que empregam o fluído supercrítico como solvente, antissolvente e soluto foram apresentados. Além disso, as recentes descobertas sobre a aplicação de fluido supercrítico para a formação de partículas de compostos bioativos foram discutidas. Esta primeira etapa teve como principal objetivo discutir sobre os fundamentos dos métodos que empregam o fluido supercrítico como antissolvente, focando no método de extração supercrítica de emulsões (SFEE - Supercritical Fluid Extraction of Emulsions). A revisão mostrou que o SFEE combina as técnicas de emulsificação e as baseadas na utilização do fluido supercrítico como antissolvente, permitindo a obtenção de partículas em escala nanométrica. O produto resultante do SFEE é uma suspensão em água e adicionais processos tornam-se necessários para obtenção do produto em pó, que podem levar ao aumento do tamanho das partículas obtidas.

Dentro deste contexto, o **Capítulo 3 -** ***MICRONIZATION AND ENCAPSULATION: APPLICATION OF SUPERCRITICAL FLUIDS IN WATER REMOVAL*** apresenta os métodos que empregam o fluido supercrítico com o objetivo de remover água. O histórico, a descrição de cada processo, as principais aplicações e a influência dos parâmetros operacionais foram discutidas para os processos CAN-BD (Carbon dioxide-Assisted Nebulisation with a Bubble Dryer) e PGSS (Particles from Gas-Saturated Solutions)-drying. Esses processos são baseados no simples conceito de expandir uma solução aquosa saturada com CO_2 supercrítico através de um atomizador. A revisão

mostrou o potencial da aplicação desses processos para obtenção de produtos para a indústria de alimentos, que é algo ainda pouco explorado na literatura. Adicionamente verificou-se a potencialidade de se utilizar ambos os processos para a eliminação de água de emulsões óleo em água, na qual o óleo é a fase dispersa e a água é a fase contínua, como as que serão preparadas contendo o extrato rico em δ-tocotrienol (Capítulo 6).

Uma vez apresentado os diversos processos para formação de partículas baseados na utilização de fluidos supercríticos, um estudo sobre a validação da unidade SAS/SFEE foi realizado e está apresentado no **Capítulo 4 -** ***EXPERIMENTAL DESIGN FOR THE MICRONIZATION OF IBUPROFEN SODIUM SALT BY SUPERCRITICAL CARBON DIOXIDE ANTISOLVENT PROCESS.*** Sal de ibuprofeno sódico foi utilizado como substância modelo para os processos de micronização via SAS precipitation. Essa substância foi selecionada por haver muitas informações sobre o sistema Ibuprofeno sódico-CO_2 na literatura. O efeito das condições operacionais (temperatura, pressão, vazão da solução, vazão do CO_2, tipo de injetor e concentração de ibuprofeno sódico na solução etanólica) no rendimento de precipitação, teor de solvente residual, morfologia das partículas e consumo energético por unidade de produto processado foi investigado utilizando o método split-plot. Sal de ibuprofeno sódico foi micronizado com sucesso via SAS precipitation utilizando a unidade construída, demonstrando que com uma seleção adequada das condições operacionais é possível obter micropartículas com diferentes morfologias.

Dentre os compostos bioativos de interesse das sementes de urucum encontram-se os δ-tocotrienóis por apresentarem propriedades antioxidantes e atividade vitamínica, comumente denominada de vitamina E. Desta forma, o **Capítulo 5** - ***FORMULATING TOCOTRIENOL-RICH OIL AS AN O/W MINI-EMULSION BY USING NONPURIFIED AQUEOUS EXTRACT FROM BRAZILIAN GINSENG ROOTS AS A BIOSURFACTANT*** apresenta um estudo sobre formulação de emulsões para aumentar o valor agregado dos extratos das sementes de urucum obtidos por extração supercrítica (SFE), que poderão ser utilizados para a formulação de novos produtos alimentícios. Albuquerque (2013) obteve as condições otimizadas de processo SFE com maior rendimento em extrato, rico em δ-tocotrienol, que foram utilizadas neste estudo. Para a proteção dos extratos de altas temperaturas, oxidação e da luz ultravioleta e para aumentar a

biodisponibilidade do δ-tocotrienol, emulsões, contendo o extrato rico em δ-tocotrienol e extrato biossurfactante de raiz de ginseng, foram formuladas utilizando o homogeneizador do tipo dispersor de fase múltipla e ultrassom. Um sistema modelo de emulsão óleo em água contendo óleo de soja e saponina comercial como biossurfactante foi preparado. A influência do processo de emulsificação, densidade energético, concentração do biossurfactante, tipo de óleo e de biossurfactante no tamanho de gota e estabilidade da emulsão também foram investigados. Este estudo foi muito importante, pois mostrou a capacidade do biossurfactante de extrato de ginseng que pode ser uma escolha muito atrativa para a formulação de emulsões de produtos alimentícios e bebidas. Além disso, os resultados mostraram que o uso do ultrassom e do bissurfactante de raiz de ginseng possibilitou a obtenção de emulsões com menores tamanhos de gota. O processo empregado de emulsificação influenciou estatisticamente a estabilidade das emulsões.

Finalmente, o **Capítulo 6 - *CONCLUSÕES GERAIS*** apresenta os principais resultados obtidos em cada um dos capítulos apresentados neste trabalho. Além disso, está apresentada também a memória do período do doutorado com todos os trabalhos acadêmicos realizados paralelamente.

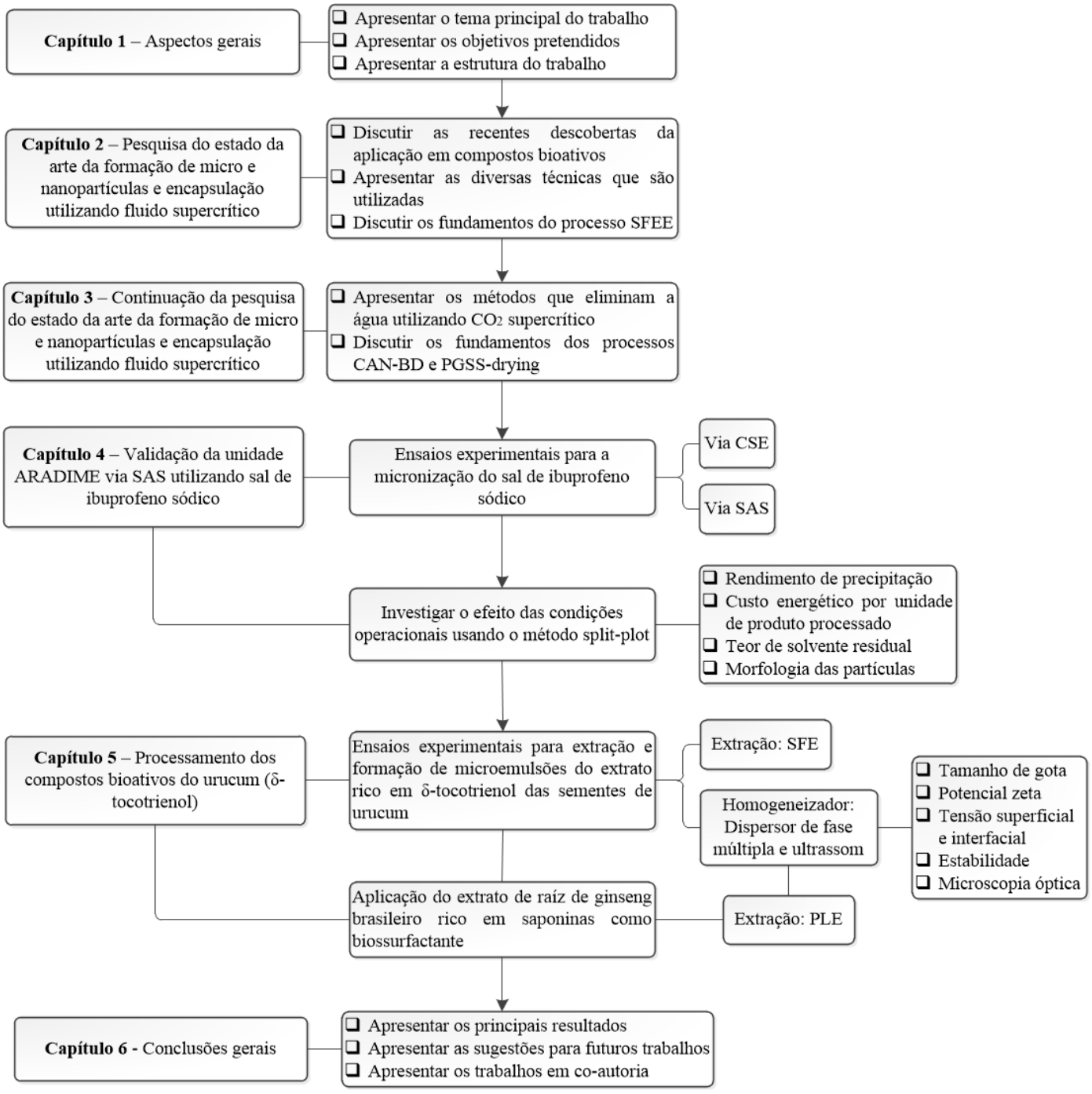

Figura 1.3: Esquema das etapas do desenvolvimento da tese de doutorado e as atividades realizadas.

Referências

ABBAS, S. et al. An overview of ultrasound-assisted food-grade nanoemulsions. **Food Engineering Reviews,** v. 5, n. 3, p. 139-157, 2013. ISSN 1866-7910.

ABIDI, S. Chromatographic analysis of tocol-derived lipid antioxidants. **Journal of Chromatography A,** v. 881, n. 1, p. 197-216, 2000.

AGGARWAL, B. B. et al. Tocotrienols, the vitamin E of the 21st century: its potential against cancer and other chronic diseases. **Biochemical Pharmacology,** v. 80, n. 11, p. 1613-1631, 2010.

ALBUQUERQUE, C. L.; MEIRELES, M. A. A. Defatting of annatto seeds using supercritical carbon dioxide as a pretreatment for the production of bixin: Experimental, modeling and economic evaluation of the process. **The Journal of Supercritical Fluids,** v. 66, p. 86-95, 2012. ISSN 0896-8446.

ALBUQUERQUE, C. L. C. **Obtenção de sementes desengorduradas e de óleo rico em tocotrienóis de urucum por extração supercrítica: estudo dos parâmetros de processo, do aumento de escala e da viabilidade econômica**. Tese (Doutorado em Engenharia de Alimentos). Universidade Estadual de Campinas, São Paulo. 2013.

ANSELMO, G.; MATA, M.; RODRIGUES, E. Comportamento Higroscópico do extrato seco de urucum (Bixa orellana L.). **Ciência Agrotecnologia,** v. 6, p. 1888-92, 2008.

ANTON, N.; BENOIT, J.-P.; SAULNIER, P. Design and production of nanoparticles formulated from nano-emulsion templates—a review. **Journal of Controlled Release,** v. 128, n. 3, p. 185-199, 2008. ISSN 0168-3659.

BARBOSA-FILHO, J. M. *Bixa orellana*: Retrospectiva de usos populares, atividades biológicas, fitoquímica e emprego na fitocosmética, no continente americano. In: Simpósio Brasileiro do Urucum—SIMBRAU, 2006, João Pessoa, Brasil.

DESAI, K. G. H.; JIN PARK, H. Recent developments in microencapsulation of food ingredients. **Drying technology,** v. 23, n. 7, p. 1361-1394, 2005.

DUARTE, F. A. **Emprego de ultrassom para a oxidação e separação de compostos orgânicos sulfurados em hidrocarbonetos e determinação de enxofre por técnicas espectrométricas e cromatográficas**. Tese (Doutorado em Química). Universidade Federal de Santa Maria, Rio Grande de Sul. 2009.

FREGA, N.; MOZZON, M.; BOCCI, F. Identification and estimation of tocotrienols in the annatto lipid fraction by gas chromatography-mass spectrometry. **Journal of the American Oil Chemists' Society,** v. 75, n. 12, p. 1723-1727, 1998.

HE, W. Z. et al. Precipitation of ephedrine by SEDS process using a specially designed prefilming atomizer. **The Journal of supercritical fluids,** v. 31, n. 1, p. 101-110, 2004.

KALANI, M.; YUNUS, R.; ABDULLAH, N. Optimizing supercritical antisolvent process parameters to minimize the particle size of paracetamol nanoencapsulated in L-polylactide. **International Journal of Nanomedicine,** v. 6, p. 1101-1105, 2011.

MAJERIK, V. et al. Bioavailability enhancement of an active substance by supercritical antisolvent precipitation. **The Journal of Supercritical Fluids,** v. 40, n. 1, p. 101-110, 2007.

MATTEA, F.; MARTIN, A.; J. COCERO, M. Co-precipitation of β-carotene and polyethylene glycol with compressed CO2 as an antisolvent: Effect of temperature and concentration. **Industrial & Engineering Chemistry Research,** v. 47, n. 11, p. 3900-3906, 2008.

MCCLEMENTS, D. J. **Food emulsions: principles, practices, and techniques**. New York: CRC press, 2004.

NITSCHKE, M.; PASTORE, G. M. Biossurfactantes: propriedades e aplicações. **Química Nova,** v. 25, n. 5, p. 772-776, 2002.

OLIVEIRA, J. S. **Caracterização, extração e purificação por cromatografia de compostos de urucum (*Bixa orellana* L.)**. Tese (Doutorado em Engenharia Química). Universidade Federal de Santa Catarina, Florianópolis. 2005.

PAPAS, A. M. Tocopherols and Tocotrienols as Byproducts of Edible Oil Processing. In: SHAHIDI, F. (Ed.). **Nutraceutical and Specialty Lipids and Their Co-products**: Taylor & Francis Group, 2006. p.469-481.

QURESHI, A. A. et al. Dietary alpha-tocopherol attenuates the impact of gamma-tocotrienol on hepatic 3-hydroxy-3-methylglutaryl coenzyme A reductase activity in chickens. **The Journal of Nutrition,** v. 126, n. 2, p. 389-394, 1996.

REVERCHON, E. Supercritical antisolvent precipitation of micro-and nano-particles. **The Journal of Supercritical Fluids,** v. 15, n. 1, p. 1-21, 1999.

SANTOS, D. T. **Extração, micronização e estabilização de pigmentos funcionais: construção de uma unidade multipropósito para desenvolvimento de processos com fluídos pressurizados**. Tese (Doutorado em Engenharia de Alimentos). Universidade Estadual de Campinas, São Paulo. 2011.

SMITH, J. Annatto extracts: chemical and technical assessment. **FAO - Food and agriculture organization of the United Nations**, p. 1-21, 2006.

SUBRA, P.; JESTIN, P. Powders elaboration in supercritical media: comparison with

conventional routes. **Powder Technology,** v. 103, n. 1, p. 2-9, 1999.

TABERNERO, A.; DEL VALLE, E. M. M.; GALÁN, M. A. Supercritical fluids for pharmaceutical particle engineering: Methods, basic fundamentals and modelling. **Chemical Engineering and Processing: Process Intensification,** v. 60, p. 9-25, 2012.

TAN, B. Appropriate spectrum vitamin E and new perspectives on desmethyl tocopherols and tocotrienols. **The Journal of the American Nutraceutical Association,** v. 8, n. 1, p. 35-42, 2005.

TAN, B. Tocotrienols: The New Vitamin E. **http://www.spacedoc.com/tocotrienols**, 2011. Acesso em: Maio de 2013.

YEO, S.-D.; KIRAN, E. Formation of polymer particles with supercritical fluids: a review. **The Journal of Supercritical Fluids,** v. 34, n. 3, p. 287-308, 2005.

YORK, P. Supercritical fluids: realising potential. **Chemistry World,** v. 2, n. 2, p. 50-53, 2005. ISSN 1473-7604.

CAPÍTULO 2 - TRENDS IN PARTICLE FORMATION OF BIOACTIVE COMPOUNDS USING SUPERCRITICAL FLUIDS AND NANOEMULSIONS

M. Thereza M. S. Gomes, Diego T. Santos and M. Angela A. Meireles

Artigo publicado no periódico *Food and Public Health* 2012, 2(5): 142-152

ISSN: 2162-8440 DOI: 10.5923/j.fph.20120205.05

AVISO DE DIREITO DE AUTOR

Food and Public Health 2012, 2(5): 142-152
DOI: 10.5923/j.fph.20120205.05

Trends in Particle Formation of Bioactive Compounds Using Supercritical Fluids and Nanoemulsions

M. Thereza M. S. Gomes, Diego T. Santos, M. Angela A. Meireles*

LASEFI/DEA/FEA (School of Food Engineering)/UNICAMP (University of Campinas), Cidade Universitária "Zeferino Vaz", R. Monteiro Lobato, 80; 13083-862, Campinas, SP, Brazil

Abstract This review discusses the recent developments in the application of supercritical fluid technologies for the production of composites or encapsulates of bioactive compounds. Various supercritical particle formation technologies are briefly described, including processes in which the supercritical fluid acts as a solute, solvent, and antisolvent. The main features and mechanisms of antisolvent techniques that contribute to the understanding of the fundamentals of the Supercritical Fluid Extraction of Emulsions (SFEE) process are described. The published literature on SFEE, including the results and perspectives of its application in various industrial fields, are discussed. This article is the first comprehensive review specifically focused on the formation of particles using the SFEE technique.

Keywords SAS, SFEE, Supercritical, Bioactive Compounds, Novel Processing Techniques

1. Introduction

Particle formation and encapsulation technologies are widely employed in the pharmaceutical, cosmetic, and food industries. Examples of classical micronization processes include spray drying, spray chilling and spray cooling; extrusion coating; fluidized bed coating; liposome entrapment; coacervation; inclusion complexation; centrifugal extrusion and rotational suspension separation[1]. However, all of these techniques have inherent limitations.

Supercritical fluids have been used as solvents, solutes, and antisolvents for micro- and nanoparticle formation in a variety of compounds and have overcome all of the limitations of the traditional techniques. These limitations include poor control of particle size and morphology, degradation of thermosensitive compounds and low encapsulation efficiency[2]. The possibility of obtaining solvent-free microparticulate particles with a narrow size distribution curve using supercritical fluids is very attractive[3].

Supercritical fluids, which were first discovered in 1879, have an exceptional solubility for solids and liquids compared with liquid or gaseous fluids. Variations in the operating conditions to increase the solvation power make this technology a solid option for the recovery of several types of substances. The properties of these fluids have been extensively explored in the extraction and/or separation steps to obtain valuable compounds, such as flavors, colorants, and other biomolecules[4]. A promising new field for supercritical fluids is the formation of particles containing these compounds.

The aim of this review is to discuss several of the recent developments in the application of supercritical fluid technologies for the production of composites or encapsulates of bioactive compounds. Bioactive compounds are extranutritional constituents that typically occur in small quantities in nature, are part of the food chain, and have an effect on human health. In this review, the various supercritical particle formation technologies are briefly described. The main features and mechanisms of the antisolvent techniques that primarily contribute to understanding the fundamentals of the Supercritical Fluid Extraction of Emulsions (SFEE) process and the results of and perspectives on applying these techniques in various industrial fields are discussed.

2. Principles of Particle Formation

Encapsulation has been defined as packaging solid, liquid or gaseous materials into microcapsules that release their contents at controlled rates over prolonged periods of time under specific conditions [5],[6]. The size of the particles formed through encapsulation may be classified as follows: macro (>5000 μm), micro (1.0–5000 μm), and nano (<1.0 μm) [7]. Different morphologies can be obtained depending on the physicochemical properties of the core and wall materials and the encapsulation techniques used during production. In general, the two main structures are mononuclear capsules, which contain one core material

* Corresponding author:
meireles@fea.unicamp.br (M. A. A. Meireles)
Published online at http://journal.sapub.org/fph

enveloped by a carrier material, and aggregates, which consist of many core materials embedded in a matrix of coating material [8],[9].

Composites are frequently produced by the simultaneous precipitation of the core and coating materials, which leads to the dispersion of the core material particles into a matrix of coating material. Encapsulates are produced when the coating material is precipitated as a thin shell over a previously existing particle of the core material [10]. Both types are produced for multiple purposes, such as controlling the release of core material in a desired quantity and location, increasing the dissolution rate of slightly water-soluble materials and modifying the surface properties of particles used in pharmaceutics, catalysts, cosmetics, the printing industry and energetic materials [11]. Figure 1 shows the general structures of encapsulates and composites.

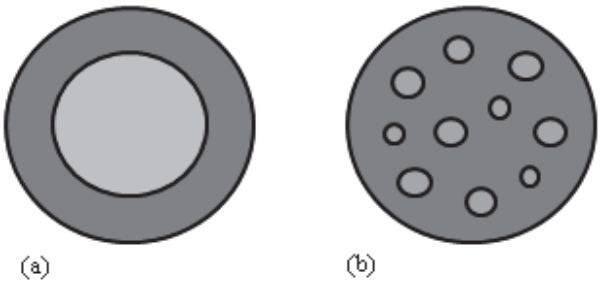

Figure 1. The structures of (a) an encapsulate and (b) a composite

In the food industry, the primary reasons that the encapsulation process is applied are summarized as follows[5], [12]: (i) to protect unstable materials from degradation; (ii) to decrease the evaporation or transfer rates of the core material to the outside environment; (iii) to modify the physical characteristics of the original material to be easier to handle; (iv) to control the release of the core material; (v) to mask the odor or taste of the core material; (vi) to dilute the core material when small amounts are required, yet still achieve a uniform dispersion in the host material; and (vii) to separate components within a mixture that would otherwise react with one another.

Nanoencapsulation offers numerous benefits. The application of this technique in the food industry has received attention from the scientific community due to its potential to protect and improve the efficiency of delivering bioactive compounds in functional foods to improve human health [13].

3. Particle Formation by Nano- and Microencapsulation

There are several studies that describe the nano- and microencapsulation technologies that are used to encapsulate bioactive compounds [6], [9], [14-16]. Microencapsulation techniques can be divided into chemical processes, such as molecular inclusion and interfacial polymerization, physicochemical techniques, such as coacervation and liposome entrapment, and physical processes, including spray drying, spray chilling or spray cooling; extrusion; co-crystallization and fluidized bed coating. Additional information on conventional techniques is provided in [5] and [17].

There are specific features and characteristics that are disadvantages in each process, such as thermal denaturing, large residual solvent concentrations, and difficulties in controlling particle size and size distribution during processing. These limitations may affect particle stability, flow properties, and delivery efficiency [18].

The use of supercritical fluids as an alternative medium for nano- and microencapsulation can improve the results obtained using conventional techniques. Published reviews indicate that these methods have the potential to overcome the drawbacks previously described [19-23].

4. Nano- and Microencapsulation Using Supercritical Fluids

Carbon dioxide is the primary fluid applied to produce composite particles using supercritical fluid methods[11] because it enables the process to be performed at near ambient temperatures in an inert atmosphere, which avoids the degradation of the bioactive compounds. The supercritical region can be achieved at moderate pressures and temperatures (Tc = 304.2 K, Pc = 7.38 MPa). A number of modified processes that use supercritical fluids in particle formation have been described in the literature. These processes are classified according to the role of the supercritical fluid in the process, as follows: solvent[Rapid Expansion of Supercritical Solutions (RESS)]; solute[Particles from Gas-Saturated Solutions (PGSS)]; or antisolvent[Supercritical AntiSolvent (SAS)], including its numerous modifications [24]. These classifications are briefly described in the following sections, and additional details regarding these methods can be found in other reviews [10], [11], [19], [23-25].

4.1. Supercritical CO_2 as a Solvent

The first review article on applying the supercritical fluid method in particle design focused on the RESS method, which was the first method used to produce particles [26].

In the RESS process, the substance to be powdered is first dissolved in a supercritical fluid. This mixture is then depressurized through a nozzle, which leads to the rapid precipitation of the dissolved matter as the supercritical fluid vaporizes. The absence of liquid organic solvents, the mild processing temperatures, and the purity of the final product make this process particularly attractive for biomedical applications [27]. Many drugs, such as salicylic acid [28], naproxen [29], ibuprofen [30], griseofulvin and β-sitosterol [31], have been micronized using the RESS technique.

4.2. Supercritical CO_2 as a Solute

The solubility of compressed gases in liquids is generally quite high. Production of particles using the gas-saturated

solution (PGSS) process is based on the high solubility of supercritical CO_2 in many substances, including molten polymers, oils and fats [32]. The PGSS process consists of solubilizing supercritical CO_2 in melted or liquid-suspended substance(s), which leads to a gas-saturated solution that is expanded through a nozzle to form fine particles through precipitation after rapid expansion as a consequence of a drastic reduction in solubility [33]. The PGSS process has been applied in various fields to produce products ranging from inorganic powders to pharmaceutical compounds. Jung & Perrut [19] and [34] list several applications of this method for food and food-related products.

Another application of the PGSS process is drying liquid solutions to produce fine powders, or PGSS-drying [34]. Varona et al.[35] recently used PGSS-drying to encapsulate lavandin oil in starches by removing the water from an oil-in-water emulsion stabilized with N-octenyl succinic anhydride (OSA) starches as surfactants.

4.3. Supercritical CO_2 as an Antisolvent

Supercritical antisolvent precipitation is also known as GAS (gas antisolvent), PCA (precipitation by compressed antisolvent), ASES (aerosol solvent extraction system), SEDS (solution enhanced dispersion by supercritical fluids), and SAS (supercritical antisolvent) [36]. These processes are essentially the same, with differences in the feed mode of the solvent and antisolvent, which can be co-current or counter-current, depending on the type of injector used, and can use batch or semi-continuous modes [37].

Encapsulation using the SAS technique is based on the same simple principles of the RESS method in which a core material and a carrier are co-precipitated together [2]. This process is well known and has been applied to several types of compounds, including explosives [38], polymers [39], [40], pharmaceuticals[41], [42], and pigments [43]. The SAS method has been thoroughly reviewed by [36]. The advanced application of supercritical fluids in micro/nanoencapsulation technology, with the emulsion process referred to as Supercritical Fluid Extraction of Emulsions (SFEE), will be evaluated in this review.

4.4. Supercritical Fluid Extraction of Emulsions (SFEE)

SFEE combines the emulsion techniques and the SAS processes. Emulsion techniques generally require large quantities of organic solvents, and their removal involves additional separation techniques and the use of high temperatures. In addition, SAS is not able to produce particles within the nanometric scale, and the resulting products have an increased tendency for particle agglomeration [10]. To overcome these disadvantages, Chattopadhyay et al. [44] combined the two technologies and patented a new encapsulation method termed the Supercritical Fluid Extraction of Emulsions (SFEE). This method allows the removal of organic solvents during the process and enables the production of nanoscale particles that improve the solubility of bioactive compounds in aqueous solutions, which increases their bioavailability.

The SAS method is based on combining the substance to be micronized or encapsulated dissolved in an organic solvent with a supercritical fluid, which acts as an antisolvent. Upon mixing, the supercritical fluid saturates and depletes the liquid solvent by decreasing its solvation power through extraction, and the solute precipitates as microparticles. If a wall material is also dissolved in the organic solvent, composites or encapsulates are formed by co-precipitation with the solute [10], [19]. The experimental setup and principles of the SFEE process are basically the same as those of SAS, but in SFEE, supercritical CO_2 is used as an antisolvent to eliminate the organic solvent from the droplets of an oil-in-water (O/W) emulsion [45]. An O/W emulsion containing the core materials to be precipitated dissolved in its dispersed phase (e.g., a conventional organic liquid solvent) is injected into the precipitation vessel with a CO_2 flow rate. The final product is a micro- or nanosuspension of the substance in water.

The differences in the SAS and SFEE processes are as follows: (a) in SFEE, an emulsion containing the substance to be precipitated dissolved in its dispersed phase is injected, whereas in SAS, a simple solution of the substances is injected; (b) SFEE requires additional steps to produce a powdery product because an aqueous product is formed; (c) the preparation of the initial materials is more complex in SFEE; and (d) emulsion droplet size distribution is a controlling parameter in addition to the other parameters involved in the SAS process (e.g., pressure, temperature, flow rate, and concentration)[10]. However, the SFEE technology is a promising method for producing nanometer particles of natural substances in water [46]. Narrower size distributions can be produced by SFEE because particle size is strictly related to the droplet size and distribution of the starting emulsion, and particle agglomeration can be prevented by the water/surfactant external phase [47]. Using the same pressure, temperature, and solution flow rate for both the SFEE and SAS methods, Shekunov et al. [45] observed a substantial difference in the resulting size and shape of the particles. SFEE produced prismatic crystals with a volume-weighted diameter typically between 0.5 and 1 μm, whereas SAS produced longer crystal dimensions of between 20 and 200 μm and a volume-weighted diameter above 10 μm. Thus, a 10-fold reduction in the particle size was achieved using SFEE compared with the particles produced using SAS.

Mattea et al. [48] described the phenomenon that occurs during the SFEE process by investigating a system composed of a β-carotene + dichloromethane-CO_2-water + starch-based surfactant. Each drop of the organic solvent behaved as a miniature gas antisolvent precipitator, and multiple particles formed inside the drop. Depending on the CO_2 pressure and temperature, the solubility of CO_2 in the aqueous and organic phases changed and caused swelling and shrinking of the drop due to the diffusion of supercritical CO_2 into the drop and dichloromethane out of the drop.

4.5. SFEE steps

4.5.1. Emulsion Preparation

Before initiating the SFEE process, an oil-in-water emulsion must be prepared. In general, these emulsions are prepared with the aid of surfactants.

Certain of the surfactant materials used to prepare the O/W emulsion have a double functionality in the SFEE process as both a surfactant to stabilize the emulsion and a coating material in the final dry product [46]. Surfactants also act as protective layers and reduce the agglomeration of the final particles[45],[49]. Mezzomo et al. [50] used a Pluronic F127 surfactant/coating material to encapsulate the extract from pink shrimp residue and observed that the emulsion was not stable due to incorrect Hydrophilic-Lipophilic Balance (HLB) values from the surfactant. The authors then used a modified starch (Hi-Cap 100) to achieve high encapsulation efficiency. Additional research is needed to optimize the effectiveness of SFEE for encapsulation.

When using a polymer without emulsification properties as a coating material, such as poly-lactic-co-glycolic acid (PLGA), surfactants are only used to stabilize the emulsion. Polyvinyl alcohol (PVA) is the most popular surfactant used in the production of PLGA-stable nanoparticles in the SFEE process.

From a food application perspective, the use of food-grade surfactants is important. Studies that have used food-grade surfactants for bioactive compound encapsulation via SFEE are extremely scarce. In the literature, all of the studies are related to the precipitation of carotenoids using a modified starch as the surfactant [46], [48], [50], [51]. Table 1 in section 4.8 lists all of the surfactants that have been tested using the SFEE process.

Silva et al. [52] provided an overview of the surfactants used in nanoemulsion production for food applications. The authors focused on nanoemulsion production methods, which are classified as either high-energy or low-energy.

There are a number of mechanisms available for the production of emulsions. High-speed stirring mixers [46],[47],[51], high-pressure homogenization [45], [53], [54], and ultrasonication [55-58] have been used to form fine emulsions for use in the SFEE process. Microfluidization is an additional alternative for preparing submicron emulsions. Jafari et al.[59] investigated the efficiency of sonication and microfluidization in the production of nanoemulsions and reported that the microfluidizer produced emulsions with narrower size distributions, whereas sonication was a better option in terms of operation and cleaning.

Emulsification is one of the important steps in the SFEE process. An advantage of this process is that growth of the particles is limited by the size of the emulsion droplets [49]. However, stable emulsions are required, and the droplets must be protected against flocculation followed by creaming or sedimentation. Coalescence via collisions and Ostwald ripening, which is a molecular diffusion degradation, are the primary reasons for instability in nanoemulsions. Additional details regarding the principles of the formation and stabilization of nanoemulsions are provided in a review article by Tadros et al. [60].

Abismaïl et al. [61] reported that smaller average drops can be obtained using ultrasound. Ultrasound requires less surfactant, consumes less energy and produces emulsions that are less polydispersed and more stable compared with the emulsions produced by mechanical processes. Furlan et al. [57] studied the influence of sonication duration on the final particle size distribution. The authors concluded that the duration of sonication slightly influenced the average particle size but had a strong influence on the particle size distribution.

4.5.2. SFEE Processing

The SFEE process can be performed in a batch, semi-continuous or continuous mode using a similar apparatus. In the SFEE batch mode, an aliquot of the emulsion is placed into the precipitation vessel to be processed. In the semi-continuous mode, the aqueous suspension is removed from the bottom of the precipitation vessel when the extraction process is complete. In the continuous mode, the suspension is continuously removed through a needle valve [45], [53], [58]. Chattopadhyay et al. [53] observed that there were no differences in mean particle size and morphology between the batch and continuous modes.

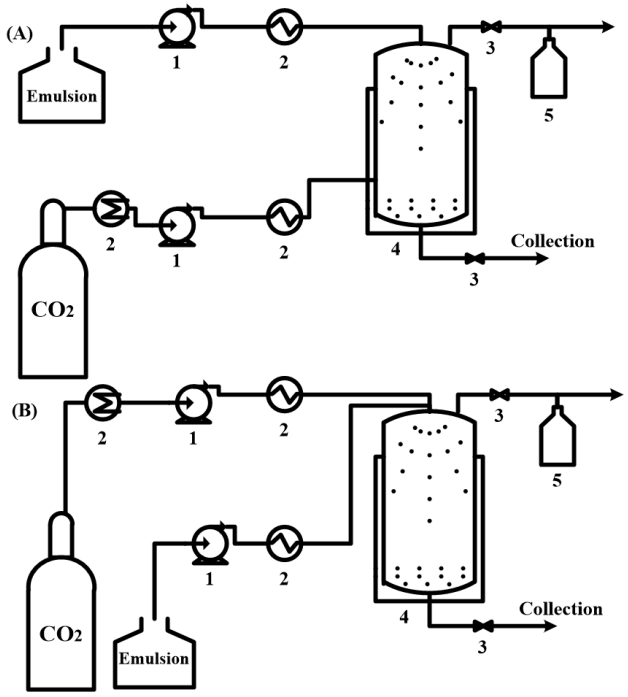

Figure 2. A schematic diagram of the SFEE apparatus. (A) Counter-current; (B) Co-current; 1, Pump; 2, Heat exchangers; 3, Valves; 4, Precipitation vessel; 5, Flash tank separator

A schematic representation of the different SFEE processes is presented in Figure 2. Briefly, the O/W emulsion and the antisolvent fluid are continuously injected

into the precipitation vessel, resulting in organic solvent extraction and particle precipitation due to contact between the supercritical fluid and the organic phase. The organic solvent diffuses into the water, followed by subsequent extraction of the solvent from the drop to achieve supersaturation and precipitation of the solute and surfactant [53].

The process can be co- or counter-current in that the antisolvent can be introduced in the top [49], [57] or the bottom [53],[58] of the precipitation vessel. The antisolvent is first injected into the precipitation vessel through a frit [54] or a nozzle[57] until the desired pressure, temperature, and flow rate are reached and maintained constant. According to Shekunov et al. [45], the use of a frit maximizes the mass-transfer efficiency during organic solvent extraction. The O/W emulsion is then injected at the desired flow rate through a capillary [58] or a nozzle [45], which breaks the emulsion into droplets to increase the surface area in contact with the antisolvent, until a selected amount is processed. The ratio between the antisolvent and emulsion flow rates, the temperature, and the pressure are maintained constant during the SFEE process. The effluent CO_2 and organic solvent exit from the top of the vessel into a flash tank separator to recycle both of the solvents. After the extraction process is complete, the antisolvent flow is maintained constant for a specific period of time to eliminate the remaining organic solvent from the suspension.

4.5.3. Elimination of Water

After SFEE processing, the final product is an aqueous micro- or nanosuspension. Water can subsequently be removed by conventional drying processes, such as spray drying, lyophilization, and microwaving. The high temperature used in most conventional dryers is unsuitable for drying suspensions of bioactive compounds because it accelerates the degradation process. This step can also promote destabilization of the nanoparticles dissolved in water, leading to an increase in the particle size. Santos et al.[51] and Mezzomo et al. [50] spray dried nanosuspensions to produce a dry powder, which increased the size of the particles due to the precipitation of the surfactant during the spray drying process. Most previous studies regarding SFEE did not remove the water, and there is a lack of research evaluating the influence of this step on particle destabilization.

4.6. The Effects of Various Parameters in the SFEE Process

4.6.1. Particle Size

The effects of various parameters in the SFEE process on precipitate particle size have been evaluated by several authors.

No significant changes in particle size have been observed by varying the operating parameters, such as pressure, temperature, processing time and solvent/antisolvent flow rates, in the SFEE process [46], [47], [53].

The literature shows that the primary parameters responsible for particle size control are the emulsion droplet size, solute/solution concentration and organic solvent content in the emulsion [45]. The literature confirms that the particle size is influenced more by the nature of the emulsions than by the mass transfer conditions [47], [53].

The literature reports that an increase in organic solvent and polymer concentration alters the particle size. Shekunov et al. [45] observed a reduction in particle size with a decrease in the organic solvent and solute concentrations. According to Chattopadhyay et al. [53] and [54], an increase in the organic solvent concentration in the emulsion can lead to the increased aggregation of the emulsion droplets, resulting in the precipitation of larger particles. Solute and polymer concentrations can be associated with specific functional groups in these compounds, which can change the interfacial tension of the emulsion droplets. The increase in particle size based on the solute concentration is likely due to an increase in the surface tension of the organic solution, resulting in emulsions with larger droplets.

In general, an increasing amount of surfactant leads to a decrease in particle size until a minimum value is reached. However, continuously increasing the amount of surfactant in water decreases the polydispersity index of the final product [57]. Kluge et al. [62] studied the effects of PLGA concentrations on the organic droplets at two different emulsion stirring rates and observed that increasing PLGA concentrations led to a higher viscosity of the dispersed organic phase, which favors the formation of larger droplets during emulsification. The authors also observed that the average particle size decreased with an increased emulsion stirring rate, whereas the particle size distributions generally became narrower [47], [53].

4.6.2. Stability of the Emulsion

The stability of the emulsion is related to the interfacial tension. If the interfacial tension increases as a result of a mass transfer of CO_2 to the drop, the emulsion becomes destabilized. Emulsion destabilization also occurs during the depressurization step due to the intense stirring caused by CO_2 release from the organic phase [46], [48].

Contact between the emulsion and CO_2 to achieve precipitation through the antisolvent effect must occur over a short period of time to minimize the possibility of emulsion destabilization prior to precipitation. However, the elimination of the remaining organic solvent may be slower because emulsion destabilization is no longer an issue after the particles have been produced [46].

Varona et al. [35] observed that the stability of the emulsion is drastically reduced when the pressure is increased. Although temperature has a minor effect, stability is related to the creaming effect. According to Chattopadhyay et al. [53], high temperatures and pressures can affect the stability of the emulsion by altering the surfactant-organic phase interactions. In general, a high

concentration of surfactant increases the stability of the emulsion [63].

4.6.3. Elimination of Solvent

The operating pressure and temperature conditions are selected to facilitate the maximum extraction of the organic phase of the emulsion with minimal loss of the solute and polymer due to dissolution in CO_2 and to avoid the loss of any emulsion that may wash out in the CO_2 stream [47],[53].

Mattea et al. [48] concluded that at pressures below the critical point pressure of CO_2-solvent mixtures, the swelling caused by CO_2 can be overcome by the diffusion of the solvent out of the drop due to the lower solubility of CO_2 in water. Thus, shrinking of the drop can be observed over time.

Chattopadhyay et al.[53] and Della Porta & Reverchon[47] observed an increased organic solvent extraction rate with an increased CO_2 flow. The efficiency of the solvent extraction increased with pressure, which was basically independent of the solution flow rate under the conditions investigated by Shekunov et al. [45].

4.6.4. Encapsulation Efficiency

The effectiveness of SFEE in encapsulation can be associated with several parameters, such as polymer type, solute concentration and emulsion formation[50]. Other factors that can influence the encapsulation efficiency include the nucleation rate of the compounds, the size of the formed particles, and the interactions between the carrier material and the solute[51]. Higher solute solubility in the antisolvent can result in a higher loss of the solute, which decreases the encapsulation efficiency due to dissolution in the antisolvent + organic solvent flow.

The CO_2 flow rate is directly related to the rate of solvent extraction from the emulsion droplet and solute/carrier material losses [47], which have a significant effect on the encapsulation efficiency [51]. Santos et al. [51] observed that a high emulsion flow rate resulted in high encapsulation efficiency, whereas an increased concentration of the surfactant/carrier material led to decreases in encapsulation efficiency. No significant changes were observed by varying the pressure.

4.7. Limitations to the SFEE Process

The most obvious drawback of SFEE is that the resulting suspension is an aqueous product instead of dry particles. Additional steps are required to produce a powdery product, which can lead to an increase in particle sizes due to agglomeration.

This technique has only been applied in the precipitation of solid solutes. Martín et al. [32] suggested the use of SFEE as a possible alternative for the production of compounds extracted from micelles loaded with essential oils, which can have a high viscosity.

Another limitation of this technique is that it is only suitable for the encapsulation of hydrophobic compounds. Kluge et al. [62] observed that solvent extraction from an emulsion, similar to the SFEE process, is not ideal for the encapsulation of hydrophilic compounds.

In the SFEE process, it is not possible to operate in a completely miscible zone. Due to the nature of the emulsion, there is additional resistance to the transport of CO_2 into the organic solvent droplet produced by the water from the emulsion. Different parameters, such as the droplet size when exiting the mixers and the design of the mixer, can affect the feasibility of the process [49].

Figure 3 represents a decision-making diagram for evaluating whether the SFEE process can be applied to encapsulate the solute of interest. This diagram must be considered based on certain conditions because temperature and pressure play an important role during the process. As shown in Table 1, the temperature and pressure for the SFEE process selected in most of the studies were 45°C and 8 MPa, respectively. These conditions were selected based on the solubility of the solute in the solvent and antisolvent. Consequently, the maximum extraction of the organic phase of the nanoemulsion with minimum solute and carrier material losses due to dissolution in CO_2 render the process viable [51].

It is important to note that when using a solute in solid form, the final product is a micelle system with powder inside at ambient temperature, but when using a solute with a viscous component that needs to be dissolved in an organic solvent to be pumped, the viscous compound is in the core of the micelle.

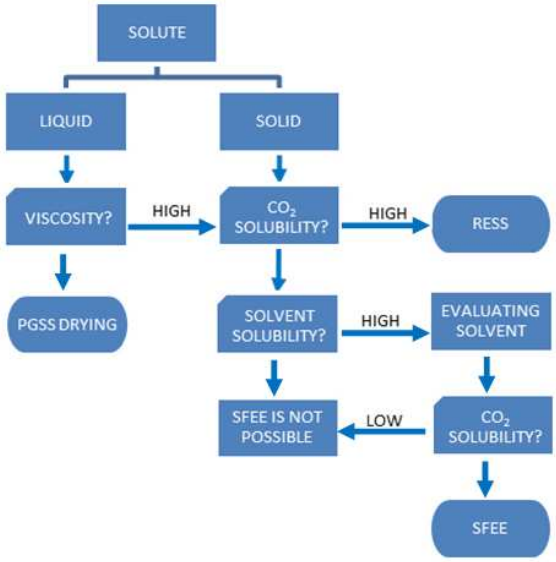

Figure 3. Diagram of a decision-making tree for the SFEE process

4.8. Applications

A variety of active pharmaceutical and food ingredients have been processed using the SFEE process. Reported applications of SFEE are presented in Table 1. Shekunov et al.[45] evaluated the SFEE method for the production of micro- and nanoparticles of cholesterol acetate, griseofulvin and megestrol acetate utilizing both batch and continuous processing for drug delivery applications. Chattopadhyay et

al.[53] successfully fabricated composite micro- and nanoparticles using a model system consisting of indomethacin, ketoprofen, and the biodegradable polymers poly(lactic/glycolic) acid and Eudragit RS to form composite particles ranging between 100 and 200 nm in size. SFEE has been used to produce nanoparticles of water-insoluble drugs combined with lipids for pulmonary delivery [54].

The compounds lysozyme (hydrophilic) and ketoprofen (hydrophobic) have been incorporated in poly-lactic-co-glycolic acid (PLGA) using the SFEE process [55],[62]. These authors investigated the phase equilibrium established between ketoprofen and PLGA to further underline the potential of SFEE to serve as a viable manufacturing technique and to highlight a novel application opportunity for this process [56]. In the SFEE processing of PLGA, variations in the PLGA concentration and stirring rates during the preparation of the emulsion have produced particles of pure PLGA with average sizes ranging between 100 nm and several µm with very narrow size distributions. PLGA has been used as a drug delivery system for magnetite nanocrystals stabilized by ricinoleic acid via SFEE[57].

Della Porta & Reverchon [47] evaluated the effectiveness of the supercritical extraction of CO_2 from the oil phase of oil-in-water emulsions to obtain spherical PLGA/piroxicam nanostructured microspheres. This process was described as occurring very rapidly due to the enhanced mass transfer of supercritical CO_2, resulting in the precipitation of microparticles with a narrower particle size distribution and preventing droplet coalescence or aggregation. Mayo et al.[58] demonstrated that the SFEE process allowed high actual loading of pDNA (19.7%, w/w), a high loading efficiency (>98%), and low residual solvents (<50 ppm) in preparing gene delivery nanoparticles.

Table 1. Reported Applications of SFEE

Core material	Surfactant/Polymer	Solvent	Operating parameters	Results and observations	References
Cholesterol acetate (CA)	Polyvinyl alcohol (PVA)	Ethyl acetate	Pressure: 8 MPa Temperature: 35 °C CO_2 flow: 12 kg·h^{-1} Emulsion flow: 1.200 ml·h^{-1}	Particle size: 100-1000 nm Emulsion size: 200-1000 nm Residual solvent (MA): <20 ppm Morphology (GF and MA): crystalline	[45]
Megestrol acetate (MA)	Tween 80	Toluene			
Griseofulvin (GF)	Lecithin	Dichloromethane			
	Polyvinyl pyrrolidone (PVP)	Dichloromethane; Ethyl acetate			
	PVA	Ethyl acetate			
Indomethacin (IN) Ketoprofen (KP)	PVA/PLGA; PVA/Eudragit RS	Ethyl acetate	Pressure: 8 MPa Temperature: 45 °C CO_2 flow: 12 kg·h^{-1} Emulsion flow: 1.200 ml·h^{-1}	Particle size: 0.1-2 µm Residual solvent: <50 ppm	[53]
Solid lipid formulations	Soy lecithin	Chloroform	Pressure: 8 MPa Temperature: 35 °C CO_2 flow: 2.4 kg·h^{-1} Emulsion flow: 120 ml·h^{-1}	Particle size: < 50 nm Residual solvent: <20 ppm	[54]
Lysozyme	PVA/PLGA	Ethyl acetate	Pressure: 8 MPa Temperature: 45 °C CO_2 flow: 4.8 kg·h^{-1} Emulsion flow: 120 ml·h^{-1}	Particle size: 100 nm-several µm with very narrow size distributions Encapsulation efficiency: >48.5%	[62]
Ketoprofen	PVA/PLGA	Ethyl acetate	Pressure: 8 MPa Temperature: 45 °C CO_2 flow: 4.8 kg·h^{-1}	Particle size: 100-200 nm	[55]

			Emulsion flow: 120 ml·h^{-1}		
Ketoprofen	PVA/PLGA	Ethyl acetate	Pressure: 8 MPa Temperature: 45 °C CO_2 flow: 4.8 kg·h^{-1} Emulsion flow: 120 ml·h^{-1}	Morphology: Spherical amorphous nanoparticles	[56]
Ricinoleic acid-stabilized magnetic nanocrystals	PVA/PLGA	Dichloromethane	Not available	Morphology: Janus type, with the magnetite accumulated on one hemisphere of the particle	[57]
Plasmid DNA (pDNA)	PVA/PLGA	Ethyl acetate	Pressure: 8 MPa Temperature: 45 °C CO_2 flow: ~240 ml·h^{-1} Emulsion flow: 24 ml·h^{-1}	Loading of pDNA: 19.7%, w/w Loading efficiency: >98% Residual solvent: <50 ppm	[58]
Piroxicam	PVA/PLGA	Ethyl acetate	Pressure: 8.5-15 MPa Temperature: 38 °C CO_2 flow: 0.1-0.5 kg·.h^{-1}	Particle size: 1-3 μm Residual solvent: <40 ppm Encapsulation efficiency: 90-95%	[47]
β-carotene	OSA-modified starch	Dichloromethane	Pressure: 8-13 MPa Temperature: 35-50 °C CO_2 flow: 2-4 kg·h^{-1} Emulsion flow: 0.3-1 kg·h^{-1}	Particle size: 400 nm in suspension in an aqueous medium	[46]
	Tween 20 + Span 20				
β-carotene	OSA-modified starch	Dichloromethane	Pressure: 5 and 10 MPa Temperature: 35 °C	Drop undergoes swelling and shrinking processes due to the diffusion of CO_2 into the drop and dichloromethane out of the drop	[48]
β-carotene	OSA-modified starch	Dichloromethane	Pressure: 9-13 MPa Temperature: 50 °C CO_2 flow: 3 kg·h^{-1} Emulsion flow: 150-330 ml·h^{-1}	Particle size: 344 – 366 nm Residual solvent: <10 ppm Encapsulation efficiency: 34-89%	[51]
Lycopene					
Shrimp residue extract enriched in astaxanthin	Hi-Cap 100 (modified starch)	Dichloromethane	Pressure: 10 MPa Temperature: 40 °C CO_2 flow: 4 kg·h^{-1} Emulsion flow: 240 ml·h^{-1}	Particle size: 0.7±0.1 μm Encapsulation efficiency: 93.1%	[50]

In the food industry, SFEE technology was used to form particles from carotenoids, which are an important class of bioactive compounds, to improve the stability and dissolution rates in water and to facilitate the dosing and handling of the product. Mattea et al. [49] published a review of the developments in carotenoid particle formation and co-precipitation with biodegradable polymers using supercritical fluids as an antisolvent, including the use of GAS, SAS, and SFEE. The same authors presented the feasibility of using antisolvent techniques to precipitate β-carotene from dichloromethane in a water emulsion, resulting in a suspension of sub-micron and nanoparticles

with final organic solvent concentrations as low as 1 ppm [46]. Santos et al. [51] recently produced sub-micrometer particles of β-carotene and lycopene in an aqueous medium using SFEE.

Mezzomo et al. [50] were the first researchers to apply SFEE in the co-precipitation of a complex mixture of bioactive compounds using a modified starch. The authors studied the encapsulation of extracts enriched in astaxanthins, the most representative carotenoid from crustaceans like shrimp, to obtain nanoemulsions with a high encapsulation efficiency and low particle size.

5.Conclusions and Perspectives

From a scientific point of view, particle design using the SFEE process is an attractive option due to the possibility of obtaining solvent-free particles with a narrow size distribution curve in addition to avoiding the degradation of thermosensitive compounds. The concept of using SFEE in an industrial context is currently under development. The primary factor limiting this process is that the final product is a suspension of the desired compound in water. The pharmaceutical industry represents a major focus for particles produced using SFEE technology.

Although SFEE has not been widely used for food applications, recent studies applied the technique to the formation of particles from carotenoids, which are an important class of bioactive compounds. Additional bioactive compounds and core materials must be explored in the near future. The results of these researches will have a positive impact in public health: (1) if the target compounds are drugs then, due to increased efficacy smaller amounts of drugs will be needed to treat illness or (2) if bioactive compounds are the target substances then we can expect that new foods can be formulated incorporating these particles.

ACKNOWLEDGEMENTS

Maria Thereza M. S. Gomes would like to thank the CNPq (process 140641/2011-4) for a doctoral fellowship. Diego T. Santos would like to thank the FAPESP (process 10/16485-5) for a postdoctoral fellowship. The authors acknowledge financial support from CNPq and FAPESP.

REFERENCES

[1] Bernard F. Gibbs, Selim Kermasha, Inteaz Alli, Catherine N. Mulligan, Encapsulation in the food industry: a review, Taylor & Francis Group, International Journal of Food Sciences and Nutrition, vol. 50, no.3, pp. 213–224, 1999.

[2] Diego T. Santos, M. Angela A. Meireles, Carotenoid pigments encapsulation: fundamentals, techniques and recent trends, Bentham Open, The Open Chemical Engineering Journal, vol.4, pp.42–50, 2010.

[3] Ireneo Kikic, Michele Lora, A thermodynamic analysis of three-phase equilibria in binary and ternary systems for applications in rapid expansion of a supercritical solution (RESS), particles from gas-saturated solutions (PGSS), and supercritical antisolvent (SAS), American Chemical Society, Industrial & Engineering Chemistry Research, vol.36, no.12, pp.5507–5515, 1997.

[4] Camila G. Pereira, M. Angela A. Meireles, Supercritical fluid extraction of bioactive compounds: fundamentals, applications and economic perspectives. Springer Science, Food and Bioprocess Technology, vol. 3, no.3, pp.340–372, 2010.

[5] Kashappa G. H. Desai, Hyun J. Park, Recent developments in microencapsulation of food ingredients, Taylor & Francis Group, Drying Technology, vol.23, no.7, pp.1361–1394, 2005.

[6] Claude P. Champagne, Patrick Fustier, Microencapsulation for the improved delivery of bioactive compounds into foods, Science Direct, Current Opinion in Biotechnology, vol.18, no.2, pp.184–190, 2007.

[7] Seid M. Jafari, Elham Assadpoor, Yinghe He, Bhesh Bhandari, Encapsulation efficiency of food flavours and oils during spray drying, Taylor & Francis Group Drying Technology, vol. 26, no.7, pp.816–835, 2008.

[8] Peter M. M. Schrooyen, Roelof van der Meer, Cornelis G. De Kruif, Microencapsulation: its application in nutrition, Proceedings of the Nutrition Society, vol.60, no.4, pp.475–479, 2001.

[9] San S. Kuang, Jorge C. Oliveira, Abina M. Crean, Microencapsulation as a tool for incorporating bioactive ingredients into food, Taylor and Francis Group, Critical Reviews in Food Science and Nutrition, vol.50, no.10, pp.951–968, 2010.

[10] María J. Cocero, Ángel Martín, Facundo Mattea, Salima Varona, Encapsulation and co-precipitation processes with supercritical fluids: fundamentals and applications, Elsevier, The Journal of Supercritical Fluids, vol.47, no.3, pp.546–555, 2009.

[11] Masoud Bahrami, Sima Ranjbarian, Production of micro- and nano-composite particles by supercritical carbon dioxide, Elsevier, The Journal of Supercritical Fluids, vol.40, no.2, pp.263–283, 2007.

[12] Fereidoon Shahidi, Xiao-Q. Han, Encapsulation of food ingredients, Taylor & Francis Group, Critical Reviews in Food Science and Nutrition, vol.33, no.6, pp.501–547, 1993.

[13] Suresh Neethirajan, Digvir S. Jayas, Nanotechnology for the food and bioprocessing industries, Springer Science, Food and Bioprocess Technology, vol.4, no.1, pp.39–47, 2011.

[14] Amparo L. Rubio, Rafael Gavara, Jose M. Lagaron, Bioactive packaging: turning foods into healthier foods through biomaterials, Elsevier, Trends in Food Science & Technology, vol.17, no.10, pp.567–575, 2006.

[15] Job Ubbink, Jessica Krüger, Physical approaches for the delivery of active ingredients in foods, Elsevier, Trends in Food Science & Technology, vol.17, no.5, pp.244–254, 2006.

[16] Mary A. Augustin, Yacine Hemar, Nano- and

micro-structured assemblies for encapsulation of food ingredients, The Royal Society of Chemistry, Chemical Society Reviews, vol.38, no.4, pp.902–912, 2009.

[17] Atmane Madene, Muriel Jacquot, Joël Scher, Stéphane Desobry, Flavour encapsulation and controlled release – a review, Institute of Food Science and Technology Trust Fund, International Journal of Food Science and Technology, vol.41, no.1, pp.1–21, 2006.

[18] Daniel J. Jarmer, Corinne S. Lengsfeld, Theodore W. Randolph, Manipulation of particle size distribution of poly(L-lactic acid) nanoparticles with a jet-swirl nozzle during precipitation with a compressed antisolvent, Elsevier, The Journal of Supercritical Fluids, vol.27, no.3, pp.317–336, 2003.

[19] Jennifer Jung, Michel Perrut, Particle design using supercritical fluids: Literature and patent survey, Elsevier, The Journal of Supercritical Fluids, vol.20, no.3, pp.179–219, 2001.

[20] Yukiya Hakuta, Hiromichi Hayashi, Kunio Arai, Fine particle formation using supercritical fluids, Elsevier, Current Opinion in Solid State and Materials Science, vol.7, no.4-5, pp.341–351, 2003.

[21] Zeljko Knez, Eckhard Weidner, Particles formation and particle design using supercritical fluids, Elsevier, Current Opinion in Solid State and Materials Science, vol.7, no.4-5, pp.353–361, 2003.

[22] Alireza Shariati, Cor J. Peters, Recent developments in particle design using supercritical fluids, Elsevier, Current Opinion in Solid State and Materials Science, vol.7, no.4-5, pp.371–383, 2003.

[23] Sang -D. Yeo, Erdogan Kiran, Formation of polymer particles with supercritical fluids: a review, Elsevier, The Journal of Supercritical Fluids, vol.34, no.3, pp.287–308, 2005.

[24] Ángel Martín, María J. Cocero, Micronization processes with supercritical fluids: fundamentals and mechanisms, Elsevier, Advanced Drug Delivery Reviews, vol.60, no.3, pp.339–350, 2008.

[25] Jacques Fages, Hubert Lochard, Jean -J. Letourneau, Martial Sauceau, Elisabeth Rodier, Particle generation for pharmaceutical applications using supercritical fluid technology, Elsevier, Powder Technology, vol.141, no.3, pp.219– 226, 2004.

[26] Jean W. Tom, Pablo G. Debenedetti, Particle formation with supercritical fluids – a review, Elsevier, Journal of Aerosol Science, vol.22, no.5, pp.555–584, 1991.

[27] Pablo G. Debenedetti, Jean W. Tom, Xianmin Kwauk, Sang -D. Yeo, Rapid expansion of supercritical solutions (RESS): fundamentals and applications, Elsevier, Fluid Phase Equilibria, vol.82, pp.311–321, 1993.

[28] Michael Türk, Ralph Lietzow, Formation and stabilization of submicron particles via rapid expansion processes, Elsevier, The Journal of Supercritical Fluids, vol.45, no.3, pp.346–355, 2008.

[29] Michael Türk, Dennis Bolten, Formation of submicron poorly water-soluble drugs by rapid expansion of supercritical solution (RESS): results for Naproxen, Elsevier, The Journal of Supercritical Fluids, vol.55, no.2, pp.778–785, 2010.

[30] Ali Z. Hezave, Feridun Esmaeilzadeh, Micronization of drug particles via RESS process, Elsevier, The Journal of Supercritical Fluids, vol.52, no.1, pp.84–98, 2010.

[31] Michael Türk, Peter Hils, Britta Helfgen, Karlheinz Schaber, Hans -J. Martin, Martin A. Wahl, Micronization of pharmaceutical substances by the rapid expansion of supercritical solutions (RESS): a promising method to improve bioavailability of poorly soluble pharmaceutical agents, Elsevier, The Journal of Supercritical Fluids, vol.22, no.1, pp.75–84, 2002.

[32] Ángel Martín, Huu M. Pham, Andreas Kilzer, Sabine Kareth, Eckhard Weidner, Micronization of polyethylene glycol by PGSS (particles from gas saturated solutions)-drying of aqueous solutions, Elsevier, Chemical Engineering and Processing, vol.49, no.12, pp.1259–1266, 2010.

[33] Kullaiah Byrappa, Satoshi Ohara, Tadafumi Adschiri, Nanoparticles synthesis using supercritical fluid technology – towards biomedical applications, Elsevier, Advanced Drug Delivery Reviews, vol.60, no.3, pp.299–327, 2008.

[34] Eckhard Weidner, High pressure micronization for food applications, Elsevier, The Journal of Supercritical Fluids, vol.47, no.3, pp.556–565, 2009.

[35] Salima Varona, Sabine Kareth, Ángel Martín, María J. Cocero, Formulation of lavandin essential oil with biopolymers by PGSS for application asbiocide in ecological agriculture, Elsevier, The Journal of Supercritical Fluids, vol.54, no.3, pp.369–377, 2010.

[36] Ernesto Reverchon, Supercritical antisolvent precipitation of micro- and nano-particles, Elsevier, The Journal of Supercritical Fluids, vol.15, no.1, pp.1–21, 1999.

[37] Renata Adami, Libero S. Osséo, Rainer Huopalahti, Ernesto Reverchon, Supercritical AntiSolvent micronization of PVA by semi-continuous and batch processing, Elsevier The Journal of Supercritical Fluids, vol.42, no.2, pp.288–298, 2007.

[38] Chang -K. Kim, Byung -C. Lee, Youn -W. Lee, Hyoun S. Kim, Solvent effect on particle morphology in recrystallization of HMX (cyclotetramethylenetetranitramine) using supercritical carbon dioxide as antisolvent, Springer Science, Korean Journal of Chemical Engineering, vol.26, no.4, pp.1125–1129, 2009.

[39] Ernesto Reverchon, Giovanna D. Porta, Igor M. Rosa, Pascale Subra, Didier Letourneur, Supercritical antisolvent micronization of some biopolymers, Elsevier, The Journal of Supercritical Fluids, vol.18, no.3, pp.239–245, 2000.

[40] Lei Yang, Jin -M. Huang, Yuan -G. Zu, Chun -H. Ma, Han Wang, Xiao -W. Sun, Zhen Sun, Preparation and radical scavenging activities of polymeric procyanidins nanoparticles by a supercritical antisolvent (SAS) process, Elsevier, Food Chemistry, vol.128, no4, pp.1152–1159, 2011.

[41] Ruggero Bettini, R. Menabeni, Roberto Tozzi, Marco B. Pranzo, Irene Pasquali, Michele R. Chierotti, Roberto Gobetto, Luca Pellegrino, Didanosine polymorphism in a supercritical antisolvent process, Wiley Periodicals, Journal of Pharmaceutical Sciences, vol.99, no.4, pp.1855–1870, 2010.

[42] Ron T. Y. Lima, Wai K. Nga, Reginald B. H. Tan, Amorphization of pharmaceutical compound by co-precipitation using supercritical anti-solvent (SAS)

process (Part I), Elsevier, The Journal of Supercritical Fluids, vol.53, no.1-3, pp.179–184, 2010.

[43] Ángel Martín, Facundo Mattea, Laura Gutiérrez, Félix Miguel, María J. Cocero, Co-precipitation of carotenoids and biopolymers with the supercritical anti-solvent process, Elsevier, The Journal of Supercritical Fluids, vol.41, pp.138–147, 2007.

[44] Pratibhash Chattopadhyay, Boris Y. Shekunov, Jeff S. Seitzinger, Robert W. Huff, Particles from supercritical fluid extraction of emulsion, US Patent N° 0026319 A1, 2004.

[45] Boris Y. Shekunov, Pratibhash Chattopadhyay, Jeff Seitzinger, Robert Huff, Springer Science, Nanoparticles of poorly water-soluble drugs prepared by supercritical fluid extraction of emulsions. Pharmaceutical Research, vol.23, no.1, pp.196–204, 2006.

[46] Facundo Mattea, Ángel Martín, Arán M. -Gago, María J. Cocero, Supercritical antisolvent precipitation from an emulsion: β-Carotene nanoparticle formation, Elsevier, The Journal of Supercritical Fluids, vol.51, no.2, pp.238–247, 2009.

[47] Giovanna D. Porta, Ernesto Reverchon, Nanostructured microspheres produced by supercritical fluid extraction of emulsions, Wiley Periodicals, Biotechnology and Bioengineering, vol.100, no.5, pp.1020–1033, 2008.

[48] Facundo Mattea, Ángel Martín, Constantin Schulz, Philip Jaeger, Rudolf Eggers, María J. Cocero, Behavior of an organic solvent drop during the supercritical extraction of emulsions, American Institute of Chemical Engineers, AIChE Journal, vol.56, no.5, pp.1184–1195, 2010.

[49] Facundo Mattea, Ángel Martín, María J. Cocero, Carotenoid processing with supercritical fluids, Elsevier, Journal of Food Engineering, vol.93, no.3, pp.255–265, 2009.

[50] Natália Mezzomo, Esther de Paz, Marcelo Maraschin, Ángel Martín, María J. Cocero, Sandra R.S. Ferreira, Supercritical anti-solvent precipitation of carotenoid fraction from pink shrimp residue: effect of operational conditions on encapsulation efficiency, Elsevier, The Journal of Supercritical Fluids, vol.66, pp.342–349, 2012.

[51] Diego T. Santos, Ángel Martín, M. Angela A. Meireles, María J. Cocero, Production of stabilized sub-micrometric particles of carotenoids using supercritical fluid extraction of emulsions, Elsevier, The Journal of Supercritical Fluids, vol.61, pp.167–174, 2012.

[52] Hélder D. Silva, Miguel Â. Cerqueira, António A. Vicente, Nanoemulsions for food applications: development and characterization nanotechnology for the food and bioprocessing industries, Springer Science, Food and Bioprocess Technology, vol.5, pp.854–867, 2012.

[53] Pratibhash Chattopadhyay, Robert Huff, Boris Y. Shekunov, Drug encapsulation using supercritical fluid extraction of emulsions, Wiley Periodicals, Journal of Pharmaceutical Sciences, vol.95, no.3, pp.667–679, 2006.

[54] Pratibhash Chattopadhyay, Boris Y. Shekunov, Dong -S. Yim, David Cipolla, Brooks Boyd, Stephen Farr, Production of solid lipid nanoparticle suspensions using supercritical fluid extraction of emulsions (SFEE) for pulmonary delivery using the AERx system, Elsevier, Advanced Drug Delivery Reviews, vol.59, no.6, pp.444–453, 2007.

[55] Johannes Kluge, Francesco Fusaro, Marco Mazzotti, Gerhard Muhrer, Production of PLGA micro- and nanocomposites by supercritical fluid extraction of emulsions: II. Encapsulation of Ketoprofen, Elsevier, The Journal of Supercritical Fluids, vol.50, no.3, pp.336–343, 2009.

[56] Johannes Kluge, Marco Mazzotti, Gerhard Muhrer, Solubility of Ketoprofen in colloidal PLGA, Elsevier, International Journal of Pharmaceutics, vol.399, no.1-2, pp.163–172, 2010.

[57] Marco Furlan, Johannes Kluge, Marco Mazzotti, Marco Lattuada, Preparation of biocompatible magnetite–PLGA composite nanoparticles using supercritical fluid extraction of emulsions, Elsevier, The Journal of Supercritical Fluids, vol.54, no.3, pp.348–356, 2010.

[58] Aaron S. Mayo, Balamurali K. Ambati, Uday B. Kompella, Gene delivery nanoparticles fabricated by supercritical fluid extraction of emulsions, Elsevier, International Journal of Pharmaceutics, vol.387, no.1-2, pp.278–285, 2010.

[59] Seid M. Jafari, Yinghe He, Bhesh Bhandari, Nano-emulsion production by sonification and microfluidization – a comparison, Taylor & Francis Group, International Journal of Food Properties, vol.9, no.3, pp.475–485, 2006.

[60] Tharwat Tadros, Paqui Izquierdo, Jordi Esquena, Conxita Solans, Formation and stability of nano-emulsions, Elsevier, Advances in Colloid and Interface Science, vol.108-109, pp.303–318, 2004.

[61] B. Abismaïl, Jean P. Canselier, Anne M. Wilhelm, Henri Delmas, Christophe Gourdon, Emulsification by ultrasound: drop size distribution and stability, Elsevier, Ultrasonics Sonochemistry, vol.6, no.1-2, pp.75–83, 1999.

[62] Johannes Kluge, Francesco Fusaro, Nathalie Casas, Marco Mazzotti, Gerhard Muhrer, Production of PLGA micro- and nanocomposites by supercritical fluid extraction of emulsions: I. Encapsulation of lysozyme, Elsevier, The Journal of Supercritical Fluids, vol.50, no.3, pp.327–335, 2009.

[63] Esther de Paz, Ángel Martín, Antonio Estrella, Soraya R. -Rojo, Ana A. Matias, Catarina M. M. Duarte, María J. Cocero, Formulation of β-carotene by precipitation from pressurized ethyl acetate-on-water emulsions for application as natural colorant, Elsevier, Food Hydrocolloids, vol.26, no.1, pp.17–27, 2012.

CAPÍTULO 3 - MICRONIZATION AND ENCAPSULATION: APPLICATION OF SUPERCRITICAL FLUIDS IN WATER REMOVAL

M. Thereza M. S. Gomes, Diego T. Santos and M. Angela A. Meireles

Capítulo de livro publicado no livro *"Conventional and advanced food processing technologies", Editor: Suvendu Bhattacharya, Wiley-Blackwell, UK, 2014.*

ISBN: 9781118406281 DOI: 10.1002/9781118406281

AVISO DE DIREITO DE AUTOR

11

Micronization and Encapsulation: Application of Supercritical Fluids in Water Removal

M. Thereza M. S. Gomes, Diego T. Santos and M. Angela A. Meireles

LASEFI/DEA/FEA (School of Food Engineering)/UNICAMP (University of Campinas), Campinas, Brazil

11.1 Introduction

Encapsulation is defined as the process of forming a thin shell over a solid, liquid or gaseous material, which is completely contained within the capsule wall, and micronization is defined as the process of reducing the particle size and obtaining micro- or even nano-sized particles (Cocero *et al.*, 2009).

Production of ultrafine (micro- or nano-sized) particles with desired properties and precise control of particle size and morphology is one of the objectives of many industries. Conventional processes for particle formation suffer from limitations in producing a desirable final product. The use of supercritical fluids for particle sizing and design represents an attractive alternative to create micro- and nano-sized particles with controlled particle size and narrow particle size distribution. Furthermore, these processes offer a wide control of particle morphology, obtain solvent-free products and avoid thermal degradations due to the low level of the operating temperatures (since in most cases carbon dioxide is the supercritical fluid) (Cocero *et al.*, 2009; Gomes *et al.*, 2012).

Conventional and Advanced Food Processing Technologies, First Edition.
Edited by Suvendu Bhattacharya.

Many different processes for particle formation using supercritical fluids have been proposed; in each one, the supercritical fluids perform different functions, such as solvent (rapid expansion of supercritical solutions (RESS)), antisolvent (supercritical antisolvent (SAS) precipitation), co-solvent or solute (particles from gas-saturated solutions (PGSS)) and propellant (carbon dioxide-assisted nebulization with a bubble dryer (CAN-BD)) (Martín *et al.*, 2010a). Due to the different process arrangements and apparatuses used in these particle formation processes, different acronyms are also used by the various authors to promote the uniqueness of the process, despite not being very different one from the other.

In particular, the methods referred to as CAN-BD and PGSS drying allow the production of ultrafine particles of water-soluble compounds. These processes micronize or encapsulate the desired compound or compounds by removing the water. The main target of them is to obtain stabilized dry powders. These technologies are promising when applied to proteins or other biomolecules that may be denatured by conventional drying processes like spray drying. Different from freeze drying, it is also possible to control the particle size and particle size distribution using these processes (Perrut, 2004). Furthermore, the time required for drying by freeze drying is much longer (hours rather than seconds) and there is no need for additional milling or micronization steps (Sievers *et al.*, 2001). Spray drying and freeze drying are two of the most successful conventional methods used to produce particles by removing water. Table 11.1 shows the main limitations of both techniques.

Table 11.1 Limitations of spray drying and freeze drying methods

Conventional method	Principle of operation	Limitation	Reference
Spray drying	Atomization with a nozzle or spinning wheel of a mixture (core and carrier materials) into a hot-air desiccant into a chamber	Problems with efficient particle collection and the potential instability of materials sensitive to high temperatures	Prinn, Costantino and Tracy (2002); Martín *et al.* (2010a); Santos and Meireles (2010)
Freeze drying	Water is removed from the frozen state by vacuum sublimation, maintaining the drying chamber pressure and temperature below the triple point of water	Long processing time, expensive process costs and difficult to control the particle size	Perrut (2004); Martín *et al.* (2010a); Santos and Meireles (2010)

The present chapter describes the basic aspects of CAN-BD and PGSS drying processes for the production of ultrafine particles. For each technique, the history, the process description and the influence of process variables have been discussed. Recent developments focused on processing of food ingredients using these methods are also presented.

11.2 Supercritical fluid

A supercritical fluid is defined as a fluid whose pressure and temperature are simultaneously higher than those at the critical point (Figure 11.1). Its solvency power is enhanced due to its higher density, which is very similar to those of liquids (100–900 kg/m^3 at 7.5–50 MPa). Furthermore, these fluids have the main characteristics of gases such as low viscosity, large diffusivity and small surface tension, which are favourable attributes for several processes (Skala and Orlovic, 2006). Carbon dioxide is a fluid widely applied to produce fine particles using supercritical fluid methods. The main advantages of CO_2 are its nontoxicity, nonflammability, its relatively low critical temperature (T_C = 304.2 K) and pressure (P_C = 7.38 MPa), it is inexpensive and recyclable. In addition, it can be completely separated from the final product by expansion and then liquefied for recycling purpose.

11.3 Developmental stages

Carbon dioxide-assisted nebulization with a bubble dryer (CAN-BD) was developed based on the same concept of the PGSS technique and patented

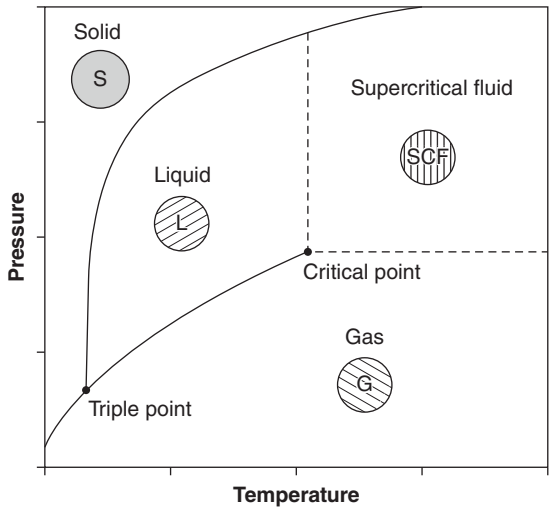

Figure 11.1 Pressure–temperature phase diagram of a single substance

by Sievers and co-author in 1997 (Sievers and Karst, 1997). These authors proposed a modification to the PGSS process that allowed expanding the process application for the use of any compound that is water soluble (Nunes and Duarte, 2011). In the PGSS concept, a gas-saturated solution is expanded through a nozzle to an atmospheric pressure. During the expansion, the gas dissolved into the solution is suddenly vaporized and the intense cooling due to the Joule–Thomson effect during CO_2 expansion promotes particle formation (Martín and Weidner, 2010). In the CAN-BD process, an aqueous solution mixed with CO_2 is expanded to atmospheric pressure through a flow restrictor to generate aerosols of microbubbles and microdroplets. This process is available commercially (Sievers, Best and Cape, 2008). Since the first patent in 1997, several modifications were proposed in order to make the CAN-BD process more versatile; these variants are referred to as supercritical-assisted atomization (SAA) and supercritical enhanced atomization (SEA), proposed by Padrela *et al.* (2010) and Reverchon (2002), respectively.

Another modification of the PGSS process is PGSS drying. The main difference between the two techniques is that in PGSS drying, the coating material is fed to the static mixer in an aqueous solution (Martín *et al.*, 2010a). This process was patented by Weidner and co-workers in 2000 (Weidner *et al.*, 2000). In this technique, the particles do not need to be dried with the help of N_2 inert flux as in CAN-BD. Although the published papers mostly focus on drugs and polymers, some authors demonstrated that this technique is also feasible for food applications (Weidner, 2009). This process exists at the pilot and industrial scale, providing a basis for the demonstration of its technical and economic feasibility for some industrial applications (Nunes and Duarte, 2011; Weidner 2009).

11.4 Process description and influence of process parameters

11.4.1 CAN-BD

Process description The CAN-BD process consists of mixing a stream of compressed CO_2 with an aqueous solution or dispersion containing the solute of interest during a short time in a 'low-dead-volume' tee (< 1 μL). A quantity of CO_2 is solubilized in water and an emulsion is formed. Carbon dioxide is a suitable compressible fluid because it has a good solubility in water (1.6 mole % at 336 K and 10 MPa) and its use enhances the expansion process. The emulsion so formed is rapidly decompressed to atmospheric pressure through a flow restrictor (or a capillary tube) by expansion into a drying chamber that generates an aerosol of very fine droplets of liquid-carrying microbubbles of gas (Sievers *et al.*, 1999). This plume of microbubbles and

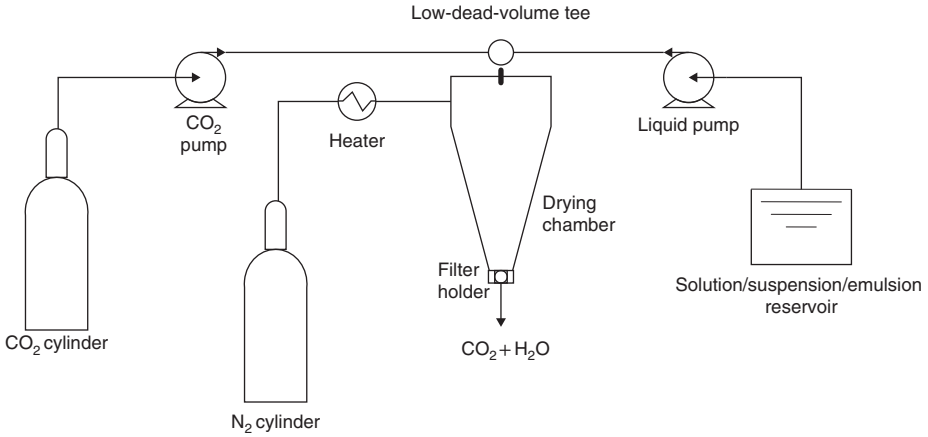

Figure 11.2 Schematic diagram of the carbon dioxide-assisted nebulization with a bubble dryer (CAN-BD) process

microdroplets is further dried by contact with a stream of inert N_2 warmed at temperatures between 298 and 348 K, much lower than those currently used in spray drying (Perrut, 2004). CAN-BD has been used with aqueous and organic solvents. Figure 11.2 represents a schematic diagram of the CAN-BD process.

There are two versions of this process, static and dynamic. The static version involves the pre-mixing of the supercritical CO_2 and the aqueous solution, and after the equilibrium is approached, the mixture in a high pressure chamber is allowed to expand to atmospheric pressure. The dynamic version involves continuous intimate mixing of the aqueous solution and the supercritical CO_2 (Cape *et al.*, 2008).

The CAN-BD process provides a more efficient atomization because, after the primary atomization, the release of CO_2 produces a secondary atomization, producing smaller droplets. This technique does not differ much from the classical aerosol method. Due to the very short contact time between the compressible CO_2 and the aqueous solution, the CO_2 is far from dissolving to saturation in the aqueous solution, unlike the PGSS and PGSS drying. It is noteworthy that owing to the depressurization of the CO_2, a sharp temperature decrease takes place (the Joule–Thomson effect) both in the tee and in the restrictor, which also must be heated to avoid plugging. The temperature required can damage some thermolabile compounds, which can be solved by applying a vacuum in the drying chamber (Tabernero, Valle and Galán, 2012; Charbit, Badens and Boutin, 2004).

Influence of process parameters The CAN-BD process has been developed mainly for industrial purposes. Therefore, there are not many published papers that investigated the influence of the operational parameters on particle characteristics. In a first study, Sievers *et al.* (1999) produced fine

particles of pharmaceuticals and other materials by aerosolization in a low-volume mixing device. The authors observed that the desired fine aerosols are obtained when a 'low-dead-volume' tee (< 1 μL) was used, but under the same conditions, using a normal 1/16 in (0.159 cm) tee with a volume of about 50 μL, no aerosol was obtained. Furthermore, a water stream rather than an aerosol resulted when the CO_2 tee inlet pressure was set at 5.5 MPa instead of at 10.3 MPa.

Sievers *et al.* (1999) also noted that the size distribution of the particles suspended in the formed aerosol depended on the concentration of the precursors in the aqueous solution. Increasing the concentration of the precursors a narrower size range was obtained. The results of process parametric studies for ethanolic solutions containing beta-methasone as well as aqueous solutions containing mannitol or myo-inositol indicated that the ratio of CO_2 to the solution mass flow rate has a significant influence on the particle size. By manipulating this ratio, the particle size of fine powders generated by the CAN-BD process can be controlled from nanometre size to micrometre size (Huang *et al.*, 2003).

According to Sievers *et al.* (2000), spherical morphology might be expected for particles formed by drying microbubbles or droplets. Liquid droplets synthesized by aerosol methods maintain a spherical shape to minimize surface energy. However, these authors observed that differences in drying conditions can lead to different morphologies of particles of the same drug. Lifeboat-shaped particles of cromolyn sodium were obtained when the aerosol plume was bubble-dried using the dynamic method by mixing with dry nitrogen at temperatures between 348 and 368 K. Nonetheless, when cromolyn sodium was dried at or near room temperature by passing the aerosol plume over the concentrated sulfuric acid, more nearly spherical particles were observed. The concentrated sulfuric acid was alternatively used as a desiccant to dry the aerosol plume diluted with nitrogen before collection on a filter.

Applications The CAN-BD process has been applied to obtain powders from water solutions of pharmaceuticals (Sievers *et al.*, 2007), proteins (Cape *et al.*, 2008) and other water-soluble compounds. Table 11.2 summarizes the various substances that have been processed into particles using the CAN-BD technique.

Despite the potential of CAN-BD to dry water-soluble compounds for food applications, data for this process are scarcely available in the literature. Dried powders of extracts from natural sources using the CAN-BD technique have been obtained (Andersson *et al.*, 2012; Herrero *et al.*, 2010) and the process was patented in 2009 as an on-line process in one step combining the pressurized hot water extraction (PHWE) and the drying of the extract by the CAN-BD process, named as water extraction and particle formation on-line (WEPO) (Figure 11.3) (Ibáñez *et al.*, 2009). This promising process

Table 11.2 Summary of particles produced via carbon dioxide-assisted nebulization with a bubble dryer (CAN-BD) process

Substance	Solvent/nebulization fluid	Operational conditions	Results	References
Enzyme α1-antitrypsin	Water/CO_2	Mixing tee pressure: 8.27 MPa Mixing tee temperature: room temperature Solution flow rate: 0.3–0.5 mL/min N_2 drying gas flow rate: 15–30 L/min Drying temperature: 313 K	Particle formation type: micronization Morphology: spherical Moisture content: 1.8% Particle size: 1.9 — 2.2 μm	Cape *et al.* (2008)
Trypsinogen (protein)	Water/CO_2	Mixing tee pressure: 8.27 MPa Mixing tee temperature: room temperature Solution flow rate: 0.3–0.5 mL/min N_2 drying gas flow rate: 15–30 L/min	Particle formation type: micronization Morphology: dimpled raisin-like Particle size: 0.86–1.4 μm	Cape *et al.* (2008)
NaCl	Water/CO_2	Mixing tee pressure: 8 MPa Mixing tee temperature: room temperature Solution flow rate: 0.3 mL/min Nebulizing fluid flow rate: 1–3 mL/min N_2 drying gas flow rate: 15 L/min Drying temperature: 333–353 K	Particle formation type: micronization Morphology: hollow clusters Particle size: 2–5 μm	Sievers *et al.* (2003)
Palmitic acid	Ethanol/CO_2	Mixing tee pressure: 8 MPa Mixing tee temperature: room temperature Solution flow rate: 0.3 mL/min Nebulizing fluid flow rate: 1–3 mL/min N_2 drying gas flow rate: 15 L/min Drying temperature: 333–353 K	Particle formation type: micronization Morphology: flat, leaf-shaped Particle size: 1 μm	Sievers *et al.* (2003)

Table 11.2 (*continued*)

Substance	Solvent/nebulization fluid	Operational conditions	Results	References
Lysozyme and lactate dehydrogenase	Water/CO_2	Mixing tee pressure: 10.34 MPa Mixing tee temperature: >305 K Solution flow rate: 0.3 mL/min N_2 drying gas flow rate: 15 L/min Drying temperature: <343 K	Particle formation type: micronization Morphology: spherical Moisture content: <4% Particle size: 1–3 μm	Sellers *et al.* (2001)
Onion extract	Water/CO_2	Mixing tee pressure: 8 MPa Mixing tee temperature: 393 K Solution flow rate: 0.2–0.3 mL/min Nebulizing fluid flow rate: 3–10 mL/min Drying temperature: 393 K	Particle formation type: micronization Morphology: spherical Moisture content: 4 % Particle size: < 4 μm	Andersson *et al.* (2012)
Rosemary extract	Water/CO_2	Mixing tee pressure: 8 MPa Mixing tee temperature: 473 K Solution flow rate: 0.2 mL/min Drying temperature: 343 K	Particle formation type: micronization	Herrero *et al.* (2010)

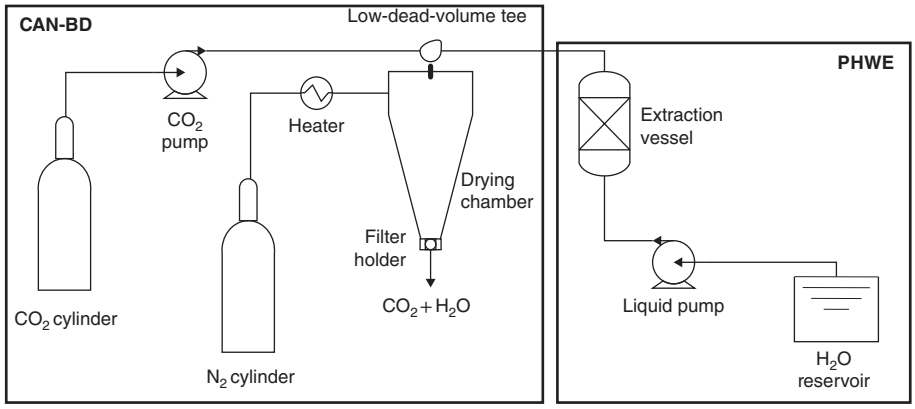

Figure 11.3 Schematic diagram of the WEPO process

was suitable to obtain fine powder with particle sizes smaller than 4 μm in diameter with an intact antioxidant capacity of great interest for food and cosmetic industries. Andersson *et al.* (2012) compared the particles obtained by WEPO with the ones obtained by PHWE followed by freeze drying. Despite having similar results in terms of antioxidant capacity, concentration of quercetin derivatives and water content, the WEPO process was able to produce smaller and well-defined spherical particles. According to Herrero *et al.* (2010), the results obtained via WEPO are promising considering the time saving due to the absence of a later drying process.

11.4.2 PGSS drying

Process description The PGSS drying process (Figure 11.4) consists of mixing an aqueous solution with supercritical CO_2 using a static mixer at the desired temperature and pressure. Aqueous suspensions (Paz, Martín and Cocero, 2012) and oil-in-water emulsions (Varona *et al.*, 2010) also can be fed to the static mixer. In this mixer, a certain amount of water is extracted by CO_2 despite supercritical CO_2 being partly dissolved in the liquid solution. This biphasic mixture is expanded down to atmospheric conditions through a nozzle into a thermally insulated spray tower (Varona *et al.*, 2010). The expansion of the CO_2 dissolved into the liquid promotes the formation of fine droplets. In addition, evaporation of the remaining water takes place due to pre-selected temperature conditions in the spray tower. Water is exhausted together with CO_2 by a blower (supercompressor) from the spray tower. In order to achieve a good water and CO_2 removal from the powder, the conditions in the spray tower have to be above the dew line of the water–CO_2 mixture because in this region one single gas phase is obtained. Knowledge of the vapour–liquid equilibrium (VLE) diagram of this mixture is needed

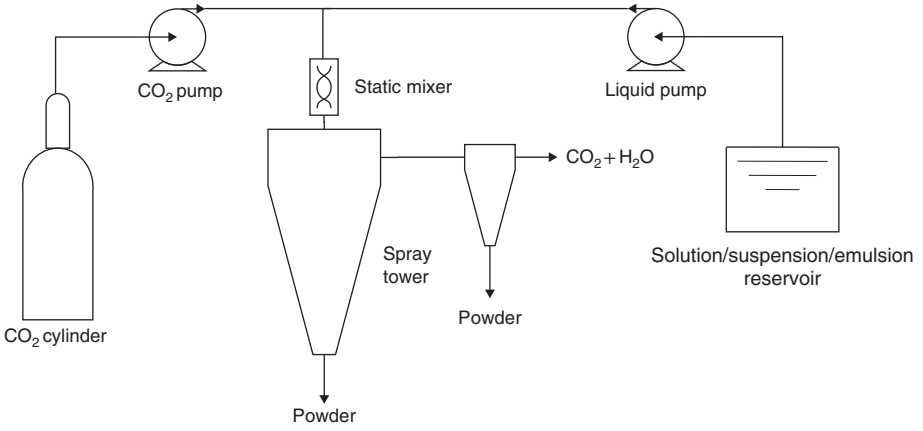

Figure 11.4 Schematic diagram of the PGSS drying process

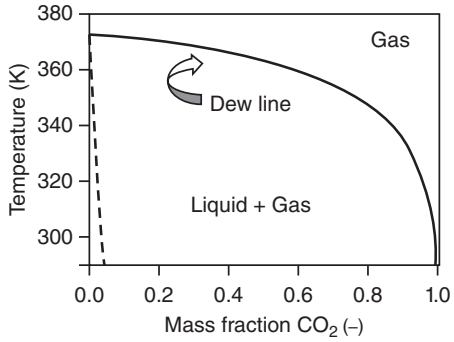

Figure 11.5 Temperature–composition diagram for water and carbon dioxide at atmospheric pressure

to choose between different strategies for water removal. For instance, the temperature in the spray tower can be increased and therefore less CO_2 is used; the other option is to work at a lower temperature and thus it is necessary to increase the mass flow of CO_2 to remove the same amount of water (Figure 11.5) (Pham, Pollak and Petermann, 2012; Martín and Weidner, 2010; Meterc, Petermann and Weidner, 2008). Finally, the produced powder is collected inside the spray tower with a cyclone. Particles are collected at the bottom of the spray tower and CO_2 together with evaporated water leave the tower through its upper part. A cyclone separator is used to recover fine powder entrapped in the effluent gas (Martín *et al.*, 2010b). This process provides an inert atmosphere (CO_2 atmosphere without oxygen), avoiding the possibility of oxidation (Tabernero, Valle and Galán, 2012).

Influence of process variables The literature provides a detailed experimental analysis of the influence of different process and design variables

and parameters (temperature, pressure, flow rates, design of the static mixer, concentration of carrier material, etc.) on particle size, residual moisture, encapsulation efficiency and morphology of the particles obtained by PGSS drying.

Particle size Experimental results demonstrated that one of the major parameters influencing the particle size is the ratio of the gas to solution flow rate. The particle size decreases as the ratio of gas to solution flow rate increases, due to a more efficient atomization and faster precipitation (Martín *et al.*, 2010b). A reduction of particle size was also observed by Martín *et al.* (2010b) when the number of mixing elements was increased from 0 to 5. The authors concluded that with five mixing elements, a saturation of the liquid phase with CO_2 was achieved. The use of mixing elements favours the contact between the aqueous and gas phases, leading to a more efficient supercritical fluid dissolution into the liquid phase, and improves atomization and particle formation in the spray tower. Varona, Martín and Cocero (2011) observed that the higher carrier material concentration has made the atomization more difficult; this is due to the higher emulsion viscosity which produced bigger particles.

Pre-expansion temperature and pressure are important parameters to determine the extraction conditions in the static mixer. These parameters have to be chosen in order to promote a higher concentration of CO_2 in the gas-saturated solution, which enhances the atomization process and leads to the formation of smaller particles (Paz, Martín and Cocero, 2012).

Residual moisture The main parameters that influence the residual moisture are the ratio of the gas to liquid flow rate, pre-expansion temperature and pressure. The decrease of residual moisture with the ratio of the gas to liquid flow rate has a direct consequence for the mass balance (Martín *et al.*, 2010b). Martín and Weidner (2010) showed that a mass balance can be used to calculate the minimum gas/liquid flow rate required for the complete evaporation of water.

Martín *et al.* (2010b) observed a direct relationship between pre-expansion and post-expansion temperatures. As a result of the conservation of energy during the expansion, when the pre-expansion temperature is higher, the temperature in the spray tower is also higher, being more favourable for water evaporation. On the other hand, the increase of the residual moisture when pre-expansion pressure increases is a consequence of the reduction in the spray tower temperature due to the Joule–Thomson effect.

Morphology Particle morphology is directly related to the residual moisture content of particles. When the water has not been successfully removed,

a paste or gel is obtained instead of a solid powder. When the water concentration is lower, the solid powder normally is produced and consists of spherical particles (Pham, Pollak and Petermann, 2012; Martín *et al.*, 2010b).

Varona *et al.* (2010) observed that two main different particle morphologies like spheres and needles were obtained, depending on the pre-expansion conditions. The generation of spheres is favoured by a high pre-expansion temperature and pressure.

Encapsulation efficiency The influence of different parameters on encapsulation efficiency has been investigated by Varona *et al.* (2011, 2010) and Paz, Martín and Cocero (2012). When the pre-expansion temperature is increased, more water is extracted in the static mixer. With a concentrated solution already formed in the static mixer, particles can more easily be surrounded by a shell of carrier material that can be maintained upon drying in the spray tower, leading to the production of microcapsules and an increase in the encapsulation efficiency (Paz, Martín and Cocero, 2012; Varona, Martín and Cocero, 2011).

The observations of Varona, Martín and Cocero (2011) and Paz, Martín and Cocero (2012) diverge with respect to the influence of the concentration of the carrier material on encapsulation efficiency. This divergence may be associated with the different characteristics between the encapsulated materials in the two cases (liquid oil droplets and solid particles).

The pre-expansion pressure and the ratio of gas to product flow rate have a smaller effect on lavandin essential oil encapsulation in modified starch in the conditions investigated by Varona *et al.* (2010). However, in another work, Varona, Martín and Cocero (2011) observed a reduction of lavandin essential oil encapsulation in soybean lecithin when the ratio of gas to product flow rate was increased due to a partial extraction of the oil by supercritical CO_2. However, this effect was not observed by Paz, Martín and Cocero (2012) because the solubility of β-carotene in CO_2 in the conditions studied was very low.

Applications The PGSS drying process has been successfully applied to produce fine particles of polymers and natural compounds. Table 11.3 summarizes the compounds processed by the PGSS drying technique.

Published papers have demonstrated that PGSS drying is feasible for food applications. PGSS drying extends the applicability of PGSS to water-soluble compounds. Application of PGSS drying has been investigated for polymers. Polyethylene glycol (PEG) (Martín *et al.*, 2010b) and polyethylene oxide (PEO) (Pham, Pollak and Petermann, 2012) were dried and micronized by this technique. These polymers can be used as a carrier material for developing formulations of food and pharmaceutical compounds. In addition, the literature provides some natural compounds successfully treated by PGSS drying.

Table 11.3 Summary of particles produced from aqueous solutions using PGSS-drying process

Substance	Solvent	Operational conditions	Results	References
Polyethylene glycol	Water	Pre-expansion pressure: 6.1–15.1 MPa Pre-expansion temperature: 353–414 K Post-expansion temperature: 281–325 K Solution flow rate: 0.5–6 kg/h CO_2 flow rate: 26–100.4 kg/h Gas/liquid flow ratio: 6–139	Particle formation type: micronization Morphology: spherical Moisture content: < 1 % Particle size: 10–20 μm	Martín *et al.* (2010b)
Green tea extracts	Water	Pre-expansion pressure: 5.9–10 MPa Pre-expansion temperature: 383–418 K Post-expansion temperature: 306–352 K	Particle formation type: micronization Morphology: spherical Moisture content: 5.95–13.05% Particle size: < 10 μm	Meterc, Petermann and Weidner (2008)
Gelatine	Water	Pre-expansion pressure: 7.5–8.5 MPa Pre-expansion temperature: 413–433 K Post-expansion temperature: 333–343 K Gas/liquid flow ratio: 20–50	Particle formation type: micronization Moisture content: 8–13% Particle size: 300 μm	Reibe *et al.* (2008)
β-Carotene	Water	Pre-expansion pressure: 8–10 MPa Pre-expansion temperature: 373–403 K Post-expansion temperature: 313–353 K Gas/liquid flow ratio: 21–37	Particle formation type: encapsulation Morphology: agglomerated spheres Particle size: 10–500 μm Encapsulation efficiency (carrier material): 30–60% (soybean lecithin)	Paz, Martín and Cocero (2012)
Lavandin essential oil	Water	Pre-expansion pressure: 6-10 MPa Pre-expansion temperature: 377–403 K Gas/liquid flow ratio: 5–35	Particle formation type: encapsulation Morphology: aggregated spheres Particle size: 1.4–25 μm Encapsulation efficiency (carrier material): 6–14.5% (soybean lecithin)	Varona, Martín and Cocero (2011)
Lavandin essential oil	Water	Pre-expansion pressure: 9–12.1 MPa Pre-expansion temperature: 373–404 K Post-expansion temperature: 333–348 K Solution flow rate: 2.4–4.1 kg/h CO_2 flow rate: 72–91 kg/h Gas/liquid flow ratio: 22.4–41.2	Particle formation type: encapsulation Morphology: spheres and needles Moisture content: 5% Particle size: 15–194 μm Encapsulation efficiency (carrier material): 6–55% (starch)	Varona *et al.* (2010)

PGSS drying was reported on drying green tea extracts containing antioxidant polyphenols. Dried and free-flowing powders were obtained without degradation of the active ingredients because of an oxygen-free atmosphere and low drying temperatures required by this technique, making this process very promising for sensitive substances (Meterc, Peterson and Weidner, 2008). It is possible to produce fine and microbiologically stable gelatin powders having a relatively small amount of CO_2. With the spray drying process it is common to dry aqueous solutions with very low amounts (5%, wt) of high molecular mass gelatin because higher viscosities lead to a blockage of the nozzle due to the formation of fibres and filaments. Therefore, the PGSS drying technology allows a dried food ingredient to be achieved with a considerably reduced energy demand (Reibe *et al.*, 2008).

Lavandin oil-loaded microcapsules have been prepared by using a modified starch, which performed the double function of the surfactant and carrier material (Varona *et al.*, 2010). The encapsulation efficiency varied from 6 to 55%. Particle sizes varied between 15 and 194 μm, with a residual moisture content of about 5%, similar to the water content in unprocessed modified starch. Varona, Martín and Cocero (2011) also studied the formulation of emulsions of lavandin essential oil with liposomes, using soybean lecithin as the carrier material. PGSS drying was effective in micronizing soy lecithin, forming spherical aggregated particles. The low efficiency of encapsulation (6–14.5%) thus obtained can be improved by modifying the process conditions in order to increase the solubility of carbon dioxide in the emulsion in the static mixer. β-Carotene was also encapsulated in soybean lecithin using the PGSS drying process. Dried particles of 10–500 μm were obtained with β-carotene encapsulation efficiencies up to 60% (Paz, Martín and Cocero, 2012).

11.5 Conclusions and future perspectives

CAN-BD and PGSS drying processes use supercritical fluid for water removal. These methods are based on the very simple concept of expanding an aqueous solution saturated with a supercritical fluid, preferably CO_2, through a restriction device. Emulsions and suspensions have also been used. Although no studies reported the use of emulsions via CAN-BD, this operation is possible and extends its applicability. Despite the fact that most published papers explored applications related to the pharmaceutical industry, the present chapter shows the feasibility of applying these processes for producing products for the food industry. Further, the possibility of operating on a large scale exists due to the several advantages presented over the conventional process. The reasons are the prevention of product degradation, control of product characteristics and achievement of a product of good quality due to the closed and inert system used. It is also possible

to couple a process such as WEPO, which combines bioactive compounds (food ingredients) extraction to on-line particle formation. It is a highly promising area and is suitable to obtain desired particles with a reduced time of preparation.

Abbreviations

CAN-BD	Carbon dioxide-assisted nebulization with a bubble dryer
PEG	Polyethylene glycol
PGSS	Particles from gas-saturated solutions
PHWE	Pressurized hot water extraction
PEO	Polyethylene oxide
RESS	Rapid expansion of supercritical solutions
SAA	Supercritical-assisted atomization
SAS	Supercritical antisolvent
SEA	Supercritical enhanced atomization
VLE	Vapour-liquid equilibrium
WEPO	Water extraction and particle formation on-line

Acknowledgements

M. Thereza M. S. Gomes would like to thank the CNPq (Process 140641/2011-4) for a doctoral fellowship. Diego T. Santos would like to thank the FAPESP (Process 10/16485-5) for a postdoctoral fellowship. The authors acknowledge the financial support from CNPq and FAPESP.

References

Andersson, J.M., Lindahl, S., Turner, C. and Rodriguez-Meizoso, I. (2012) Pressurised hot water extraction with on-line particle formation by supercritical fluid technology. *Food Chemistry*, **134**, 1724–1731.

Cape, S.P., Villa, J.A., Huang, E.T.S., Yang, T.-H., Carpenter, J.F. and Sievers, R.E. (2008) Preparation of active proteins, vaccines and pharmaceuticals as fine powders using supercritical or near-critical fluids. *Pharmaceutical Research*, **25**, 1967–1990.

Charbit, G., Badens, E. and Boutin, O. (2004) Methods of particle production. In: York, P., Kompella, U.B. and Shekunov, B.Y. (eds), *Supercritical Fluid Technology for Drug Product Development*. Informa Healthcare, Marcel Dekker, Aix-en-Provence, France.

Cocero, M.J., Martín, A., Mattea, F. and Varona, S. (2009) Encapsulation and co-precipitation processes with supercritical fluids: fundamentals and applications. *Journal of Supercritical Fluids*, **47**, 546–555.

Gomes, M.T.M.S., Santos, D.T. and Meireles, M.A.A. (2012) Trends in particle formation of bioactive compounds using supercritical fluids and nanoemulsions. *Food and Public Health*, **2**, 142–152.

Herrero, M., Plaza, M., Cifuentes, A. and Ibáñez, E. (2010) Green processes for the extraction of bioactives from rosemary: chemical and functional characterization via ultra-performance liquid chromatography-tandem mass spectrometry and *in-vitro* assays. *Journal of Chromatography A*, **217**, 2512–2520.

Huang, E.T.S., Cape, S.P., Alargov, D.K., Villa, J.A., Meresman, H., Rinner, L., Liang, C. and Sievers, R.E. (2003) Nanoparticle and microparticle generation with super or near critical carbon dioxide. In: 6th International Symposium on *Supercritical Fluids*, Versailles, France.

Ibáñez, I., Cifuentes, A., Rodriguez-Meizoso, I., Mendiola, J.A., Reglero, G., Señorans, F.J. and Turner, C. (2009) Device and process for the on-line extraction and drying of complex extracts. Spanish Patent P200900164.

Martín, Á. and Weidner, E. (2010). PGSS-drying: mechanisms and modeling. *Journal of Supercritical Fluids*, **55**, 271–281.

Martín, Á., Varona, S., Navarrete, A. and Cocero, M.J. (2010a) Encapsulation and co-precipitation processes with supercritical fluids: applications with essential oils. *The Open Chemical Engineering Journal*, **4**, 31–41.

Martín, Á., Pham, H.M., Kilzer, A., Kareth, S. and Weidner, E. (2010b) Micronization of polyethylene glycol by PGSS (particles from gas saturated solutions)-drying of aqueous solutions. *Chemical Engineering and Processing*, **49**, 1259–1266.

Meterc, D., Petermann, M. and Weidner, E. (2008) Drying of aqueous green tea extracts using a supercritical fluid spray process. *Journal of Supercritical Fluids*, **45**, 253–259.

Nunes, A.V.M. and Duarte, C.M.M. (2011) Dense CO_2 as a solute, co-solute or co-solvent in particle formation processes: a review. *Materials*, **4**, 2017–2041.

Padrela, L., Rodrigues, M.A., Velaga, S.P., Fernandes, A.C., Matos, H.A. and Azevedo, E.G. (2010) Screening for pharmaceutical cocrystals using the supercritical fluid enhanced atomization process. *Journal of Supercritical Fluids*, **53**, 156–164.

Paz, E., Martín, A. and Cocero, M.J. (2012) Formulation of β-carotene with soybean lecithin by PGSS (particles from gas saturated Ssolutions)-drying. *Journal of Supercritical Fluids*, **72**, 125–133.

Perrut, M. (2004) Applications of supercritical fluid solvents in the pharmaceutical industry. In: Marinsky, J.A., Sen Gupta, A.K. and Marcus, Y. (eds), *Ion Exchange and Solvent Extraction*. *A Series of Advances*. CRC Press, Champigneulles, France, pp. 1–35.

Pham, M., Pollak, S. and Petermann, M. (2012) Micronisation of poly(ethylene oxide) solutions and separation of water by PGSS-drying. *Journal of Supercritical Fluids*, **64**, 19–24.

Prinn, K.B, Costantino, H.R. and Tracy, M. (2002) Statistical modeling of protein spray drying at the lab scale. *AAPS Pharmacological Science and Technology*, **3**, 1–8.

Reibe, C., Alessi, P., Knez, Z. and Weidner, E. (2008) Micronization of high viscous biopolymers. In: Proceedings of the 11th European Meeting on *Supercritical Fluids*, Barcelona, Spain.

Reverchon, E. (2002) Supercritical-assisted atomization to produce micro- and/or nanoparticles of controlled size and distribution. *Industrial and Engineering Chemistry Research*, **41**, 2405–2411.

Santos, D.T. and Meireles, M.A.A. (2010) Carotenoid pigments encapsulation: fundamentals, techniques and recent trends. *The Open Chemical Engineering Journal*, **4**, 42–50.

Sellers, S.P., Clark, G.S., Sievers, R.E. and Carpenter, J.F. (2001) Dry powders of stable protein formulations from aqueous solutions prepared using supercritical CO_2-assisted aerosolization. *Journal of Pharmaceutical Sciences*, **90**, 785–797.

Sievers, R.E., Best, J.A. and Cape, S.P. (2008) Human-powered dry powder inhaler and dry powder inhaler compositions. US Patent 0035143 A1.

Sievers, R.E., and Karst, U. (1997) Methods for fine particle formation. US Patent 5,639,441.

Sievers, R.E., Karst, U., Milewski, P.D., Sellers, S.P., Miles, B.A., Schaefer, J.D., Stoldt, C.R. and Xu, C.Y. (1999) Formation of aqueous small droplet aerosols assisted by supercritical carbon dioxide. *Aerosol Science and Technology*, **30**, 3–15.

Sievers, R.E., Milewski, P.D., Sellers, S.P., Miles, B.A., Korte, B.J., Kusek, K.D., Clark, G.S., Mioskowski, B. and Villa, J.A. (2000) Supercritical and near-critical carbon dioxide assisted low-temperature bubble drying. *Industrial and Engineering Chemistry Research*, **39**, 4831–4836.

Sievers, R.E., Huang, E.T.S., Villa, J.A., Kawamoto, J.K., Evans, M.M. and Brauer, P.R. (2001) Low-temperature manufacturing of fine pharmaceutical powders with supercritical fluid aerosolization in a bubble dryer. *Pure and Applied Chemistry*, **73**, 1299–1303.

Sievers, R.E., Huang, E.T.S., Villa, J.A., Engling, G. and Brauer, P.R. (2003) Micronization of water-soluble or alcohol-soluble pharmaceuticals and model compounds with a low temperature bubble dryer. *Journal of Supercritical Fluids*, **26**, 9–16.

Sievers, R.E., Quinn, B.P., Cape, S.P., Searles, J.A., Braun, C.S., Bhagwat, P., Rebits, L.G., McAdams, D.H., Burger, J.L., Best, J.A., Lindsay, L., Hernandez, M.T., Kisich, K.O., Iacovangelo, T., Kristensen, D. and Chen, D. (2007) Near-critical fluid micronization of stabilized vaccines, antibiotics and anti-virals. *Journal of Supercritical Fluids*, **42**, 385–391.

Skala, D. and Orlovic, A. (2006) Particle production using supercritical fluids. In: Hsu, J.-P. and Spasic, A.M. (eds), *Micro-, Nano-, and Atto-Engineering*. CRC Press, Belgrade, Serbia and Montenegro, pp. 641–678.

Tabernero, A., Valle, E.M.M. and Galán, M.A. (2012) Supercritical fluids for pharmaceutical particle engineering: methods, basic fundamentals and modelling. *Chemical Engineering and Processing*, **60**, 9–25.

Varona, S., Martín, A. and Cocero, M.J. (2011) Liposomal incorporation of lavandin essential oil by a thin-film hydration method and by particles from gas-saturated solutions. *Industrial and Engineering Chemistry Research*, **50**, 2088–2097.

Varona, S., Kareth, S., Martín, Á. and Cocero, M.J. (2010) Formulation of lavandin essential oil with biopolymers by PGSS for application as biocide in ecological agriculture. *Journal of Supercritical Fluids*, **54**, 369–377.

Weidner, E. (2009) High pressure micronization for food applications. *Journal of Supercritical Fluids*, **47**, 556–565.

Weidner, E., Kilzer, A., Petermann, M., Pross, A., Lucas, H.W. and Stepanski, H. (2000) Verfahren zur Erzeugung von Polyurethanpartikeln (Process for producing polyurethane particles). Deutsches Patent DE 100 40 551.7.

CAPÍTULO 4 - EXPERIMENTAL DESIGN FOR THE MICRONIZATION OF IBUPROFEN SODIUM SALT BY SUPERCRITICAL CARBON DIOXIDE ANTISOLVENT PROCESS

M. Thereza M. G. Rosa, Diego T. Santos, Ademir J. Petenate, M. Angela A. Meireles

Artigo experimental submetido a um periódico.

Experimental design for the micronization of ibuprofen sodium salt by supercritical carbon dioxide antisolvent process

M. Thereza M. G. Rosa[a], Diego T. Santos[a,b], Ademir J. Petenate[c], M. Angela A. Meireles[a]

[a]*LASEFI/DEA/FEA (School of Food Engineering)/ UNICAMP (University of Campinas),R. Monteiro Lobato, 80; CEP: 13083-862, Campinas, SP, Brazil*

[b]*Industrial Process and Energy Systems Engineering (IPESE), Swiss Federal Institute of Technology Lausanne (EPFL), Station 9; CH-1015, Lausanne, Switzerland*

[c]*EDTI – Process Improvement; Rua José Ponchio Vizzari, 312; Campinas, SP; CEP: 13085-170; Brazil*

Author for correspondence*: gomes.mtms@gmail.com; Phone: 0055-19-3521-4033 Fax: 0055-19-3521-4027 (M. Thereza M. G. Rosa)

Abstract

Ibuprofen sodium salt micronization by supercritical carbon dioxide antisolvent (SAS) precipitation was investigated in order to better understand this alternative process aiming at industrial applications. Ethanol and CO_2 was used as solvent and antisolvent, respectively, and the effect of the operating conditions on the precipitation yield, energy consumption per unit of manufactured product, residual organic solvent content and particle morphology were evaluated using split-plot experimental design and analysis of variance (ANOVA) method. Focusing on energy saving, a SAS process was simulated using the SuperPro Designer simulation platform. Selecting appropriate process conditions has been shown to facilitate the production of sheet-like morphologie, the best for tableting purposes, with high precipitation yield (70%) and low residual solvent content (4.7 $mg \cdot kg^{-1}$). For the lower energy cost per unit of manufactured product the process must be operated at solution flow rate of 1 $mL \cdot min^{-1}$ and concentration of ethanolic solution of 0.04 $g \cdot mL^{-1}$.

Keywords

Supercritical antisolvent process; Precipitation; Split-plot experimental design; Conventional solvent evaporation; Microparticles.

INTRODUCTION

The use of supercritical fluids is getting more important in pharmaceutical fields. Supercritical fluid technologies for precipitating pharmaceutical substances offer several advantages over conventional ones, such as low energy requirements, low thermal and chemical degradation of products and the production of solvent-free particles with narrow particle size distributions (Knez and Weidner, 2003). Microparticles and nanoparticles can be formed directly from drug solutions in a single-step supercritical fluid process and this would be an excellent alternative, since high energy milling and long processing times can lead to contamination, batch variation, downstream processing difficulties, and compromised stability (Hu et al., 2004).

Ibuprofen is a nonsteroidal anti-inflammatory drug (NSAID) among the most widely used to treat pain, inflammation and fever. Ibuprofen is a white powder with a slight characteristic odor, a melting point of 348–351 K and a molecular weight of 206.28 $g \cdot mol^{-1}$ (Linstrom and Mallard, 2003). The low solubility of ibuprofen in aqueous media (<1 $mg \cdot mL^{-1}$) limits the dissolution and absorption rates into the organism. This limitation can be overcome by the use of ibuprofen sodium salt, which can be easily dissolved in aqueous media to provide faster and greater pain relief. Furthermore, the salt is cheaper and has a higher melting temperature (493 K), which facilitates the tableting process (Gruber and Reher, 2004). Tablets are the most widely used form of commercially available pharmaceutical formulations. The manufacture of tablets by direct compression requires uniform mixing between the excipients and the drug. This content uniformity is promoted by using smaller particles (Kayrak et al., 2003). Moreover, reducing the particle sizes results in a higher bioavailability of the tablet when disintegrates in the body due to increasing its surface area (Newa et al., 2008). Micronization procedures can modify particle

size, porosity, and density, and the drug may be mixed with pharmaceutical excipients using small-particle technologies to maximize delivery to the desired target for drug administration (Rogers et al., 2001).

Processes that employ supercritical carbon dioxide as a solvent have been successfully used by several researchers to micronize pure ibuprofen due to its high solubility in supercritical CO_2. Pathak et al. (2006) and Kayrak et al. (2003) obtained micro- and nanoparticles via these processes. However, due to the low solubility of ibuprofen sodium salt in supercritical CO_2, processes that use supercritical CO_2 as an antisolvent must be employed, such as supercritical carbon dioxide antisolvent (SAS) precipitation; the details of this process was reported recently by Gomes et al. (2012).

Bakhbakhi et al. (2013) and Martín et al. (2009) micronized successfully ibuprofen sodium using the SAS process. Martín et al. (2009) presented a study of the influence of different operating parameters on the purity, particle size, morphology and polymorphism of ibuprofen sodium. Similarly Bakhbakhi et al. (2013) supplemented this study extending the range of the operating parameters evaluated. On the other hand, neither used experimental design approach and proper statistical analysis during their scientific studies.

Theoretically, a number of parameters have simultaneous effect on a process. However, application of experimental design approach is the most effective way to identify the most significant parameters and their interactions, and to achieve a competent result by few experimental trials (Sharif et al., 2014). Although a huge number of parameters can influence the SAS process, some of them might not have effect on it at statistically significant levels. In this context, the objective of this work was to identify which operating parameters (pressure, temperature, CO_2 flow rate, solution flow rate, injector type and concentration of ibuprofen

sodium in the ethanol solution) have statistical significant effects on the precipitation yield, energy cost per unit of manufactured product, residual organic solvent content and particle morphology in order to better understand this alternative process aiming at industrial applications.

MATERIALS AND METHODS

Materials

Ibuprofen sodium salt (BCBC9914V, India) was purchased from Sigma-Aldrich and used as a model substance in the precipitation experiments. Ethanol (Dinâmica®, 52990, Diadema, Brazil), with a minimum purity of 99.5%, was used to prepare the ibuprofen sodium solutions. Carbon dioxide (99% purity, Gama Gases Especiais, Campinas, Brazil) was used as the antisolvent in the SAS process.

Experimental procedure

A schematic diagram of the constructed experimental setup to perform the SAS precipitation experiments on a laboratory scale is shown in Fig. 1. The procedure was performed as follows: The CO_2 from the cylinder was cooled to −10 °C using a thermostatic bath (Marconi, MA-184, Piracicaba, Brazil) to ensure that liquid CO_2 is being pumped by the air driven pump (Maximator, M111 CO_2, Germany) in a 500 mL AISI 316 stainless steel precipitation vessel with a 6.8 cm inner diameter. The precipitation vessel was fitted with an electric heating jacket and an AISI 316 stainless steel porous filter (screen size of 2 μm) fixed at the bottom of the vessel, which was used to collect the precipitated particles.

Once the desired conditions of pressure, temperature and CO_2 flow rate were achieved and remain stable, the ethanolic solution, which contains ibuprofen sodium, was introduced into the vessel by a high pressure pump (Jasco, PU-2080, Japan), which allows a maximum working solution flow rate of 10 $mL \cdot min^{-1}$. A volume of 43 mL was injected into the precipitation vessel, and 10 mL of pure ethanol was then pumped to clean the tubes. Depending on the solution flow rate used, the time allowed for precipitation was 43 or 86 min.

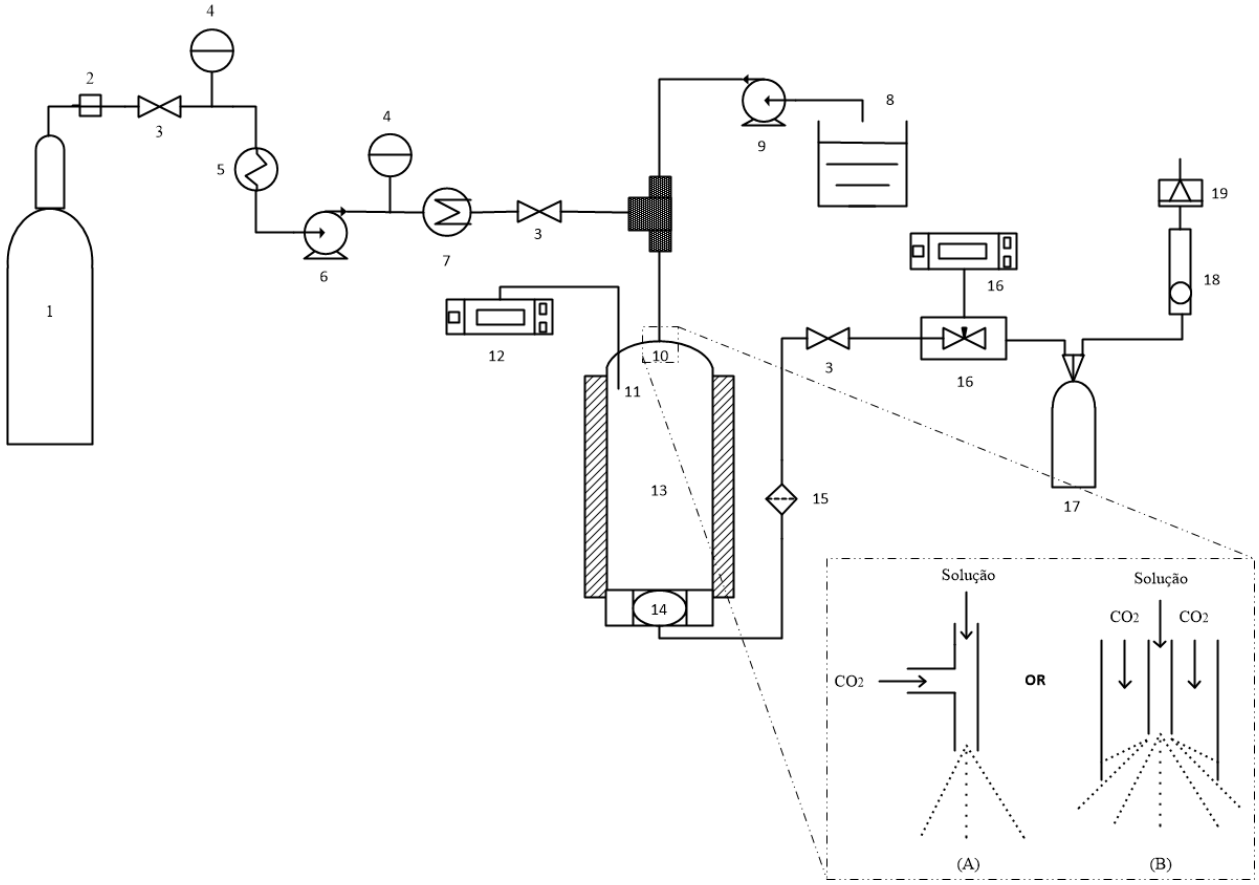

Fig. 1: Schematic diagram of the SAS apparatus. 1 CO_2 Cylinder; 2 CO_2 Filter; 3 Blocking Valves; 4 Manometers; 5 Thermostatic bath; 6 Air driven pump; 7 Heating bath; 8 Solution (solute/solvent) reservoir; 9 High pressure pump; 10 Injector; 11 Thermocouple; 12 Temperature controllers; 13 Precipitation vessel; 14 Filter; 15 Line filter; 16 Micrometric valve with a heating system; 17 Glass flask; 18 Glass float rotameter; 19 Flow totalizer.

In this work, two different injectors were used to mix CO_2 and the solution at the inlet of the precipitation vessel: i) a home-made coaxial nozzle, which consists of a stainless steel tube with an inner diameter of 1/16 in (i.d. 177.8 mm) for the solution, placed inside a 1/8 in stainless steel tube for the CO_2; ii) a commercial 1/8 in stainless steel T-fitting. The injectors were placed at the top of the precipitation vessel. Fig. 1 also shows schematic diagrams of the two injectors.

When the ethanolic solution and CO_2 were mixed, the ethanol was quickly solubilized by the supercritical CO_2, and this fluid mixture (CO_2 plus ethanol) exited the vessel and flowed to a glass flask (100 mL) connected to a micrometric valve. This valve was maintained at 393 K to avoid the freezing and blockage of the outlet caused by the Joule–Thompson effect of the expanding CO_2. Ethanol was deposited in the glass flask, and the gaseous CO_2 was discharged to the atmosphere. The temperature and pressure were measured with instruments directly connected to the precipitation vessel with accuracies of ± 2 K and ± 0.2 MPa, respectively. The CO_2 flow rate was measured using a glass float rotameter (ABB, 16/286A/2, Warminster, USA) coupled with a flow totalizer (LAO, G0,6, Osasco, Brazil).

After the injection of pure ethanol, the high pressure pump was stopped and only CO_2 was pumped, using a minimum of 300 g of CO_2 to ensure that all remaining traces of ethanol present in the precipitation vessel were removed before depressurization. Subsequently, the air driven pump was stopped, the precipitation vessel was slowly depressurized to atmospheric pressure by manually opening the valves and the particles were retained inside the precipitation vessel by a porous filter fixed at the bottom of the vessel and another placed at the vessel outlet (AISI 316 stainless steel porous line filter (Hoke, 6321G2Y, United States), porosity of 2 μm). The particles were carefully collected and stored at ambient temperature in a glass desiccator protected from light until subsequent analysis.

A conventional solvent evaporation (CSE) of ibuprofen sodium process was also used as a reference process to compare it with the SAS process. Two ethanolic solutions were prepared at 0.02 and 0.04 $g \cdot mL^{-1}$ and the ethanol was evaporated using a rotary evaporator (Tecnal, TE-211, Piracicaba, Brazil) with a vacuum control of 200 mmHg and thermostatic bath at 313 K. The ibuprofen sodium precipitates were collected from the precipitation vessel (50 mL glass flask) and stored at ambient temperature in a glass desiccator protected from light. Previous studies (Li et al., 2008, Won et al., 2005) have been used CSE method to produce microparticles of various solids (e.g. phospholipids complex of puerarin; felopidine). Despite this technique uses evaporation of a solvent, the mechanism of particle formation is similar: dissolution of the solid in an organic solvent and precipitation of the solid by elimination of the solvent. Because of this, the ibuprofen particles from CSE method were compared to the SAS method in this study.

Experiment design and statistical analysis

Fractional factorial designs are widely used in industrial experiments. Completely Randomized Design (CRD) is usually used in this situation where the treatments are completely randomized to the experimental units. In this work, an experiment with 5 factors, each at two levels, was conducted. However, it is very difficult to change the levels for the factor type of injector and a CRD would eventually require a modification of the apparatus after each experimental run. Due to time constraint and to avoid leaks, the factor type of injector was considered as a hard-to-change parameter. In this case, a fractional factorial split-plot design represents a practical design option and the experimental runs were done accordingly to this method. A discussion about this experimental design technique can be found in Box et al. (2005).

In the split-plot design the hard-to-change factor is called whole-plot and the easy-to-change factors, sub-plots. First the whole-plot factor is randomized and in the sequence the sub-plots are randomized within the whole plot. While holding the level of the factor type of injector fixed, all of the level combinations of the remaining factors are randomized in a random order was run.

The injection type (T-fitting and coaxial nozzle) was applied to the whole-plots with two replications and a 2^{5-2} fractional factorial while considering the temperature (313 and 323 K), pressure (10 and 12 MPa), concentration of ethanolic solutions (0.02 and 0.04 $g \cdot mL^{-1}$), CO_2 flow rate (500 and 800 $g \cdot h^{-1}$) and solution flow rate (0.5 e 1.0 $mL \cdot min^{-1}$) applied to the sub-plots, which totaled 32 experimental units. Treatments were deemed to be statistically significant for p-value < 0.05 (95% confidence level). Statistical analysis was conducted with MINITAB Statistical Software (Minitab Inc., State College, Pennsylvania). The data from different experiments were compared for statistical significance by analysis of variance (ANOVA).

Analysis and characterization

Determination of residual organic solvent

Gas chromatography (GC) was used to determine the residual amount of ethanol in the particles. The residual solvent was analyzed on a Shimadzu gas chromatograph (GC-17-A, Kyoto, Japan) equipped with a flame ionization detection (FID) system. Approximately 30 mg of sample was dissolved in 1 mL of toluene with the aid of an ultrasonic bath (Unique, Max Clean 1400, 40 Hz, Indaiatuba, Brazil). Sample solutions (1 µL) were introduced by direct injection on a Zebron ZB-5 capillary column from Phenomenex (30 m × 0.25 mm and 0.25 µm). The other conditions were as follows: the injection temperature was 493 K; the detector temperature was

513 K; the helium flow rate was 28 $mL \cdot min^{-1}$; the split ratio was 1:20. Helium served as the carrier gas, and the analysis was performed using an oven temperature of 313 K with a ramp of 20 $K \cdot min^{-1}$ until a temperature of 453 K was reached. The data were quantified using a calibration curve that was constructed by measuring different known concentrations of ethanol in toluene.

Determination of morphology

The morphology of ibuprofen sodium particles was examined by scanning electron microscopy (SEM; LEO Electron Microscopy/Oxford, Leo 440i, Cambridge, England) with an energy dispersive X-ray analyzer (LEO Electron Microscopy/Oxford, 6070, Cambridge, England). The samples were coated with a thin layer of gold in a Polaron sputter coater (VG Microtech, SC7620, Uckfield, England) and examined using a SEM at 20 kV accelerating voltage and 100 pA beam current. A coarse measurement of the particle size was done over the micrographs from the SEM analysis.

Simulation procedure of the studied process

The simulations were performed using the commercial simulator SuperPro Designer 6.0® process. The energy consumption per unit of manufactured product was determined for each SAS experimental process condition. This software allows the estimation of the mass and energy balance for all streams of the process. The results were normalized to determine the energy consumption (in terms of cost) per unit (1 kg) of manufactured product (particles obtained by SAS). The SAS process developed in the SuperPro Designer consisted of two pumps (one for CO_2 and one for ethanol), one precipitation vessel and two heat exchangers. The economic data

fed into the simulator are: US$ 0.091/kWh electricity, US$ 5.15/ton cooling water and US$ 20.00/ton steam (Prado et al., 2013). Utility costs comprise producing heat exchange agents and the electricity used in the processes. For the calculation of energy (utility) cost per unit of manufactured product of each experiment was taken into account the precipitation yield of each process and the volume injected into the precipitation vessel, according to Equation 1:

$$EC = \frac{\Sigma UC}{C \cdot V \cdot \frac{PY}{100}} \qquad \text{Eq. (1)}$$

where: EC is the energy cost per unit of manufactured product (US$/kg); UC is the utility cost (US$); C is the concentration of the ethanolic solution (kg/mL); V is the volume injected into the precipitation vessel (43 mL); PY is the precipitation yield (%).

RESULTS AND DISCUSSION

The effect of the temperature, pressure, CO_2 flow rate, solution flow rate, concentration of the ethanolic solution and type of injector on the characteristics of ibuprofen sodium particles obtained via SAS was investigated. The range of the experimental conditions adopted in this work was based on information from the literature (Martín et al., 2009) and preliminary tests. Table 1 shows the experimental conditions used for the SAS experiments randomized by split-plot experimental design.

The experiments were performed using typical conditions for SAS. The pressure and temperature values were chosen in order to operate the process above the critical point of the ethanol and CO_2 mixture, which was located at approximately 8.5 MPa at 313 K (Chang et al., 1998). Martín et al. (2009) did not obtain a dry ibuprofen sodium powder at subcritical conditions because the formation of particles is controlled by the fluid mechanics and the

kinetics of evaporation of the solvent under these conditions, and the time available inside the precipitation vessel was not sufficiently long to completely evaporate the solvent in their study. The operation above or below the mixture critical point results in different particle formation mechanisms in the SAS. Su et al. (2011) observed that when operating above the critical point, no droplet formation and fast mass transfer after solution injection favored the production of smaller fluticasone propionate particles.

The choice of the solution and CO_2 flow rates was related to the difficulties in producing a dry powder. Preliminary tests showed that obtaining a dry powder was not possible at higher solution flow rates and lower CO_2 flow rates. Under these conditions, the mass of CO_2 used was not sufficient to completely eliminate the organic solvent and precipitate the ibuprofen sodium. On the other hand, CO_2 flow rates higher than 1,000 $g \cdot h^{-1}$ induced in higher ibuprofen sodium loss in the downstream separator. Thus, moderate CO_2 and solution flow rates of 500-800 $g \cdot h^{-1}$ and 0.5-1.0 $mL \cdot min^{-1}$, respectively, were adopted in this study.

Influence of the operating conditions on the precipitation yield

Table 1 presents the precipitation yields obtained from each experiment. The precipitation yield ranged from 14.72 to 72.58% depending on the operating conditions used in the SAS process. A precipitation yield of 100% was obtained using the conventional solvent evaporation (CSE) method. The lower yield of the SAS experiments can be attributed to the loss of individual particles through the filters. The individual particle size was approximately 1 μm, which is smaller than the filter pore size of 2 μm. Thus, only agglomerates could be retained. Furthermore, slower precipitation kinetics can lead to a loss of ibuprofen sodium in the downstream separator. These reasons were also responsible for the low yield achieved by

Visentin's group study (Visentin et al., 2012) for the precipitation and encapsulation of rosemary antioxidants by SAS. Using a filter with a smaller pore size may result in a greater precipitation yield. However, such a filter may also clog more easily. Satisfatory yield above 85% was obtained by Su et al. (2011) in the micronization of fluticasone propionate using dichloromethane as the solvent, and a lower yield, about 70%, was obtained when occurred particle adhesion on the surface of the spiral jet mill.

Table 1: Experimental conditions from split-plot design and results obtained in each experiment.

Exp.	T (K)	P (MPa)	CO_2 flow rate ($g \cdot h^{-1}$)	Solution flow rate ($mL \cdot min^{-1}$)	Concentration of ethanolic solution ($g \cdot mL^{-1}$)	Injector	Precipitation yield (%)	Residual solvent content ($mg \cdot kg^{-1}$)	Energy consumption ($US\$ \cdot kg^{-1}$)	Morphology
12	313	10	500	0.5	0.02	Coaxial	26.77	10.1±0.5	45.04	Flake and sheet
2	313	10	500	0.5	0.04	T-fitting	41.68	9±2	14.47	Flake
31	313	10	500	1	0.02	T-fitting	27.9	5.1±0.5	21.77	Sheet
19	313	10	500	1	0.04	Coaxial	14.72	16.3±0.9	20.64	Flake
6	313	10	800	0.5	0.02	T-fitting	69.99	4.7±0.3	25.82	Sheet
15	313	10	800	0.5	0.04	Coaxial	25.44	54±1	35.52	Flake, needle and sheet
17	313	10	800	1	0.02	Coaxial	35.82	7.3±0.1	26.98	Flake, needle and sheet
32	313	10	800	1	0.04	T-fitting	66.82	9±2	7.23	Flake and needle
30	313	12	500	0.5	0.02	T-fitting	21.48	5±1	57.02	Flake and needle
23	313	12	500	0.5	0.04	Coaxial	16.92	13±1	36.19	Flake and sheet
16	313	12	500	1	0.02	Coaxial	21.33	13±1	28.72	Flake and needle
3	313	12	500	1	0.04	T-fitting	25.75	6.0±0.1	11.89	Flake and sheet
21	313	12	800	0.5	0.02	Coaxial	41.86	15±2	46.32	Needle and sheet
26	313	12	800	0.5	0.04	T-fitting	41.13	9.3±0.2	23.57	Flake
1	313	12	800	1	0.02	T-fitting	38.95	44±6	25.01	Flake and needle
10	313	12	800	1	0.04	Coaxial	35.34	6±1	13.78	Flake and needle
22	323	10	500	0.5	0.02	Coaxial	24.15	4.7±0.1	54.82	Flake and needle
29	323	10	500	0.5	0.04	T-fitting	30.48	6.1±0.6	21.72	Flake
4	323	10	500	1	0.02	T-fitting	23.45	9±1	28.55	Flake and needle
14	323	10	500	1	0.04	Coaxial	37.07	41±1	9.03	Flake
25	323	10	800	0.5	0.02	T-fitting	30.36	6.4±0.6	69.49	Sheet
18	323	10	800	0.5	0.04	Coaxial	27.32	16.6±0.3	38.61	Flake
11	323	10	800	1	0.02	Coaxial	20.68	37±2	51.36	Flake and sheet
7	323	10	800	1	0.04	T-fitting	35.88	7.0±0.1	14.8	Flake
8	323	12	500	0.5	0.02	T-fitting	19	6.7±0.3	71	Flake, needle and sheet
9	323	12	500	0.5	0.04	Coaxial	25.03	5.1±0.4	26.94	Flake and needle

24	323	12	500	1	0.02	Coaxial	29.41	3.7±0.7	22.92	Flake and needle
27	323	12	500	1	0.04	T-fitting	25.86	5.3±0.2	13.04	Flake and needle
13	323	12	800	0.5	0.02	Coaxial	25.99	21±2	81.78	Flake
5	323	12	800	0.5	0.04	T-fitting	31.98	4.3±0.3	33.23	Flake and needle
28	323	12	800	1	0.02	T-fitting	72.58	9.9±0.2	14.74	Flake and needle
20	323	12	800	1	0.04	Coaxial	53.57	27±2	9.99	Flake

SAS formulations of oxeglitazar with various solubilizing excipients was precipitated using six different organic solvents by Majerik and his group (Majerik et al., 2007a). Precipitation yield obtained varied between 28 and 91%. The authors observed that precipitation from non-chlorinated solvents resulted in low precipitation yield suggesting that these solvents act as cosolvent and increase the solubility of processed pharmaceutical ingredients in the supercritical phase. This phenomenon was considered by the authors as the main source of loss in precipitation yield using supercritical fluid antisolvents and must be considered in this work, once it was also used a non-chlorinated solvent, the ethanol.

The data from different experiments were compared for statistical significance by analysis of variance (ANOVA). The p-values for the precipitation yield are given in Table 2. According to these values, only CO_2 flow rate significantly influenced the precipitation yield (p-value < 0.05). Table 3 shows that the precipitation of ibuprofen sodium salt at CO_2 flow rate of 800 $g \cdot h^{-1}$ gave a significantly higher precipitation yield compared to precipitation at 500 $g \cdot h^{-1}$. For the interpretation of this result, it must be taken into account that an increase in the CO_2 flow rate leads to a lower contact time between CO_2 and the solute. As a result, a higher precipitation yield was achieved as a consequence of the amount of solute dissolved in supercritical CO_2 be lower and less solute be dragged. Moreover, the higher CO_2 flow rate enhanced the turbulence, due to the increase in the Reynolds number (Sui et al., 2012), which resulted in a better mixing between the solvents turbulence, and thus contribute to the precipitation process. Imsanguan et al. (2010) observed the same influence of CO_2 flow rate in the precipitation yield of andrographolide from *A. paniculata* extract using SAS process. The authors reported that CO_2 flow rate affects kinetic energy of supercritical CO_2 and the composition of the fluid phase. It is noteworthy that a maximum precipitation yield is intended and CO_2 flow rate of 800 $g.h^{-1}$

achieved optimum results, and preliminary studies showed that further increasing leads to a higher loss of the ibuprofen sodium in the downstream separator.

Table 2: P-values obtained statistically for precipitation yield, residual solvent content and energy cost per unit of manufactured product.

Parameter	Precipitation yield p-value	Residual solvent content p-value	Energy cost per unit of manufactured product p-value
Injector	0.070	0.255	0.118
Temperature	0.599	0.834	0.036
Pressure	0.867	0.558	0.550
CO_2 flow rate	0.009	0.162	0.498
Solution flow rate	0.386	0.483	0.000
Concentration of ethanolic solution	0.943	0.693	0.000

As can be observed at Table 3, the variability in precipitation yield was observed with higher CO_2 flow rate. The increase of the deviations can be related to an unstable deposition of the particles on the filter allowing the exit of them.

Table 3: Influence of statistically significant parameters on precipitation yield (%) and energy consumption per unit of manufactured product (US$·kg^{-1}).

CO_2 flow rate (g·h^{-1})	**Precipitation Yield (%)***
500	25.69±6.90
800	40.86±16.36
Solution flow rate (mL·min^{-1})	**Energy cost per unit of manufactured product (US$·kg^{-1})**
0.5	42.60±19.58
1.0	20.03±10.98
Temperature 313 K	
Concentration of ethanolic solution (g·mL^{-1})	**Energy cost per unit of manufactured product (US$·kg^{-1})**
0.02	34.58±12.96
0.04	20.41±10.78
Temperature 323 K	
Concentration of ethanolic solution (g·mL^{-1})	**Energy cost per unit of manufactured product (US$·kg^{-1})**
0.02	49.33±24.75
0.04	20.92±11.09

*Mean ± Standard deviation

Influence of operating conditions on residual organic solvent content in the micronized particles

The chromatography profile of the standard solution containing ethanol and toluene showed an ethanol peak at a retention time of 2.04 min. The resultant linear relationship between peak area (y) and ethanol concentration (x) was $y = 32719 \cdot x - 1030.3$ ($R^2 = 0.9998$).

The results presented in Table 1 show a low residual organic solvent content in the ibuprofen sodium precipitated by SAS. The residual ethanol content in the ibuprofen sodium particles was below 55 $mg \cdot kg^{-1}$ in all SAS experiments, while the ibuprofen sodium particles precipitated by CSE was 2.5 times higher, approximately 140 $mg \cdot kg^{-1}$. These concentrations are below than the suggested value of the Internal Conference on Harmonization (ICH) guideline Q3C (Impurities: Guideline for Residual Solvents), which for ethanol is 5000 $mg \cdot kg^{-1}$ (ICH, 1997). Also, the ethanol concentrations in the particles are significant different, indicating that the SAS process has technical advantages to obtain products of free solvent. Majerik et al. (2007b) also demonstrated that SAS reduces residual solvent content more efficiently than CSE. The authors observed that the residual dicloromethane content in the solid dispersions of oxeglitazar in PVP K17 (polyvinilpyrrolidone) obtained by CSE was 1.4 higher than the one obtained by SAS, and the solid dispersions of oxeglitazar in poloxamer 407 (polyoxyethylene-polyoxypropylene block copolymer) was 1.6 higher.

Similar results were obtained by Adami et al. (2008) at certain experimental conditions; they reported the production of micronized nalmefene HCl via SAS with a residual organic solvent content of 2 $mg \cdot kg^{-1}$. In a study by Kim et al. (2007), GC analysis revealed that the residual solvent (dichloromethane) content in the precipitated cilostazol via SAS was below 50

$mg \cdot kg^{-1}$, indicating that the solvent removal during SAS, depends not only on volatility of the solvent but also on other factors, such as the operating conditions and the SAS apparatus.

Depending on the operating conditions, the residual organic solvent could be reduced below to 4 $mg \cdot kg^{-1}$. The statistical analysis showed that all operating parameters evaluated did not influence the residual solvent content in the range studied (Table 2). On the other hand, an interesting behavior was observed: the experiments that resulted in the best precipitation yield also showed low residual solvent content (using a T-fitting; at high CO_2 flow rate).

Influence of operating conditions on morphology

The effect of different process parameters on the morphology of ibuprofen sodium particles obtained with the SAS process was studied. Fig. 2 shows a scanning electron microscopy (SEM) picture of unprocessed ibuprofen sodium. The unprocessed ibuprofen sodium consisted of typical agglomerated sheet-like particles (Martín et al., 2009) with particle sizes of approximately 30 µm. The morphology obtained in each experiment is presented in Table 1.

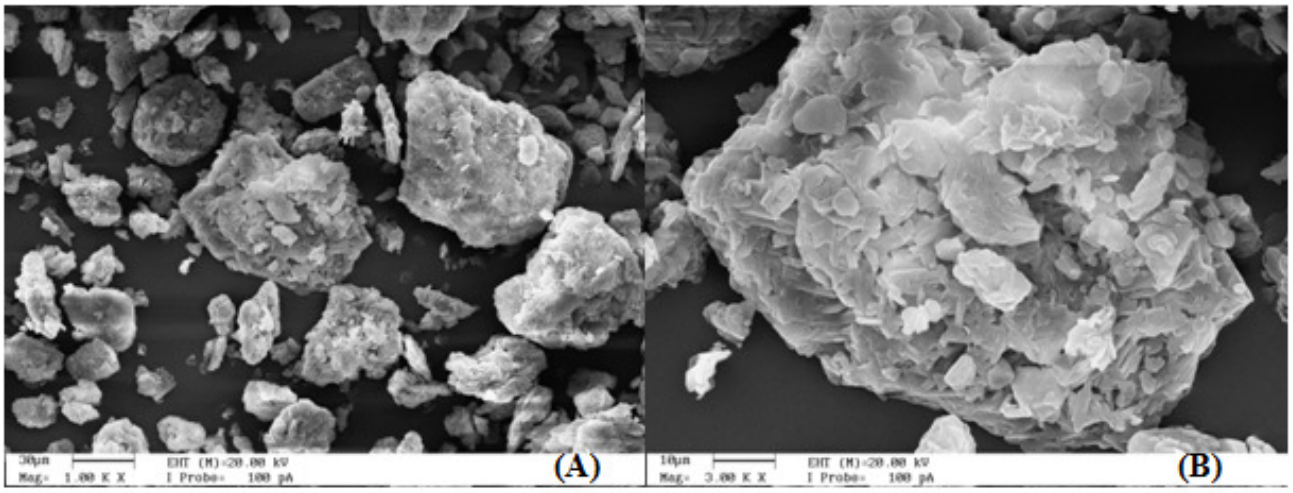

Fig. 2: SEM image of unprocessed ibuprofen sodium particles with magnification of 1000 (A) and 3000 (B).

Ibuprofen sodium particles were successfully micronized with a SAS process. Fig. 3 shows the SEM pictures of the particles obtained from various experiments listed in Table 1. The particles of ibuprofen have a trend to develop agglomerates after the SAS process, as showed in Fig. 3. A coarse measurement of the agglomerates was done over the micrographs from the SEM analysis. For example exp. 20 shows an agglomerate of ≈5 μm of diameter but Exp. 8 show a bulk set of agglomerates. The measurement was not possible for all the micrographs due to a no visible limit between agglomerates.

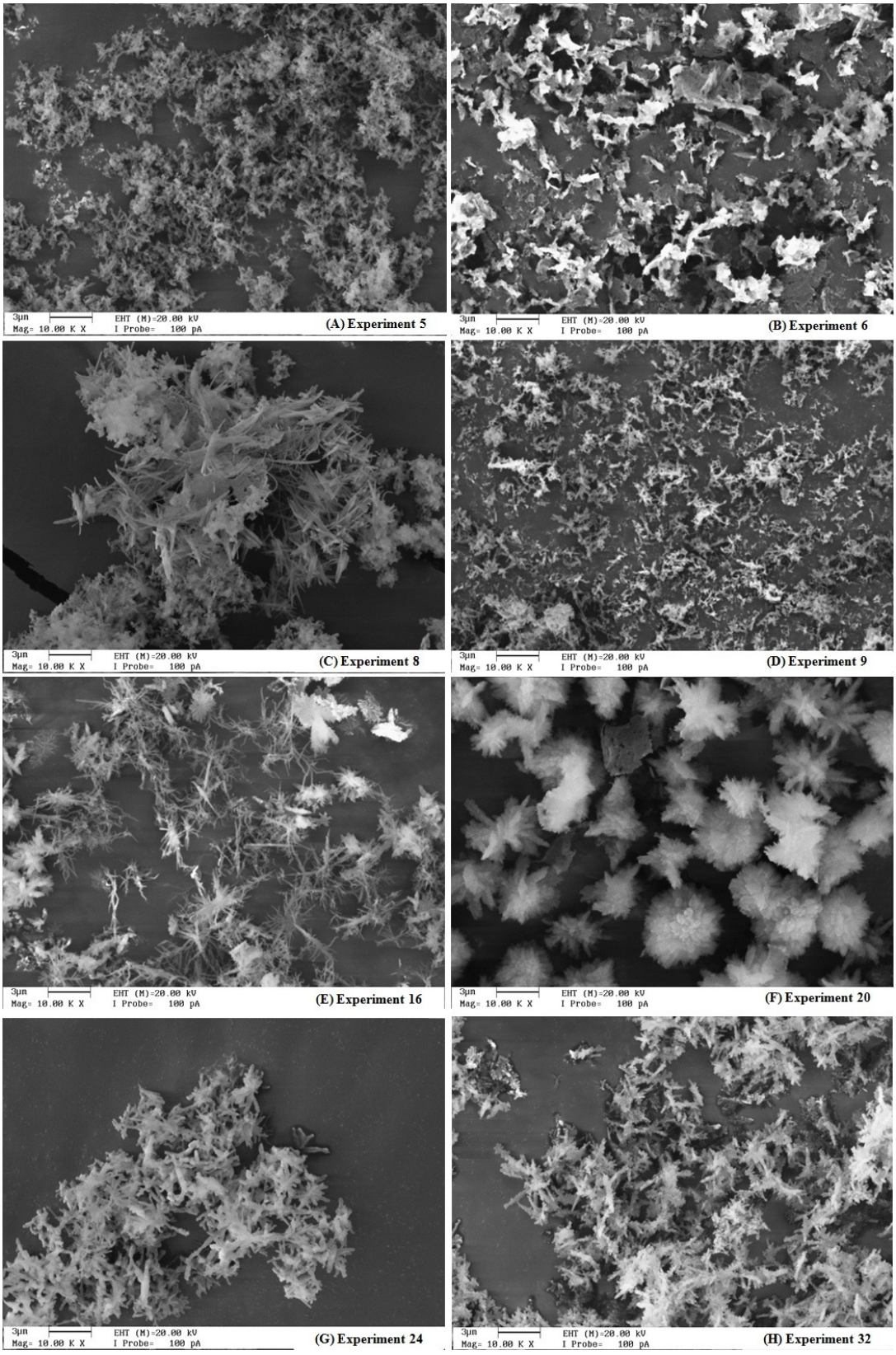

Fig. 3: (A – H) SEM images of ibuprofen sodium particles obtained by SAS process.

The particle morphology depended on the experimental conditions and included sheet-, flake- and needle- like morphologies (Fig. 3). According to Reverchon et al. (Reverchon et al., 2003), the particle morphology can be affected by many process parameters, such as the temperature, pressure, solution concentration and antisolvent to solution flow rate ratio. Moreover, the process arrangement and the apparatus can also heavily influence the product properties. In most experiments, needle-like particles of micron- to submicron size were obtained, but these particles were highly agglomerated and formed star-shaped aggregates. Nevertheless, appropriate operating conditions have been shown to generate particles that were approximately 1 μm in size. Bakhbakhi et al. (2013) also obtained submicron-sized ibuprofen sodium particles with a needle-like morphology by SAS, which corroborated our findings.

The different morphology among agglomerates from SAS and CSE process maybe trigger for a different molecular structure of the ibuprofen. Previous studies showed that ibuprofen is a polymorphic drug (Martín et al., 2009) indicating that different conditions of pressure, temperature and solvent can induce a more stable molecular structure. Therefore, the produced agglomerate can obtain different physico-chemical properties. These characterizations are beyond of this study but future research is encouraged to understand the influence of the morphology.

The results showed that higher CO_2/solution flow ratios resulted in particles with a sheet morphology that were significantly less agglomerated but bigger than the flake- and needle- like particles. This effect is particularly noticeable in the results of experiments 6, 21 and 25, which operated at CO_2/solution flow ratio of 34 and produced large sheet-like particles with a particle size of approximately 5 μm. Martín et al. (2009) attributed this effect to the increased solubility of ibuprofen sodium in the fluid due to the cosolvent effect of ethanol when the CO_2/solution

flow ratio was reduced. The cosolvent effect is well known in supercritical extraction processing and has been used to improve the solubility of otherwise difficult to solubilize compounds by altering the polarity of CO_2 (Sánchez-Camargo et al., 2011, Reverchon, 1999). As a result of the cosolvent effect, the increase in the solubility lead to slower nucleation kinetics, thus producing fewer large particles. Though not predominant, a sheet-like morphology was produced in experiments 8, 9, 12 and 29 (operated at CO_2/solution flow ratio of 21), as demonstrated in Fig. 3C. Experiments 5, 10 and 16 produced smaller particles with a needle-like morphology.

Under supercritical conditions, the density of CO_2 is influenced by pressure and temperature and plays an important role for mass transfer between organic solvents and CO_2 during particle formation (Kim et al., 2007). The SEM images indicated that the density of CO_2 can alter the particle size because it alters the mass-transfer characteristics of the process. Smaller particles were obtained using CO_2 at a density of up to 587 $kg \cdot m^{-3}$. At higher densities, larger particles were produced. Density data for carbon dioxide was taken from NIST (Linstrom and Mallard, 2001) according to the pressure and temperature used. Randolph et al. (1993) also observed that the particle size positively correlated with the CO_2 density during an investigation of L-PLA micronization, which was sprayed from a dichloromethane solution into CO_2. The authors attributed the effect to mass transport mechanisms rather than to jet breakup and hydrodynamics. Kim et al. (2007) showed that the mean particle size of cilostazol precipitated from dichloromethane and glacial acetic acid showed a good linear relation with the density of CO_2, increasing the density of CO_2 led to decreasing the particle size.

The ability to alter the sizes and morphology of drug particles is important to their formulation and administration. Pathak et al. (2006) applied Rapid expansion of a supercritical solution into a liquid solvent (RESOLV) to produce exclusively nanoscale ibuprofen particles in

aqueous suspension using polymers as stabilization agent. The authors concluded that the experimental conditions and the selection of stabilization agent in RESOLV are used to alter the sizes and morphology of the nanosized drug particles.

Ibuprofen sodium was also micronized using a conventional process, which was used as a reference process to compare with the SAS process. The SEM images of ibuprofen sodium particles obtained by conventional solvent extraction (CSE) are presented in Fig. 4. The ibuprofen sodium morphology did not change after precipitation; sheet-like particles were produced using CSE. However, the ibuprofen sodium particles obtained by CSE were 3 times bigger than those of the unprocessed ibuprofen sodium. The CSE method involves multi-stage processing to reduce the particle size and is always time-consuming. The solid obtained by Li et al. (2008) using CSE was collected and desiccated in a vacuum oven at 323 K, then pulverized and finally passed through a 180-mm sieve and Won et al. (2005) produced solid dispersions of felodipine by CSE and pulverized the product using a mill to reduce the particle size.

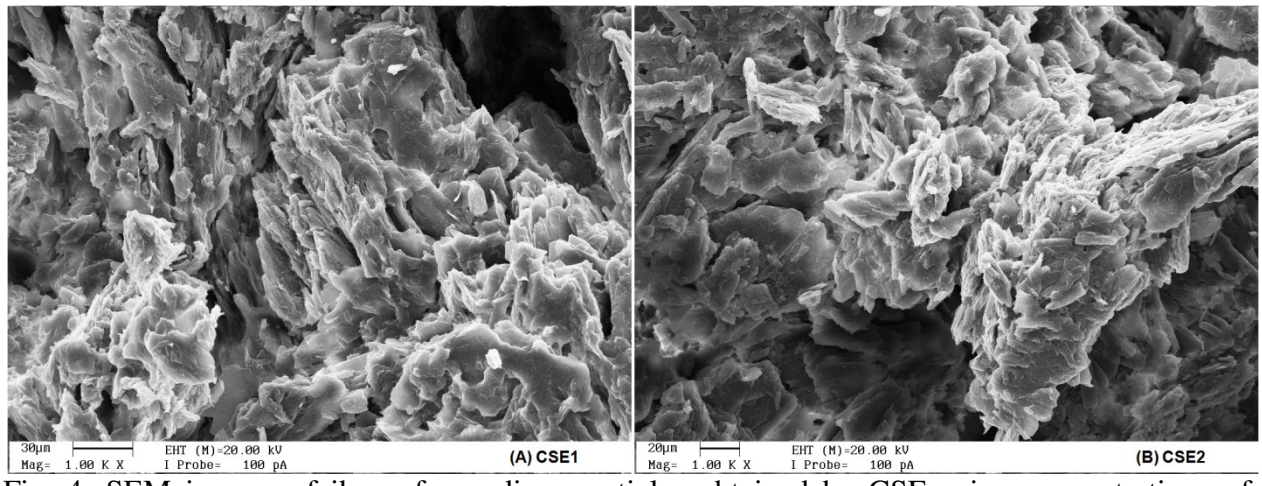

Fig. 4: SEM images of ibuprofen sodium particles obtained by CSE using concentrations of ethanolic solution of (A) 0.02 e (B) 0.04 $g \cdot mL^{-1}$.

Influence of the operating conditions on energy cost per unit of manufactured product

The effect of the operating conditions on the energy cost per unit of manufactured product was also investigated while focusing on energy savings. Table 1 shows the energy consumption (in terms of cost) per unit of manufactured product (US$·kg^{-1}) obtained in each experiment. The temperature, solution flow rate and concentration of the ethanolic solution influenced the energy consumption at statistically significant levels, as observed in Table 2. Furthermore, the statistical analysis indicated a second order relationship between the temperature and concentration of the ethanolic solution (p-value = 0.047) with a 95 % confidence level (p-value < 0.05).

Table 3 presents the solution flow rate influence and the concentration of the ethanolic solution as a function of temperature. The high cost of ibuprofen precipitation remains a barrier to its acceptance in the market. The lowest estimated energy cost per unit of manufactured product was obtained using solution flow rate of 1.0 mL·min^{-1}. The estimated energy cost to precipitate ibuprofen sodium salt at this solution flow rate was 20 US$·kg^{-1}. At high solution flow rate, lower was the process time and hence lower the energy cost. Table 3 also shows that the lowest energy consumption was obtained at concentration of ethanolic solution of 0.04g·mL^{-1} due to the higher manufactured solute mass. At this concentration, the results were independent of the temperature used, and the estimated energy cost per unit of manufactured product was approximately 20 US$·kg^{-1}. Therefore, processing at the lowest temperature is the best choice. Currently, to the best of our knowledge, no study about economic analyses in the micronization using SAS is found in the literature. According to Weidner (2009), the large amount of CO_2 required for particle micronization has a high economical impact. Therefore, to install a CO_2

recovery it could be economical and minimize environmental impact by reducing the CO_2 emissions at the atmosphere.

The cost of obtaining ultrafine ibuprofen sodium particles is compensated by an improved drug bioavailability and improved content uniformity for the tablet formulation (Kayrak et al., 2003, Newa et al., 2008). The lowest energy cost per unit of manufactured product (US$·kg^{-1}) was obtained in experiment 32, which increased final price of the manufactured product by only 1% compared to the price sold by Sigma-Aldrich®. This increase is negligible when compared to the advantages offered by the reduction of the particle size. Small micro- and nanometer-sized particles have attracted growing interest in the pharmaceutical and food industries because they endow materials with new properties that can be adopted by these industries (Sanguansri and Augustin, 2006). Notably, the energetic cost (cost of utilities) is one of five factors used to estimate the cost of manufacturing (COM) according to a methodology proposed in Turton et al. (2008). The COM is estimated as the sum of the cost of investment, the cost of operational labor, the cost of waste treatment and the cost of utilities (energetic cost). More information about each cost factor can be found in a paper by in Rosa and Meireles (2005).

Selecting appropriate conditions

In the SAS equipment used in this work, our findings indicate that to produce ibrupofen sodium salt particles with a low residual solvent, high precipitation yield and low energy consumption per unit of manufactured product, the process must operate at CO_2 flow rate of 800 g·h^{-1}, solution flow rate of 1 mL·min^{-1} and concentration of ethanolic solution of 0.04 g·mL^{-1}, which experiment 32 yields satisfactory results for all these response variables. However, flake and needle-like particles were obtained at this condition (Fig. 4H).

The particle morphology has been shown to affect the flow properties and tableting performance. Small particles with an adequate morphology could improve the bioavailability. Historically, compounds that exhibit a needle-like crystalline shape have showed poor flow properties, and ibuprofen is not any exception to this observation. Sheet-like particles show improved flow and tableting properties compared to needle-like particles (Amin and Gordon, 1984). Homogeneous sheet-like micronized particles were produced at experiment 6 (Fig. 4B), with also low residual solvent content (4.7 $mg \cdot kg^{-1}$) and high precipitation yield (70%).

CONCLUSIONS

The influence of the operating parameter during ibuprofen sodium salt SAS micronization was investigated in deep by means of experimental design and proper statistical analysis. The CO_2 flow rate influenced the precipitation yield at statistically significant levels meanwhile none operating parameters did influence the residual solvent content in the micronized particles. The temperature and concentration of the ethanolic solution influenced the energy cost at statistically significant levels. Selecting appropriate process conditions (using the T-fitting at a temperature of 313 K, pressure of 10 MPa, CO_2 flow rate of 800 $g \cdot h^{-1}$, solution flow rate of 0.5 $mL \cdot min^{-1}$ and ethanol solution concentration of 0.02 $g \cdot mL^{-1}$) has been shown to facilitate the production of homogeneous sheet-like microparticles of ibuprofen particles, the best for tableting purposes, with low residual solvent (4.7 $mg \cdot kg^{-1}$) and high precipitation yield (70%). However, our findings indicate that the lowest estimated energy cost per unit of manufactured product was obtained using solution flow rate of 1 $mL \cdot min^{-1}$ and concentration of ethanolic solution of 0.04 $g \cdot mL^{-1}$.

ACKNOWLEDGMENTS

M. Thereza M. G. Rosa thanks CNPq (140641/2011-4) for the doctoral fellowship. Diego T. Santos thanks the FAPESP (10/16485-5; 12/19304-7) for the postdoctoral fellowships. The authors acknowledge financial support from CNPq (564721/2010-7); M. Angela A. Meireles thanks CNPq for a productivity grant (302778/2007-1). The authors also thank Moysés N. Moraes for his assistance with the statistical analyses.

REFERENCES

ADAMI, R., REVERCHON, E., JÄRVENPÄÄ, E. & HUOPALAHTI, R. 2008. Supercritical antisolvent micronization of nalmefene HCl on laboratory and pilot scale. *Powder Technol,* 182**,** 105-112.

AMIN, S. I. & GORDON, R. E. 1984. *Crystallization of ibuprofen*. 4476248.

BAKHBAKHI, Y., ALFADUL, S. & AJBAR, A. 2013. Precipitation of Ibuprofen Sodium using compressed carbon dioxide as antisolvent. *Eur. J. Pharm. Sci,* 48**,** 30-39.

BOX, G. E., HUNTER, J. S. & HUNTER, W. G. 2005. *Statistics for experimenters: Design, Innovation, and Discovery,* New York, Wiley

CHANG, C. J., CHIU, K.-L. & DAY, C.-Y. 1998. A new apparatus for the determination of P-x-y diagrams and Henry's constants in high pressure alcohols with critical carbon dioxide. *J. Supercrit. Fluid,* 12**,** 223-237.

GOMES, M. T. M. S., SANTOS, D. T. & MEIRELES, M. A. A. 2012. Trends in Particle Formation of Bioactive Compounds Using Supercritical Fluids and Nanoemulsions. *Food Public Health,* 2**,** 142-152.

GRUBER, P. & REHER, M. 2004. *Dosage form of sodium ibuprofen*. 2004035024.

HU, J., JOHNSTON, K. P. & WILLIAMS III, R. O. 2004. Nanoparticle engineering processes for enhancing the dissolution rates of poorly water soluble drugs. *Drug Dev Ind Pharm,* 30**,** 233-245.

ICH 1997. International Conference on Harmonization (ICH) of Technical Requirements for the Registration of Pharmaceuticals for Human Use. *Guideline for Residual Solvents,* Step 4.

IMSANGUAN, P., PONGAMPHAI, S., DOUGLAS, S., TEPPAITOON, W. & DOUGLAS, P. L. 2010. Supercritical antisolvent precipitation of andrographolide from *Andrographis paniculata* extracts: Effect of pressure, temperature and CO2 flow rate. *Powder Technol,* 200**,** 246-253.

KAYRAK, D., AKMAN, U. & HORTAÇSU, Ö. 2003. Micronization of ibuprofen by RESS. *J. Supercrit. Fluid,* 26**,** 17-31.

KIM, M.-S., LEE, S., PARK, J.-S., WOO, J.-S. & HWANG, S.-J. 2007. Micronization of cilostazol using supercritical antisolvent (SAS) process: effect of process parameters. *Powder Technol,* 177**,** 64-70.

KNEZ, Z. & WEIDNER, E. 2003. Particles formation and particle design using supercritical fluids. *Curr. Opin. Solid. St. M,* 7**,** 353-361.

LI, Y., YANG, D.-J., CHEN, S.-L., CHEN, S.-B. & CHAN, A. S.-C. 2008. Comparative physicochemical characterization of phospholipids complex of puerarin formulated by conventional and supercritical methods. *Pharmaceut. Res,* 25**,** 563-577.

LINSTROM, P. & MALLARD, W. 2003. *NIST Chemistry, National Institute of Standards and Technology*, Gaithersburg.

LINSTROM, P. J. & MALLARD, W. 2001. *NIST chemistry webbook*, National Institute of Standards and Technology Gaithersburg, MD.

MAJERIK, V., CHARBIT, G., BADENS, E., HORVÁTH, G., SZOKONYA, L., BOSC, N. & TEILLAUD, E. 2007a. Bioavailability enhancement of an active substance by supercritical antisolvent precipitation. *J. Supercrit. Fluid,* 40**,** 101-110.

MAJERIK, V., HORVÁTH, G., SZOKONYA, L., CHARBIT, G., BADENS, E., BOSC, N. & TEILLAUD, E. 2007b. Supercritical antisolvent versus coevaporation-preparation and characterization of solid dispersions. *Drug Dev Ind Pharm,* 33**,** 975-983.

MARTÍN, Á., SCHOLLE, K., MATTEA, F., METERC, D. & COCERO, M. J. 2009. Production of polymorphs of ibuprofen sodium by supercritical antisolvent (SAS) precipitation. *Cryst. Growth D,* 9**,** 2504-2511.

NEWA, M., BHANDARI, K. H., KIM, J. O., IM, J. S., KIM, J. A., YOO, B. K., WOO, J. S., CHOI, H. G. & YONG, C. S. 2008. Enhancement of solubility, dissolution and bioavailability of ibuprofen in solid dispersion systems. *Chem. Pharm. Bull,* 56**,** 569-574.

PATHAK, P., MEZIANI, M. J., DESAI, T. & SUN, Y.-P. 2006. Formation and stabilization of ibuprofen nanoparticles in supercritical fluid processing. *J. Supercrit. Fluid,* 37**,** 279-286.

PRADO, I. M., PRADO, G. H., PRADO, J. M. & MEIRELES, M. A. A. 2013. Supercritical CO2 and low-pressure solvent extraction of mango (*Mangifera indica*) leaves: Global yield, extraction kinetics, chemical composition and cost of manufacturing. *Food Bioprod. Process,* 91**,** 656-664.

RANDOLPH, T. W., RANDOLPH, A. D., MEBES, M. & YEUNG, S. 1993. Sub-Micrometer-Sized Biodegradable Particles of Poly (L-Lactic Acid) via the Gas Antisolvent Spray Precipitation Process. *Biotechnol. Progr,* 9**,** 429-435.

REVERCHON, E. 1999. Supercritical antisolvent precipitation of micro-and nano-particles. *J. Supercrit. Fluid,* 15**,** 1-21.

REVERCHON, E., CAPUTO, G. & DE MARCO, I. 2003. Role of phase behavior and atomization in the supercritical antisolvent precipitation. *Ind. Eng. Chem. Res,* 42**,** 6406-6414.

ROGERS, T. L., JOHNSTON, K. P. & WILLIAMS III, R. O. 2001. Solution-based particle formation of pharmaceutical powders by supercritical or compressed fluid CO2 and cryogenic spray-freezing technologies. *Drug Dev Ind Pharm,* 27**,** 1003-1015.

ROSA, P. T. & MEIRELES, M. A. A. 2005. Rapid estimation of the manufacturing cost of extracts obtained by supercritical fluid extraction. *J. Food Eng,* 67**,** 235-240.

SÁNCHEZ-CAMARGO, A. P., MEIRELES, M. A. A., LOPES, B. L. F. & CABRAL, F. A. 2011. Proximate composition and extraction of carotenoids and lipids from Brazilian redspotted shrimp waste (*Farfantepenaeus paulensis). J. Food Eng,* 102**,** 87-93.

SANGUANSRI, P. & AUGUSTIN, M. A. 2006. Nanoscale materials development–a food industry perspective. *Trends Food Sci. Tech,* 17**,** 547-556.

SHARIF, K., RAHMAN, M., AZMIR, J., MOHAMED, A., JAHURUL, M., SAHENA, F. & ZAIDUL, I. 2014. Experimental design of supercritical fluid extraction–A review. *J. Food Eng,* 124**,** 105-116.

SU, C. S., LO, W. S. & LIEN, L. H. 2011. Micronization of Fluticasone Propionate using Supercritical Antisolvent (SAS) Process. *Chemical Engineering & Technology,* 34**,** 535-541.

SUI, X., WEI, W., YANG, L., ZU, Y., ZHAO, C., ZHANG, L., YANG, F. & ZHANG, Z. 2012. Preparation, characterization and *in vivo* assessment of the bioavailability of glycyrrhizic acid microparticles by supercritical anti-solvent process. *Int. J. Pharm,* 423**,** 471-479.

TURTON, R., BAILIE, R. C., WHITING, W. B. & SHAEIWITZ, J. A. 2008. *Analysis, synthesis and design of chemical processes*, Pearson Education.

VISENTIN, A., RODRÍGUEZ-ROJO, S., NAVARRETE, A., MAESTRI, D. & COCERO, M. 2012. Precipitation and encapsulation of rosemary antioxidants by supercritical antisolvent process. *J. Food Eng,* 109**,** 9-15.

WEIDNER, E. 2009. High pressure micronization for food applications. *J. Supercrit. Fluid,* 47**,** 556-565.

WON, D.-H., KIM, M.-S., LEE, S., PARK, J.-S. & HWANG, S.-J. 2005. Improved physicochemical characteristics of felodipine solid dispersion particles by supercritical anti-solvent precipitation process. *Int. J. Pharm,* 301**,** 199-208.

CAPÍTULO 5 - FORMULATING TOCOTRIENOL-RICH OIL AS AN O/W MINIEMULSION BY USING NONPURIFIED AQUEOUS EXTRACT FROM BRAZILIAN GINSENG ROOTS AS A BIOSURFACTANT

M. Thereza M. G. Rosa, Eric Keven Silva, Ademir J. Petenate, M. Angela A. Meireles

Artigo experimental submetido a um periódico.

FORMULATING TOCOTRIENOL-RICH OIL AS AN O/W MINIEMULSION BY USING NONPURIFIED AQUEOUS EXTRACT FROM BRAZILIAN GINSENG ROOTS AS A BIOSURFACTANT

M. Thereza M. G. Rosa[a], Eric Keven Silva[a], Ademir J. Petenate[b], M. Angela A. Meireles[a*]

[a]LASEFI/DEA/FEA (School of Food Engineering)/UNICAMP (University of Campinas), R. Monteiro Lobato, 80; 13083-862, Campinas, SP, Brazil

[b]DE, IMEC-UNICAMP, Cx. Postal 6065, CEP: 13083-970, Campinas, SP, Brazil

Author for correspondence*: maameireles@gmail.com; meireles@fea.unicamp.br; Phone: +55-19-3521-4033 Fax: +55-19-3521-4027 (M. A. A. Meireles)

Capítulo 5 – Formulating tocotrienol-rich oil as an O/W miniemulsion by using nonpurified aqueous extract from Brazilian ginseng roots as a biosurfactant

Abstract

The purpose of this study was to produce an oil-in-water (O/W) emulsion of δ-tocotrienol-rich oil obtained from annatto seeds by a supercritical fluid extraction process. The effects of emulsification by ultrasound (US) were evaluated and compared to emulsification by dispax reactor (DR) at similar energy densities. Nonpurified saponin-rich extract from Brazilian ginseng roots (BGR) was obtained from BGR by pressurized liquid extraction and used as a biosurfactant. A model O/W emulsion system was prepared with soybean oil and commercial saponin. The influence of the emulsification process, energy density, oil type, biosurfactant type and biosurfactant concentration on the size and stability of the resulting droplets was examined through the experimental design and proper statistical analysis. The results showed that US produced more stable emulsion with smaller droplet sizes in comparison with the DR device at the same energy density. In general, increasing the energy density helped to reduce the emulsion droplet size. The minimum average droplet size observed in the mini-emulsions was 0.35 μm. The data show that both biosurfactants were capable of forming emulsions containing relatively small droplets (< 0.83 μm) and were rather stable (96 to 99%), with some creaming. The emulsion droplets also showed a surface potential of approximately -49 mV because of the adsorbed biosurfactants, which minimized the flocculation of the oil droplets. These results indicate that BGR-extracted saponin might be an attractive biosurfactant choice for emulsion formulations for use in food and beverage products.

Keywords

Annatto seeds, Brazilian ginseng roots, δ-tocotrienol, *Pfaffia glomerata*, Saponins

Capítulo 5 – Formulating tocotrienol-rich oil as an O/W miniemulsion by using nonpurified aqueous extract from Brazilian ginseng roots as a biosurfactant

1 Introduction

Food industries have focused on nutritive and healthy food products that meet consumer demand for a healthy lifestyle, which are intended to prevent nutrition-related diseases in consumers (Menrad, 2003). Annatto (*Bixaorellana* L.) seeds contain carotenoid pigments, which are the most commonly used colorants in food processing, for example in coloring butter, cheese, ice cream, bakery products and edible oils (Smith, 2006). Moreover, the lipid fraction of these seeds is rich in tocotrienol, which health benefits are very interesting for the food industry. Tocotrienols, which are related to the tocopherol family, have received a large amount of attention recently for their important biological activities, especially for inhibiting tumor development and reducing the risk of cardiovascular disease (Sylvester and Theriault, 2003). Aggarwal et al. (2010) published an excellent review paper about tocotrienol effects on cancer, bone resorption, diabetes, and cardiovascular and neurological diseases at both preclinical and clinical levels.

Tocotrienols consist of a chromanol ring linked to a 15-carbon tail, with three trans double bonds. These compounds are made of a group of four amphipathic molecules (α-, β-, γ- and δ-) that differ in the number and position of methyl groups on the chromanol rings (Aggarwal et al., 2010, Schauss et al., 2013). Tocotrienols are present in only a very small number of plants and are especially abundant in rice bran, palm oil and annatto seeds, for which the ratio of tocopherol-to-tocotrienol in each is 50:50, 25:75 and 0.1:99.9, respectively. Tocotrienol-containing products can be a considerable source of vitamin E when consumed. Annatto seeds are described by Tan (2011) as the richest source of the most potent tocotrienol, that is, δ-tocotrienol. Tocopherol interferes with tocotrienol benefits. Annatto stands out as a superior tocotrienol source because of its unique

composition of 90% δ-tocotrienol and 10% γ-tocotrienol, without any tocopherols (Schauss et al., 2013).

By focusing on an increase in the high added value of δ-tocotrienol-rich extracts, which were obtained by using the supercritical fluid extraction process, a nonpurified aqueous extract from Brazilian ginseng roots (BGR) (*Pfaffia glomerata*) was used as a biosurfactant in the emulsification process. This extract is rich in saponins, a natural class of compounds used as a food additive for its amphiphilic properties (Mitra and Dungan, 2000).

Saponins are predominantly made of glycosides that possess one, two or three sugar chains attached to the aglycones, also called sapogenins, which are the nonpolar parts of the molecule (Oleszek and Hamed, 2010). The presence of hydrophobic and hydrophilic areas (the aglycone and sugar resides) in the saponin molecules account for the ability of this compound to reduce surface tension at phase boundaries (Mironenko et al., 2010). These compounds have been used in foods as natural surfactants; they serve as preservatives to control the microbial spoilage of food. Because of consumer preferences for natural substance, saponins have more recently been used as a natural small molecule surfactant in beverage emulsions to replace synthetic surfactants such as polysorbates (Cheok et al., 2014).

There are a number of mechanisms available to produce emulsions. According to the literature, ultrafine emulsions can be prepared by high- and low-energy emulsification methods (Yang et al., 2012). Emulsification is a process in which a system is made from two immiscible liquids (usually oil and water), one of which is dispersed as small droplets within the other (Chandrapala et al., 2012). The high-energy methods employ mechanical

or ultrasound devices that generate shearing (rotor-stator) or pressure differences (a high-pressure homogenizer or power ultrasound) to decompose the emulsion structures (Spinelli et al., 2010). Anyway, the reduction of the droplet size makes emulsions more stable.

The objective of the present work was to generate food grade oil-in-water (O/W) emulsions through mechanical stirring by the dispax reactor (DR) or power ultrasound (US), with particular emphasis on identifying equipment-related constraints. A model O/W emulsion system was prepared with soybean oil and commercial saponin as biosurfactant. The best conditions for fabricating an O/W mini-emulsion of δ-tocotrienol-rich oil with a saponin-rich extract from BGR as a biosurfactant were identified. This system may be suitable for applications in food and beverage formulations.

2 Materials and Methods

2.1 Material

Annatto seeds (*Bixa orellana* L.) of the *Piave* variety were obtained from the Agronomic Institute of Campinas, Department of Agriculture and Supply of the State of São Paulo, Brasil. The centesimal composition of this annatto was determined by using the official methods published by the AOAC (1997) for measuring the moisture, protein, ash and total lipid contents. The carbohydrate content was determined by difference. The γ-, δ-, α- and β-tocotrienol contents were determined according to AOCS (2004) method Ce 8–89.

The tocotrienol-rich oil used in this study was obtained from annatto seeds by using supercritical carbon dioxide (99% CO_2, Air Liquide, Campinas, SP, Brazil) as an extracting solvent with pilot scale equipment (Thar Technologies, model SFE-2 × 5LF-2-FMC, Pittsburgh, PA, USA) that was equipped with two 5.15 L extraction vessels and three 1 L

separators displayed in a series. The process conditions were selected from the ones that were optimized by Albuquerque and Meireles (2012). The results showed that the extract with the most concentrated δ-tocotrienol and the lowest bixin content was obtained at 313 K and 20 MPa. The static extraction time was 20 min. The extraction was performed until the solvent mass-to-feed mass ratio (S/F) was 3.5, with a constant flow rate of 100 $g \cdot min^{-1}$.

BGR saponins were obtained from Brazilian ginseng (*Pfaffia glomerata*) plants cultivated in CPQBA/UNICAMP (Campinas, SP, Brazil) and processed in our own lab as described elsewhere (Santos et al., 2012). The saponin-rich extract was obtained by using a pressurized liquid extraction system as described by Debien and Meireles (2014). In brief, the system contains an HPLC pump (Thermoseparation Products, Model ConstaMetric 3200 P/F, Riviera Beach, FL, USA), a 415 mL extraction cell containing sintered metal filters at the upper and lower parts, a jacket connected to a thermostatic bath, a block valve (Autoclave engineers, Model 10V2071 15000 psi, Erie, PA, USA) and a heated micrometering valve (Autoclave engineers, Model 10VRMM11000PSI Erie, PA, USA). The extract was prepared under conditions that were optimized by Vardanega et al. (2014) as follows: temperature of 353 K, pressure of 12 MPa, static extraction time of 10 min, and flow rate of 10 $mL \cdot min^{-1}$ over 120 min to achieve an S/F of 26. Distilled water was the solvent and BGR particles with a 7.9 μm diameter were used. Water from the extracts was removed by freeze-drying for 5 days at 60–100 μm Hg and at 223 K (Liobras, Liotop L101, São Carlos, SP, Brazil). This nonpurified extract was used as a biosurfactant.

The model O/W emulsion system was prepared with soybean oil and commercial saponin. The saponins were purchased from Sigma Aldrich Co. (8-25% Sapogenin, Lot BCBG 4489V, St. Louis, MO, USA). Soybean oil was purchased in a local supermarket.

This oil was selected because the composition of the annatto seed oil was similar to that of the soybean oil (Silva et al., 2008).

2.2 Biosurfactant characterization

To estimate the emulsification index of the biosurfactants, 2 mL of soybean oil was added to 2 mL of solution (50 mg of biosurfactant/1 mL of distilled water) in a graduated tube and vortexed at high speed for 2 min. The emulsification index (%) was calculated after 24 h by dividing the measured height of the emulsion layer by the mixture's total height and multiplying by 100 (Cooper and Goldenberg, 1987).

The determination of the critical micellar concentration (CMC) for the biosurfactants in aqueous solutions was obtained by using the surface tension method. A stock solution containing 30 $mg \cdot mL^{-1}$ of biosurfactants was prepared in distilled water; solutions of varying concentrations ranging from 30-0.1 $mg \cdot mL^{-1}$ were prepared by diluting this stock solution. The surface tension of the working solutions was measured by tensiometer (Teclis, model Tracker S, Longessaigne, Rhone-Alpes, France) at 25 °C. The surface tension-concentration plots were used to determine the CMC, and the coefficients of the adjusted cubic model were estimated by regression analysis.

2.3 Interfacial tension measurements

The interfacial tension was measured at oil-water interfaces by using a pendant drop analysis instrument (Teclis, model Tracker S, Longessaigne, Rhone-Alpes, France). The aqueous phases were prepared by mixing appropriate amounts of water and biosurfactant. The oil phase was injected into the aqueous phase and the interfacial tension was

determined by drop shape analysis after the system had time to reach equilibrium. The equilibrium time required to measure the steady state surface tension was 15 min. Rising oil drops were formed into a biosurfactant solution.

2.4 Emulsion preparation

Batch emulsification processes were conducted through mechanical agitation (DR) and power ultrasound (US). A rotor-stator type homogenizer, the Dispax Reactor (DR, Magic Lab, Module DR-UTL, IKA, Staufen, Baden-Württemberg, Germany) and an ultrasound horn (US, UNIQUE, DESRUPTOR, 19 kHz, 500 W, Indaiatuba, SP, Brazil) were used.

Oil-in-water emulsions were prepared by homogenizing a 3 wt.% lipid phase with a 97 wt.% aqueous phase. The aqueous phase consisted of biosurfactant, and the selected concentration was obtained according to the CMC analyses. Ultra-pure (MilliQ®) water was used in all experiments. O/W emulsions were prepared at room temperature and the biosurfactant was first dissolved in water; oil was then added and energy was supplied over a controlled period of time. Primary emulsions were obtained with a homogenizer (IKA, T18 basic, Wilmington, NC, USA) at 10,000 rpm for 2 min. Emulsions were obtained by using an ultrasonic horn at 200 and 400 W of the nominal applied powers (NAP) for 5 min. Emulsions were also obtained by using a rotor-stator type homogenizer at 20,000 rpm and an energy density equivalent to that of the US. Energy densities (ED) of 200 and 400 W for the US emulsifications were 600 and 1,200 $J.mL^{-1}$, respectively, and they were calculated by using Equation (1) as follows:

$$ED(J.ml^{-1}) = \frac{NAP(W) \cdot t(s)}{V(ml)} \quad (1)$$

Where ED is the energy density, NAP is the nominal applied power, t is the time and V is the volume.

The DR emulsification times were obtained with Equation (1) by substituting the calculated energy density values from the US, the solution volume (V=100 mL) and the power drawn by the DR at 20,000 rpm, as calculated by using Equation (2).

$$NAP(W) = \frac{2 \cdot \pi \cdot T(Nm) \cdot n(rpm)}{60} \quad (2)$$

where T is the torque or moment, which was 0.11 Nm at 20,000 rpm, and n is the speed. Therefore, the DR processing time was 8 min 40 s and 4 min 20 s for ED values of 1,200 and 600 $J.mL^{-1}$, respectively.

2.5 Characterization of emulsions

2.5.1 Droplet size measurement

The droplet sizes were measured by laser light scattering method in a Mastersizer 2000 with a Hydro 2000S wet dispersion unit (Malvern Instruments, Worcestershire, England, UK). The pump speed was set at 1750 rpm. The droplet sizes were measured 1 h after preparing the emulsions. The mean diameter of the droplets was calculated by using Equation (3) and expressed as the surface volume or Sauter diameter (D_{32}) as follows:

$$D_{32} = \frac{\sum n_i d_i^3}{\sum n_i d_i^2} \quad (3)$$

where n_i is the number of droplets of diameter d_i.

To determine the variations in the droplet size distributions, a term known as the 'span' was calculated by using Equation (4) and expressed as follows:

$$Span = \frac{[d(v,90) - d(v,10)]}{d(v,50)} \quad (4)$$

where d(v,10), d(v,50), and d(v,90) are the diameters at 10%, 50%, and 90% cumulative volume, respectively.

2.5.2 Zetapotential measurements

The zeta potential of each emulsion was determined by using a Zeta Potential Analyzer (Malvern Instruments, Nano Z, Malvern, England, UK) over 12 runs of three cycles each. The emulsions were diluted 50-fold in MilliQ® water prior to the measurements. Measurements were made in triplicate. The pH of the emulsions was measured by using a pH meter (Tecnal, model DM20, São Paulo, SP, Brazil).

2.5.3 Emulsion stability measurement

The emulsions were visually checked for phase separation. Twenty-five mL of freshly prepared emulsion was transferred into 25 mL graduated tubes (internal diameter, 16.4 mm; height, 165 mm), sealed with Parafilm®, and then stored at 17 °C. The emulsion stability was monitored over seven days. During storage, emulsion instability was indicated by a complete breakdown into two phases, with an opaque cream layer at the top. The emulsion stability was monitored by measuring the remaining emulsion height (RH) and

the total emulsion height (TH) in the tube. The emulsion stability was obtained as a percentage by using Equation (5) as follows:

$$ES(\%) = \frac{RH}{TH} \times 100 \quad (5)$$

2.5.4 Microscopic examination

The microstructure of selected emulsions was determined by using an optical microscope (Carl Zeiss, Axio Scope A1, Lower Saxony, Germany). A drop of each emulsion was placed on a microscope slide, covered by a cover slip, and observed at a magnification of 1000 ×.

2.5.5 Emulsion rheology measurements

The rheological characteristics and viscosity of selected emulsions were determined at 298 K in triplicate by using a rheometer (TA Instruments, AR 1500ex, New Castle, DE, USA). A double-walled concentric cylinder geometry (500 μm gap) consisting of an inner rotating acrylic cylinder (inner radius=17.53 mm, outer radius=16.02 mm) and an outer fixed stainless steel cup (inner radius=15.10 mm, outer radius=58 mm) were used for the measurements.

Flow curves were obtained by using an up-down-up step program with a different shear stress range for each sample, in which the maximum shear rate value was 300 s^{-1}. The third flow curve data were fitted to the Newtonian model (Equation 6) as follows:

$$\sigma = \eta \cdot \dot{\gamma} \quad (6)$$

where σ is the shear stress (Pa), $\dot{\gamma}$ is the shear rate (s^{-1}) and η is the viscosity (Pa·s).

2.6 Experimental design and statistical analysis

The parameters thought to affect the O/W emulsion were the emulsification method, the type of oil, the energy density, the type and the biosurfactant concentration. The effects of these operational and compositional parameters on the droplet size, zeta potential and emulsion stability were studied. The experiments were statistically designed and performed according to a 2^5 full factorial design that was completely randomized. A general linear model in MINITAB Statistical Software (Minitab Inc., State College, PA, USA) was used to conduct an analysis of variance (ANOVA) to determine the differences between treatment means. Treatment means were considered significantly different at a p-value < 0.05 (95% confidence level). Table 1 presents the randomized experimental design.

Table 1: The experimental conditions for the emulsification experiments.

Experiment	Process	Oil	Biosurfactant	Biosurfactant Concentration (%)	Energy Density ($J \cdot mL^{-1}$)
1	DR[a]	Soybean	Commercial[c]	1.5	1,200
2	US[b]	Soybean	BGR[d]	1.5	600
3	DR	Annatto	Commercial	1.5	1,200
4	DR	Annatto	BGR	3.0	600
5	US	Soybean	Commercial	1.5	600
6	US	Soybean	Commercial	3.0	1,200
7	DR	Soybean	BGR	3.0	1,200
8	US	Annatto	Commercial	3.0	600
9	DR	Soybean	BGR	1.5	1,200
10	US	Soybean	Commercial	1.5	1,200
11	US	Soybean	BGR	3.0	1,200
12	US	Annatto	Commercial	1.5	1,200
13	DR	Soybean	BGR	3.0	600
14	DR	Soybean	Commercial	1.5	600
15	US	Annatto	BGR	1.5	1,200
16	DR	Annatto	Commercial	1.5	600
17	US	Annatto	BGR	3.0	1,200
18	DR	Annatto	BGR	1.5	1,200
19	US	Annatto	Commercial	1.5	600
20	US	Soybean	BGR	1.5	1,200
21	US	Annatto	Commercial	3.0	1,200
22	DR	Soybean	Commercial	3.0	1,200
23	DR	Soybean	Commercial	3.0	600
24	DR	Annatto	Commercial	3.0	600
25	DR	Soybean	BGR	1.5	600
26	US	Soybean	BGR	3.0	600
27	US	Annatto	BGR	1.5	600
28	DR	Annatto	BGR	3.0	1,200
29	DR	Annatto	Commercial	3.0	1,200
30	US	Annatto	BGR	3.0	600
31	DR	Annatto	BGR	1.5	600
32	US	Soybean	Commercial	3.0	600

[a]Dispax Reactor
[b]Ultrasound
[c]Commercial Saponin
[d]Saponin-rich extract from Brazilian ginseng roots

3 Results and Discussion

The centesimal composition of the annatto seed sample was 10.9 ± 0.2% (w/w) moisture, 5.1 ± 0.1 % (w/w) ash, 3.5 ± 0.0 % (w/w) lipids, 8.9 ± 0.2 % (w/w) proteins, and 71.6 % carbohydrates. These values are similar to those found in the literature for annatto seeds (Albuquerque and Meireles, 2012). The amounts of γ- and δ-tocotrienols detected in the tocotrienol-rich oil and extracted from annatto seeds with supercritical CO_2 were 1.18 ± 0.05 % and 7.83 ± 0.09 %, respectively. These amounts were smaller than those obtained by Albuquerque and Meireles (2012), who generated 1.97 ± 0.04 % γ-tocotrienols and 14.6 ± 0.4 % δ-tocotrienols. These differences in the results were most likely caused by the S/F used by the authors, which was 10 times higher than that used in this work. The α- and β-tocotrienols were not observed in the sample.

The emulsification index of the BGR saponins was 25 % higher than that of the commercial saponins. The emulsification index values were 63.4 ± 0.3 % and 50.8 ± 0.6 % for BGR and commercial saponins, respectively. This finding indicates that the BGR-extracted saponins might be an attractive biosurfactant choice for emulsion formulations. Better results may be achieved by using purified BGR saponins.

3.1 Critical micellar concentration

The presence of an amphiphilic molecule in aqueous solution decreases the surface tension significantly because the surfactant concentration increases until micelles form (Xiong et al., 2008). The CMC of the biosurfactant aqueous solution was estimated to be 1.5 $mg.mL^{-1}$ for the commercial saponins and 12.1 $mg.mL^{-1}$ for the BGR saponins, which

were based on the first derivative of the cubic equation when setting $dSTF/dCON = 0$, where STF is the surface tension of the solution and CON is the biosurfactant concentration. The CMCs obtained in this experiment were far higher than the 0.75 $mg.mL^{-1}$ reported by Skurtys and Aguilera (2009) for *Quillaja* saponin. It is notable that these saponins are extracted from the bark of the *Quillaja saponaria* Molina tree that is native to the semi-arid zones of Chile.

Above and at the CMC, saponin biosurfactants begin to form aggregated structures such as micelles, which are composed of a monolayer of saponin molecules in which the anionic, hydrophilic head groups are oriented towards the surrounding aqueous solution and the nonpolar tails are oriented towards the hydrophobic center of the micelle (Chen et al., 2008). To the best of our knowledge, the CMCs have not been previously measured in extract obtained from BGR. Based on the results of this study, the selected biosurfactant concentrations were 1.5 and 3.0%, w/w, which was above the CMC, for micelle formation. Therefore, biosurfactant-to-oil mass ratios of 1:1 and 1:2 were used in this work.

3.2 Interfacial tension

Oil and water do not mix because of the high interfacial tension between these two phases. Surfactants are added to reduce interfacial tension and allow dispersed media to be created easily. Additionally, surfactants create an energy barrier between the oil droplets, which prevent the droplets from coalescing. According to the theory of interfacial tension, the molecules of one of the phases adsorb at the interface between the two liquids.

Therefore, the lower the interfacial tension, the greater the adsorption of surfactant at the interface (Abismaıl et al., 1999, Stamkulov et al., 2009, Spinelli et al., 2010).

The interfacial tension between annatto oil and water was approximately 13.4 ± 0.4 $mN \cdot m^{-1}$ and 18.0 ± 0.1 $mN \cdot m^{-1}$ between soybean oil and water. Fig. 1 shows the interfacial tension of the oil-water-biosurfactant systems as a function of time at both study concentrations. These results demonstrate the ability of both biosurfactants to lower the interfacial tension of the systems, confirming their surface activity. The commercial saponin biosurfactant causes lower interfacial tension at the oil/water interface than the BGR saponin. For *Quillaja* saponin and Tween 80 surfactants, Yang et al. (2013) observed that the interfacial tension decreased appreciably with increasing surfactant concentrations, indicating that the surfactants adsorbed in the oil-water interface, reaching approximately 5 $mN \cdot m^{-1}$ at interfacial saturation.

Fig. 1 shows that the interfacial tension between the biosurfactant solution and oil is reduced slightly with the increased biosurfactant concentration. This finding would indicate that the emulsion is close to interfacial saturation with the biosurfactants at these two concentrations. A very low interfacial tension value (~ 1 $mN \cdot m^{-1}$) was obtained between annatto oil and the commercial biosurfactant solution. This decrease in interfacial tension was associated with the low viscosity and the density difference between the phases and made drop detachment easier.

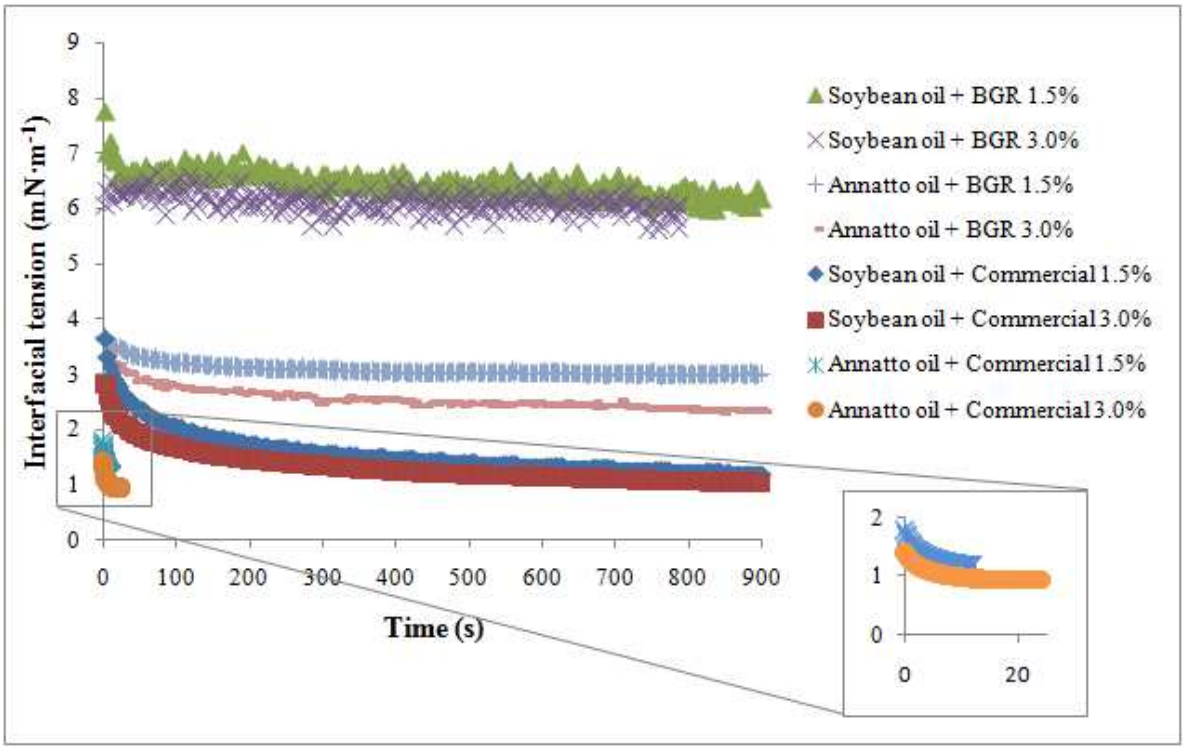

Fig. 1: Interfacial tension between the oil and aqueous phase, which contains the biosurfactant, as a function of time at both concentrations.

3.3 Emulsion droplet size

Depending on the mean droplet size of the dispersed phase, emulsions are generally classified into nano (0.01 - 0.1 µm), mini (0.1 - 1 µm) and macroemulsions (0.5- 100µm) (Windhab et al., 2005). Microemulsions are composed by swollen micelles (0.05 - 0.1 µm) with a translucent appearance, produced by self-assembly of the surfactant molecules and do not require energy for formation (low-energy process) (Santana et al., 2013). The fundamental difference between micro and nanoemulsions systems is given in terms of their thermodynamic stabilities; nanoemulsions are thermodynamically unstable, whereas microemulsions are thermodynamically stable (Mason et al., 2006, McClements, 2012). Because of the characteristic size of nanoemulsions, they appear transparent or translucent

to the naked eye and possess stability against sedimentation or creaming (Solans et al., 2005). However, both mini and macroemulsions, which are also thermodynamically unstable, tend to drop re-coalescence and phase separation (Windhab et al., 2005). Only miniemulsions were obtained in this work; their droplet sizes ranged from 0.348 ± 0.005 to 0.831 ± 0.002 μm, depending on the operational conditions. Table 2 presents the droplet size and the span of each prepared emulsion. The span values were used to express the degree of size distribution and polydispersity. The high span value of the emulsion implies a wide size distribution and a high polydispersity. The span values, shown in Table 2, are around 2, which indicate a narrow and uniform distribution (Gottlieb and Schwartzbach, 2004).

Table 2: The droplet size (μm), span (μm), emulsion stability (%), zeta potential (mV) and pH for each experiment.

Experiment	Droplet size – D_{32} (μm)	Span (μm)	Emulsion Stability (%)	Zetapotential (mV)	pH
1	0.82±0.02	2.168±0.004	97.68±0.00	-53.2±0.4	5.54±0.00
2	0.607±0.004	2.191±0.006	97.49±0.00	-53.5±0.6	5.73±0.04
3	0.590±0.008	2.26±0.03	97.41±0.00	-47.3±0.1	5.38±0.02
4	0.52±0.01	1.88±0.01	98.2±0.1	-49.9±0.9	5.42±0.01
5	0.591±0.008	2.23±0.02	99.1±0.8	-52.1±0.3	5.51±0.00
6	0.75±0.02	2.042±0.002	98.76±0.05	-53.3±0.4	5.43±0.01
7	0.710±0.001	2.02±0.02	96.6±0.3	-53.8±0.0	5.81±0.02
8	0.456±0.004	2.071±0.002	97.42±0.05	-49.3±0.4	5.39±0.01
9	0.458±0.002	2.113±0.006	98.13±0.00	-49.1±0.6	5.93±0.04
10	0.70±0.02	2.13±0.03	97.5±0.7	-54.0±1.1	5.47±0.04
11	0.436±0.006	2.02±0.01	97.9±0.2	-51.9±0.0	5.78±0.02
12	0.543±0.000	2.023±0.008	96.84±0.00	-51.4±0.2	5.34±0.01
13	0.790±0.000	2.338±0.001	95.64±0.01	-44.7±0.3	5.77±0.01
14	0.775±0.003	2.32±0.08	96.4±0.2	-56.7±0.1	5.49±0.01
15	0.348±0.005	1.76±0.03	98.3±0.2	-48.7±0.6	5.33±0.02
16	0.641±0.007	2.246±0.002	95.7±0.3	-55.5±0.6	5.28±0.01
17	0.400±0.004	1.858±0.001	98.51±0.00	-52.6±0.5	5.38±0.01
18	0.404±0.003	2.053±0.006	97.6±0.4	-49.3±0.4	5.20±0.01
19	0.440±0.002	2.039±0.002	97.79±0.05	-47.6±0.3	5.31±0.01
20	0.450±0.009	2.16±0.02	97.33±0.05	-54.1±0.6	5.91±0.01
21	0.562±0.001	2.328±0.007	96.74±0.00	-51.1±0.1	5.28±0.02
22	0.82±0.02	2.3±0.1	97.0±0.9	-50.6±1.2	5.25±0.07
23	0.831±0.002	2.086±0.008	98.9±0.9	-41.6±0.1	5.40±0.01
24	0.67±0.01	2.34±0.01	96.19±0.00	-41.5±0.2	5.38±0.01
25	0.733±0.001	2.117±0.006	96.84±0.00	-39.1±0.4	5.76±0.01
26	0.613±0.001	2.202±0.001	97.1±0.2	-35.7±0.6	5.52±0.02
27	0.501±0.008	2.179±0.008	97.95±0.01	-38.6±0.1	5.2±0.1
28	0.368±0.000	1.919±0.005	98.70±0.00	-35.6±0.4	5.35±0.01
29	0.678±0.008	2.43±0.01	96.66±0.01	-43.7±0.2	5.38±0.00
30	0.539±0.006	2.218±0.006	97.77±0.00	-50.7±0.5	5.42±0.08
31	0.484±0.003	2.179±0.001	97.6±0.2	-47.4±0.4	5.34±0.03
32	0.578±0.002	2.228±0.004	98.70±0.00	-51.0±0.4	5.40±0.02

From the analysis of variance (ANOVA) of the variables studied for the response variable emulsion droplet size (Table 3), it can be observed that the process, oil, biosurfactant, ED and the interaction between the biosurfactant and the ED had a significant influence on the emulsion droplet size with a 95% confidence level.

Table 3: An analysis of variance (ANOVA) for the studied variables on the emulsion droplet size.

Variation source	Degrees of freedom	Square sum	Meanssquare	F	*p-value*
Process	1	0.098402	0.098402	32.60	0.000
Oil	1	0.195860	0.195860	64.89	0.000
Biosurfactant	1	0.134486	0.134486	44.56	0.000
Biosurfactant concentration	1	0.012780	0.012780	4.23	0.056
Energy density	1	0.017414	0.017414	5.77	0.029
Process*Oil	1	0.012383	0.012383	4.10	0.060
Process*Biosurfactant	1	0.011877	0.011877	3.94	0.065
Process*Biosurfactant concentration	1	0.003518	0.003518	1.17	0.296
Process*Energy density	1	0.007095	0.007095	2.35	0.145
Oil*Biosurfactant	1	0.000071	0.000071	0.02	0.880
Oil*Biosurfactant concentration	1	0.000671	0.000671	0.22	0.644
Oil*Energy density	1	0.000012	0.000012	0.00	0.951
Biosurfactant*Biosurfactant concentration	1	0.000708	0.000708	0.23	0.635
Biosurfactant*Energy density	1	0.089200	0.089200	29.55	0.000
Biosurfactant concentration*Energy density	1	0.001018	0.001018	0.34	0.569
Error	16	0.048293	0.003018		
Total	31	0.633787			

Fig. 2 shows the mean values of the emulsion droplet size as a function of the statistically significant variables, which were the process, oil, biosurfactant and ED.The purpose of our initial experiments was to determine the minimum droplet size that could be produced under homogenization conditions. There is a desire to decrease the droplet size to maximize the positive attributes in a product (Henry et al., 2009). After 1 h, the droplet

sizes were somewhat different for the selected biosurfactants. BGR saponins gave the smallest droplet size. Differences in the effectiveness of the studied biosurfactants may be explained by the speed at which they adsorb to the oil-water interface, their ability to reduce the oil-water interface tension and their effectiveness at generating repulsive interactions between droplets (Jafari et al., 2008). It should be stressed that the commercial and BGR biosurfactants are actually compositionally complex mixtures. In comparison with this work, smaller droplets were achieved by Yang et al. (2013) by using Tween 80 (0.12 μm) and *Quillaja* saponin (0.17 μm) by microfluidization. However, the droplets obtained with *Quillaja* saponin were not as small as those produced by using Tween 80 under similar conditions, and thus the authors concluded that *Quillaja* saponin was capable of forming relatively small droplets. Some investigators believe that microfluidization is superior to other emulsification devices. Jafari et al. (2007) observed that the emulsion droplet size is in the order microfluidizer< US < IKA mixer, which is consistent with the results of the present work.

Henry et al. (2009) suggest that the homogenization process is the primary factor that determines the droplet size. At present, emulsions are typically prepared in the food industry by using high intensity methods (Rao and McClements, 2011). The influence of the homogenization process on the emulsion droplet size was observed. The US process yielded a smaller droplet size than the DR process at the same ED. This finding is expected because US causes more efficient droplet disruption (cavitation along with shear and inertia forces). However, the DR was a more efficient tool for dispersing the emulsion particles than the US. Although a pre-emulsion was prepared for all the processes, DR is able to

produce emulsions directly from the two separate phases, but it is always necessary to produce a pre-emulsion before the process when using US.

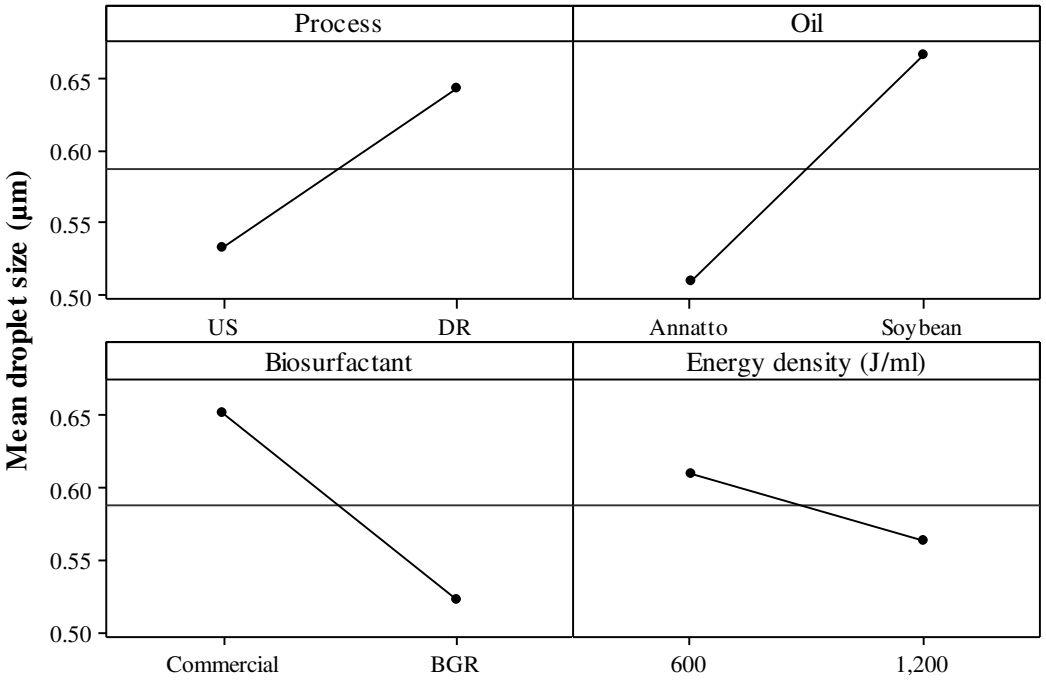

Fig. 2: A primary effects plot of the statistically significant variables on the emulsion droplet size.

The amount of shear increased with the ED at the studied ED values, and then the emulsion droplet size decreased with increasing shear. Conventionally, this finding is expected. However, some studies have demonstrated an effect described as "over-processing", in which the droplet size increases at higher power levels (Kentish et al., 2008). This effect, which is caused by re-coalescence, was observed when using commercial saponins.

The minimum droplet size that could be produced was obtained by using annatto oil and 1.5 % BGR saponins under US at 1,200 $J.mL^{-1}$, which corresponds to experiment 15. Experiment 28, which was prepared with annatto oil and 3.0 % BGR saponins under DR at

1,200 $J.mL^{-1}$, also presented a smaller emulsion droplet size. Both experiments were selected for microscopic examination and rheological behavior analysis.

3.4 Emulsion stability

The emulsion stability (ES) was investigated visually. All samples were opaque (Fig. 3) and exhibited phase separation after being stored overnight. A reversible phenomenon involving droplet aggregation and migration was observed, followed by creaming, because the density of the dispersed phase (oil) was lower than that of the continuous phase (water) (Abismaıl et al., 1999). Fungal growth was observed in some emulsions containing soybean oil on the 5^{th} day. Therefore, the ES was determined on the 4^{th} day. The ES (%) values of each experiment are shown in Table 2, ranging from 95.6 to 99.1 %, showing that the emulsions are rather stable, with some creaming. As observed in Fig. 4, the size distribution of the emulsion droplets is bimodal. The shape of the distribution curve was found to be similar at both biosurfactant concentrations. According to Dickinson et al. (2003), a bimodal droplet-size distribution was accepted an indicator of non-reversible flocculation. The size distribution behavior of the emulsions showed that the use of BGR saponins produced narrower size distributions (less span) than the use of commercial saponins (Table 2).

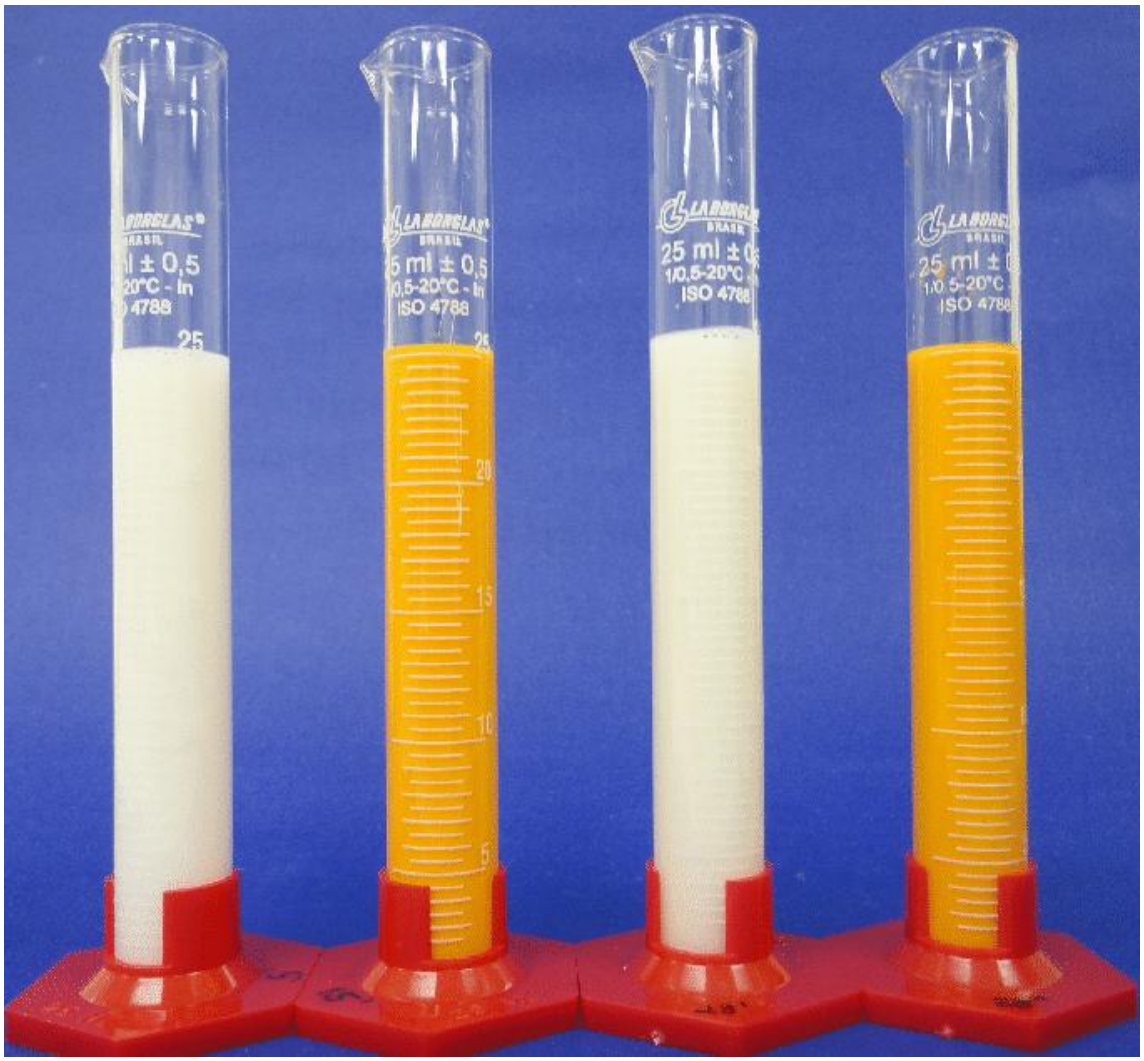

Fig. 3: The overall appearance of o/w mini-emulsions. From left to right: Experiments 5, 15, 23 and 28. Exp. 5: Soybean oil and 1.5% commercial saponins under US at 600 $J.mL^{-1}$. Exp 15: Annatto oil and 1.5% BGR saponins under US at 1,200 $J.mL^{-1}$. Exp 23: Soybean oil and 3.0% commercial saponins under DR at 600 $J.mL^{-1}$. Exp 28: Annatto oil and 3.0% BGR saponins under DR at 1,200 $J.mL^{-1}$.

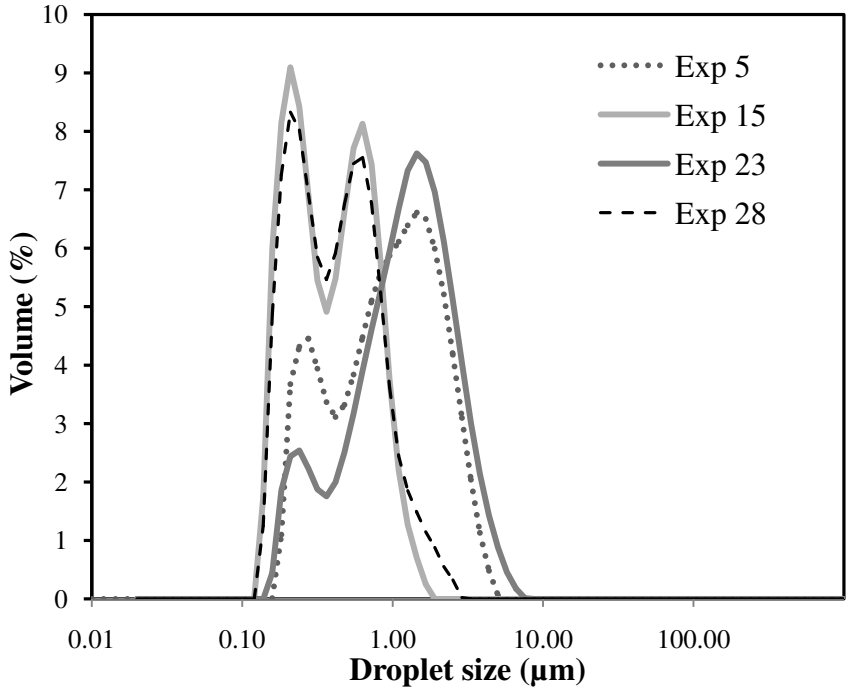

Fig. 4: The droplet size distribution of the selected emulsions. Exp. 5: Soybean oil and 1.5% commercial saponins under US at 600 $J.mL^{-1}$. Exp 15: Annatto oil and 1.5% BGR saponins under US at 1,200 $J.mL^{-1}$. Exp 23: Soybean oil and 3.0% commercial saponins under DR at 600 $J.mL^{-1}$. Exp 28: Annatto oil and 3.0% BGR saponins under DR at 1,200 $J.mL^{-1}$.

The ANOVA (Table 4) showed that only the emulsification process significantly affected the ES values. US makes emulsions more stable (Fig. 5). The mechanical vibration and acoustic cavitation from US are responsible for mixing two immiscible phases and leading to emulsion formation, and the shear forces generated by the US are responsible for a decreased emulsion droplet size that results in the stability of the emulsions (Shanmugam and Ashokkumar, 2014). Abismaıl et al. (1999) also observed a much higher stability of US-made emulsions than those prepared with an Ultra-Turrax. In another work, Shanmugam and Ashokkumar (2014) found similar results with respect to emulsion stability. They concluded that the Ultra-Turrax did not produce stable emulsions until after

20 min of processing, suggesting the superiority of the US emulsification process at a similar energy density.

Table 4: An analysis of variance (ANOVA) for the studied variables on the emulsion stability (%).

Variation source	Degrees of freedom	Square sum	Means square	F	*p-value*
Process	1	32.786	327.858	5.57	0.031
Oil	1	0.0990	0.09898	0.17	0.687
Biosurfactant	1	0.2510	0.25097	0.43	0.523
Biosurfactant concentration	1	0.0530	0.05297	0.09	0.768
Energy density	1	0.2589	0.25892	0.44	0.517
Process*Oil	1	0.3837	0.38373	0.65	0.431
Process*Biosurfactant	1	0.4408	0.44080	0.75	0.400
Process*Biosurfactant concentration	1	0.0000	0.00001	0.00	0.997
Process*Energy density	1	10.110	101.099	1.72	0.209
Oil*Biosurfactant	1	87.800	877.995	14.91	0.001
Oil*Biosurfactant concentration	1	0.0269	0.02693	0.05	0.833
Oil*Energy density	1	0.0561	0.05609	0.10	0.762
Biosurfactant *Biosurfactant concentration	1	0.2331	0.23314	0.40	0.538
Biosurfactant *Energy density	1	11.441	114.413	1.94	0.182
Biosurfactant concentration*Energy density	1	0.0358	0.03584	0.06	0.808
Error	16	94.247	0.58904		
Total	31	254.767			

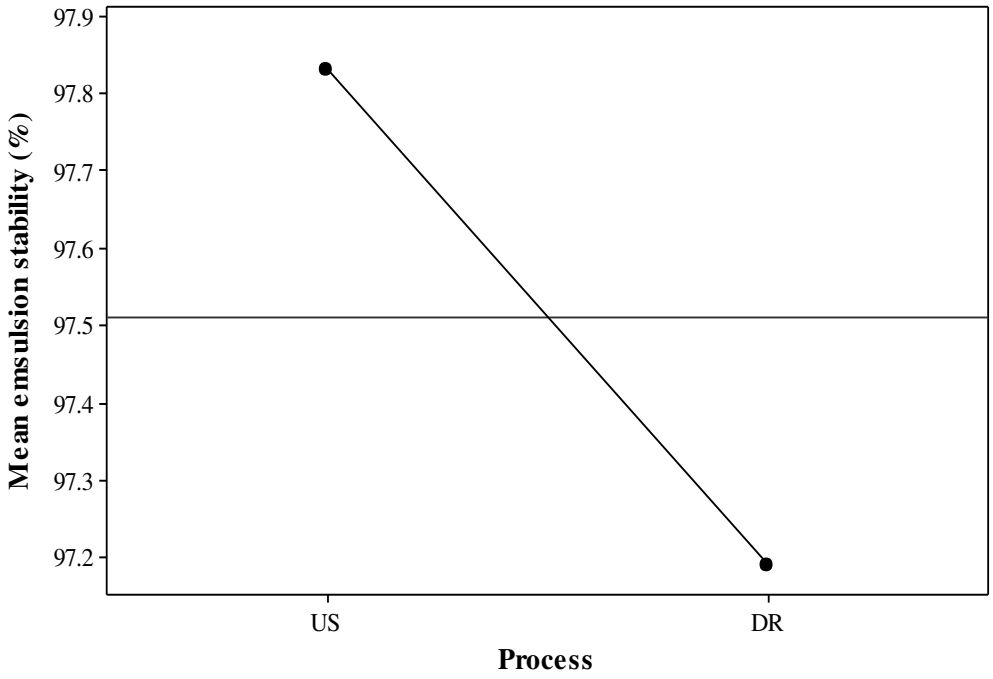

Fig. 5: A primary effect plot of the statistically significant variable on the emulsion stability (%) after 4 days at 17 °C.

The interaction effects between the oil and the biosurfactant type are presented in Fig. 6. As mentioned, the emulsions exhibited evidence of creaming, with an opaque cream layer at the top and a slightly turbid serum layer at the bottom. For the commercial saponins, the emulsions containing soybean oil were more stable. However, BGR saponins allowed for better stability with annatto oil. During the emulsification process, the commercial saponins provided easier oil incorporation than the BGR saponins, which led to oil loss during the process. The better ES obtained for annatto oil could be caused by the lower amount of incorporated oil, contributing to a smaller phase separation.

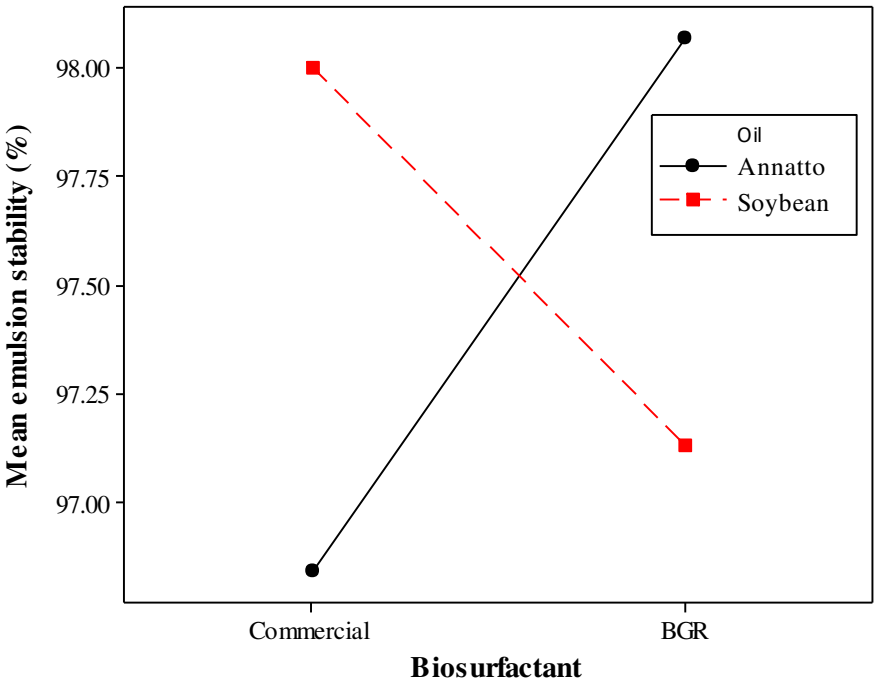

Fig. 6: An interaction effect plot of the statistically significant variable on the emulsion stability (%).

The emulsion stability can also be evaluated by the zeta potential. According to the ANOVA, there was no significant influence on the zeta potential at a 95% confidence level. A high zeta potential (positive or negative) will confer resistance to aggregation; however, when it is low, the attraction exceeds the repulsion and the dispersion will break and flocculate (Silva et al., 2012). At pH values between approximately 5.2 and 5.9, the zeta potential of the emulsions ranged from -56.7 to -35.6 mV. These values are strongly negative, which resulted in droplet-to-droplet repulsion and minimized the flocculation of the oil droplets. Salvia-Trujillo et al. (2013) studied the effects of the US parameters on the electrical charge of the lemongrass oil droplet surface, and they stated that the zeta potential of oil drops ranged between -46 ± 3 and -56 ± 6 mV when the sonication time was extended up to 3 minutes. In this study, the most stable emulsions were generated during experiments

5 and 23, both of which employed soybean oil and commercial saponins at an ED of 600 $J.mL^{-1}$, which were also selected for microscopic examination and rheological behavior. Fig. 7 shows the micrographs of the selected emulsions. The micrographs are consistent with the results obtained for the size measurement.

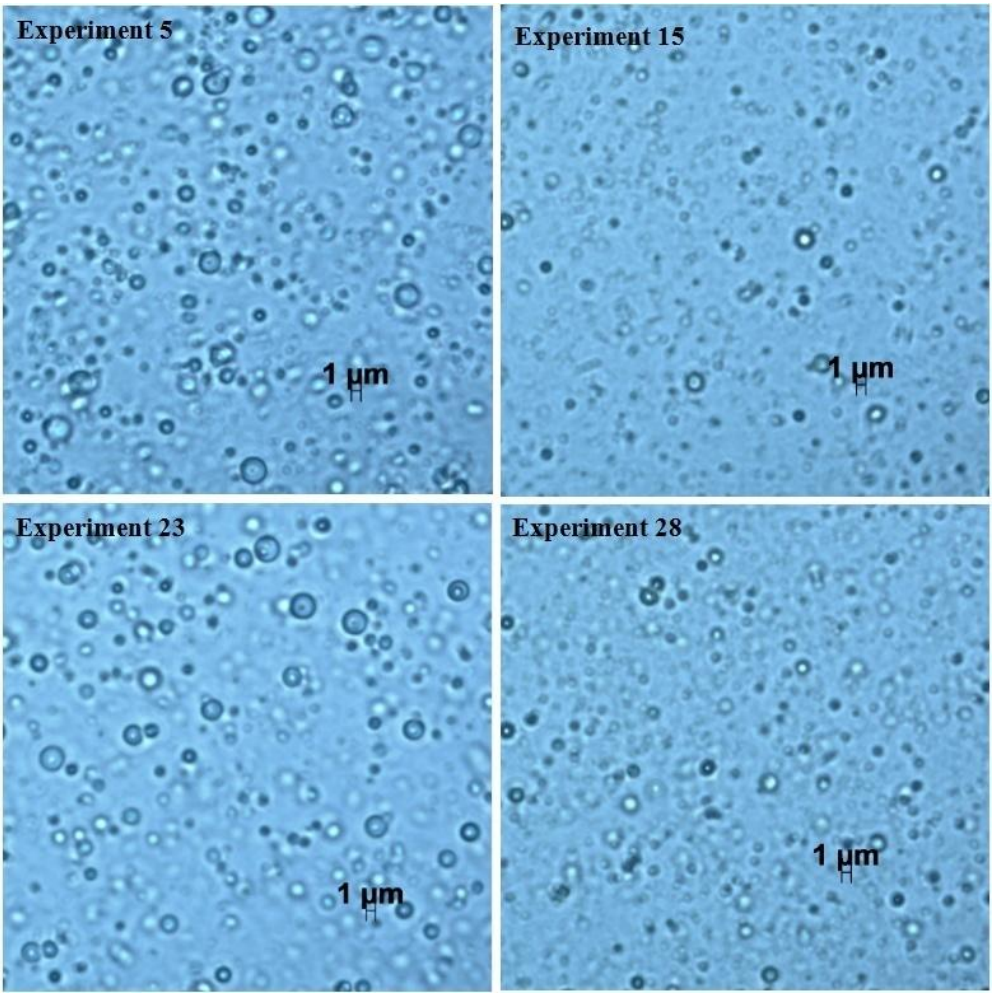

Fig. 7: Photomicrographs of the selected emulsions. Exp. 5: Soybean oil and 1.5% commercial saponins under US at 600 $J.mL^{-1}$. Exp 15: Annatto oil and 1.5% BGR saponins under US at 1,200 $J.mL^{-1}$. Exp 23: Soybean oil and 3.0% commercial saponins under DR at 600 $J.mL^{-1}$. Exp 28: Annatto oil and 3.0% BGR saponins under DR at 1,200 $J.mL^{-1}$.

3.5 Rheological behavior

Oil-in-water emulsions prepared from dilute surfactant solutions generally behave as Newtonian fluids at low values of the dispersed-phase (oil) volume fraction (Pal, 1992).

The flow curves of the selected emulsions were fitted to the Newtonian model. The relationship between the apparent viscosity and the shear rate of the selected experiments are presented in Fig. 8 and the rheological parameters in Table 5. These results show that all the emulsions presented Newtonian flow behavior and a viscosity similar to that of water. Because of the low viscosities, an anomalous flow behavior was observed at shear rates above 200 s^{-1}. At high shear rates, the systems were not performed in the laminar flow region, which is the necessary condition for rheological assays. Therefore, the flow curves of the emulsions were fitted to the Newtonian model by using shear rate data up to 200 s^{-1}. Dickinson et al. (2003) showed that the concentration of added non-ionic surfactant (Tween 20) affects the emulsion rheology. The authors observed that adding a moderately low level of Tween 20 causes the emulsion to become essentially Newtonian, with a very low viscosity. With further increases in the Tween 20 concentrations, the emulsion became destabilized as a result of surfactant-induced depletion flocculation, leading to an increase of almost three orders of magnitude in the low-stress viscosity and the onset of substantial shear-thinning behavior.

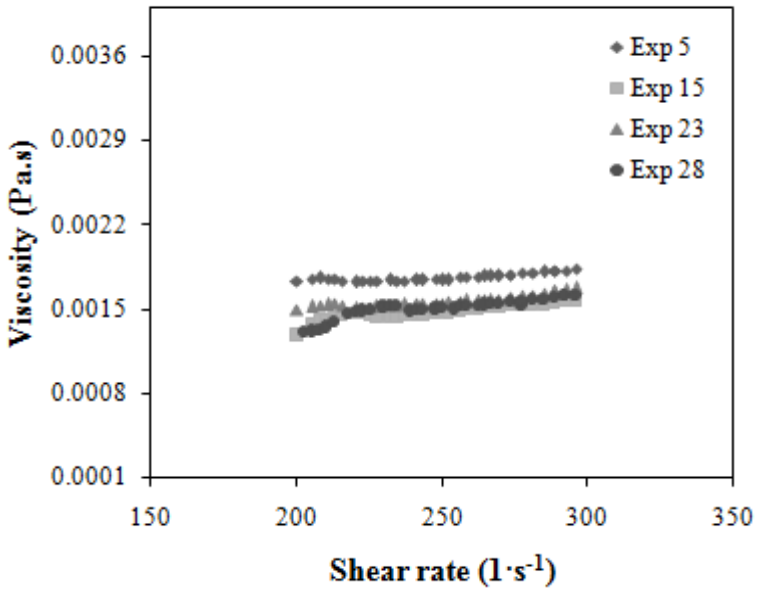

Fig.8: Viscosity-shear rate profile at 25 °C of the selected experiments.

Table 5: Rheological parameters obtained from the Newtonian model for the selected emulsions (25 °C).

Experiment	η (mPa·s)*	R^2
5	1.60 ± 0.05^{a}	0.924
15	1.285 ± 0.003^{b}	0.984
23	1.412 ± 0.004^{c}	0.960
28	1.348 ± 0.001^{bc}	0.983

*Values with the same letter are not significantly different.

4 Conclusions

We have performed a detailed study of the O/W miniemulsion preparation containing δ-tocotrienol-rich oil and a natural food-grade biosurfactant, namely the BGR saponins. The findings of our study clearly showed that the emulsification method influenced and determined the final properties of the mini-emulsions. Although US produced more stable and smaller emulsion droplet sizes when compared with the DR, the energy density is a parameter that must be considered. Overall, the miniemulsion prepared with δ-tocotrienol-rich oil and BGR saponins presented the smallest droplet size, in which enhanced the stability of these emulsions. Our results showed that BGR saponin might be an attractive biosurfactant choice for emulsion formulations. An extension of this work would require the evaluation of other factors for successful applications in the food and beverage industry, such as the taste profile, potential toxicity, reliability of supply, and cost.

ACKNOWLEDGMENTS

Maria Thereza M. G. Rosa and Eric Kevin Silva would like to thank the National Council of Technological and Scientific Development (CNPq, processes 140641/2011-4 and 140275/2014-2) for a doctoral fellowship. M. Angela A. Meireles thanks CNPq for the productivity grant (301301/2010-7). The authors acknowledge thefinancial support from CNPq and FAPESP (processes 2009/17234-9;2012/10685-8). The authors are grateful to Dr. Eliane G. Fabri from the Agronomic Institute of Campinas for donating the annatto seeds.

REFERENCES

ABISMAıL, B., CANSELIER, J. P., WILHELM, A. M., DELMAS, H. & GOURDON, C. 1999. Emulsification by ultrasound: drop size distribution and stability. *Ultrasonics Sonochemistry,* 6**,** 75-83.

AGGARWAL, B. B., SUNDARAM, C., PRASAD, S. & KANNAPPAN, R. 2010. Tocotrienols, the vitamin E of the 21st century: its potential against cancer and other chronic diseases. *Biochemical pharmacology,* 80**,** 1613-1631.

ALBUQUERQUE, C. L. & MEIRELES, M. A. A. 2012. Defatting of annatto seeds using supercritical carbon dioxide as a pretreatment for the production of bixin: Experimental, modeling and economic evaluation of the process. *The Journal of Supercritical Fluids,* 66**,** 86-95.

AOAC 1997. *Official of Analysis,* Washington, DC, Association of Official Analytical Chemists.

AOCS 2004. *Official Methods and Recommended Practices of the American Oil Chemists' Society,* Champaign, USA, American Oil Chemists' Society Press.

CHANDRAPALA, J., OLIVER, C., KENTISH, S. & ASHOKKUMAR, M. 2012. Ultrasonics in food processing. *Ultrasonics sonochemistry,* 19**,** 975-983.

CHEN, W.-J., HSIAO, L.-C. & CHEN, K. K.-Y. 2008. Metal desorption from copper (II)/nickel (II)-spiked kaolin as a soil component using plant-derived saponin biosurfactant. *Process Biochemistry,* 43**,** 488-498.

CHEOK, C. Y., SALMAN, H. A. K. & SULAIMAN, R. 2014. Extraction and quantification of saponins: A review. *Food Research International,* 59**,** 16-40.

COOPER, D. G. & GOLDENBERG, B. G. 1987. Surface-active agents from two Bacillus species. *Applied and environmental microbiology,* 53**,** 224-229.

DEBIEN, I. C. N. & MEIRELES, M. A. A. 2014. Supercritical Fluid Extraction of Beta-ecdysone from Brazilian Ginseng (*Pfaffia glomerata*) Roots. *Food and Public Health,* 4**,** 67-73.

DICKINSON, E., RADFORD, S. J. & GOLDING, M. 2003. Stability and rheology of emulsions containing sodium caseinate: combined effects of ionic calcium and non-ionic surfactant. *Food Hydrocolloids,* 17**,** 211-220.

GOTTLIEB, N. & SCHWARTZBACH, C. Development of an internal mixing two-fluid nozzle by systematic variation of internal parts. 19th Annual Meeting of ILASS (Europe) Conference Proceedings, Nottingham, UK, 2004. 97.

HENRY, J. V., FRYER, P. J., FRITH, W. J. & NORTON, I. T. 2009. Emulsification mechanism and storage instabilities of hydrocarbon-in-water sub-micron emulsions stabilised with Tweens (20 and 80), Brij 96v and sucrose monoesters. *Journal of colloid and interface science,* 338**,** 201-206.

JAFARI, S. M., ASSADPOOR, E., HE, Y. & BHANDARI, B. 2008. Re-coalescence of emulsion droplets during high-energy emulsification. *Food hydrocolloids,* 22**,** 1191-1202.

JAFARI, S. M., HE, Y. & BHANDARI, B. 2007. Production of sub-micron emulsions by ultrasound and microfluidization techniques. *Journal of Food Engineering,* 82**,** 478-488.

KENTISH, S., WOOSTER, T., ASHOKKUMAR, M., BALACHANDRAN, S., MAWSON, R. & SIMONS, L. 2008. The use of ultrasonics for nanoemulsion preparation. *Innovative Food Science & Emerging Technologies,* 9**,** 170-175.

MASON, T. G., WILKING, J., MELESON, K., CHANG, C. & GRAVES, S. 2006. Nanoemulsions: formation, structure, and physical properties. *Journal of Physics: Condensed Matter,* 18**,** R635.

MCCLEMENTS, D. J. 2012. Nanoemulsions versus microemulsions: terminology, differences, and similarities. *Soft Matter,* 8**,** 1719-1729.

MENRAD, K. 2003. Market and marketing of functional food in Europe. *Journal of food engineering,* 56**,** 181-188.

MIRONENKO, N., BREZHNEVA, T., POYARKOVA, T. & SELEMENEV, V. 2010. Determination of some surface-active characteristics of solutions of triterpene saponin derivatives of oleanolic acid. *Pharmaceutical chemistry journal,* 44**,** 157-160.

MITRA, S. & DUNGAN, S. R. 2000. Micellar properties of quillaja saponin. 2. Effect of solubilized cholesterol on solution properties. *Colloids and surfaces B: Biointerfaces,* 17**,** 117-133.

OLESZEK, W. & HAMED, A. 2010. Saponin-based surfactants. *In:* KJELLIN, M. & JOHANSSON, I. (eds.) *Surfactants from Renewable Resources.* United Kingdom: John Wiley & Sons Ltd.

PAL, R. 1992. Rheological behaviour of concentrated surfactant solutions and emulsions. *Colloids and surfaces,* 64**,** 207-215.

RAO, J. & MCCLEMENTS, D. J. 2011. Food-grade microemulsions, nanoemulsions and emulsions: fabrication from sucrose monopalmitate & lemon oil. *Food Hydrocolloids,* 25**,** 1413-1423.

SALVIA-TRUJILLO, L., ROJAS-GRAÜ, A., SOLIVA-FORTUNY, R. & MARTÍN-BELLOSO, O. 2013. Physicochemical characterization of lemongrass essential oil–alginate nanoemulsions: effect of ultrasound processing parameters. *Food and Bioprocess Technology,* 6**,** 2439-2446.

SANTANA, R., PERRECHIL, F. & CUNHA, R. 2013. High-and low-energy emulsifications for food applications: a focus on process parameters. *Food Engineering Reviews,* 5**,** 107-122.

SANTOS, D. T., BARBOSA, D. F., BROCCOLO, K., GOMES, M. T. M. S., VARDANEGA, R. & MEIRELES, M. A. A. 2012. Pressurized organic solvent extraction with on-line particle formation by supercritical anti solvent processes. *Food and Public Health,* 2**,** 231-240.

SCHAUSS, A. G., ENDREDD, J. R. & CLEWELL, A. 2013. Safety of unsaturated Vitamin E Tocotrienols ans their isomers. *In:* TAN, B., WATSON, R. R. & PREEDY, V. R. (eds.) *Tocotrienols: vitamin E beyond tocopherols.* Boca Raton: CRC Press.

SHANMUGAM, A. & ASHOKKUMAR, M. 2014. Ultrasonic Preparation of Stable Flax seed Oil Emulsions in Dairy Systems–Physicochemical Characterization. *Food Hydrocolloids,* 39**,** 151-162.

SILVA, G., GAMARRA, F., OLIVEIRA, A. & CABRAL, F. 2008. Extraction of bixin from annatto seeds using supercritical carbon dioxide. *Brazilian Journal of Chemical Engineering,* 25**,** 419-426.

SILVA, H. D., CERQUEIRA, M. Â. & VICENTE, A. A. 2012. Nanoemulsions for food applications: development and characterization. *Food and Bioprocess Technology,* 5**,** 854-867.

SKURTYS, O. & AGUILERA, J. 2009. Formation of O/W macroemulsions with a circular microfluidic device using saponin and potato starch. *Food hydrocolloids,* 23**,** 1810-1817.

SMITH, J. 2006. Annatto extracts–chemical and technical assessment. *Chemical and Technical Assessment Manual***,** 1-21.

SOLANS, C., IZQUIERDO, P., NOLLA, J., AZEMAR, N. & GARCIA-CELMA, M. 2005. Nano-emulsions. *Current Opinion in Colloid & Interface Science,* 10**,** 102-110.

SPINELLI, L. S., MANSUR, C. R., GONZÁLEZ, G. & LUCAS, E. F. 2010. Evaluation of process conditions and characterization of particle size and stability of oil-in-water nanoemulsions. *Colloid journal,* 72**,** 56-65.

STAMKULOV, N. S., MUSSABEKOV, K. B., AIDAROVA, S. B. & LUCKHAM, P. F. 2009. Stabilisation of emulsions by using a combination of an oil soluble ionic surfactant and water soluble polyelectrolytes. I: emulsion stabilisation and interfacial tension measurements. *Colloids and Surfaces A: Physicochemical and Engineering Aspects,* 335**,** 103-106.

SYLVESTER, P. & THERIAULT, A. 2003. Role of tocotrienols in the prevention of cardiovascular disease and breast cancer. *Current Topics in Nutraceutical Research,* 1**,** 121-136.

TAN, B. 2011. *Tocotrienols: The New Vitamin E* [Online]. Spacedoc. Available: http://www.spacedoc.com/tocotrienols [Accessed 18 june 2014.

VARDANEGA, R., SANTOS, D. T. & MEIRELES, M. A. M. Obtaining bioactive compounds from Brazilian ginseng roots using pressurized water. European meeting on supercritical fluids, 2014.

WINDHAB, E., DRESSLER, M., FEIGL, K., FISCHER, P. & MEGIAS-ALGUACIL, D. 2005. Emulsion processing—from single-drop deformation to design of complex processes and products. *Chemical Engineering Science,* 60**,** 2101-2113.

XIONG, J., GUO, J., HUANG, L., MENG, B. & PING, Q. 2008. Self-micelle formation and the incorporation of lipid in the formulation affect the intestinal absorption of Panax notoginseng. *International journal of pharmaceutics,* 360**,** 191-196.

YANG, Y., LESER, M. E., SHER, A. A. & MCCLEMENTS, D. J. 2013. Formation and stability of emulsions using a natural small molecule surfactant: Quillaja saponin (Q-Naturale®). *Food hydrocolloids,* 30**,** 589-596.

YANG, Y., MARSHALL-BRETON, C., LESER, M. E., SHER, A. A. & MCCLEMENTS, D. J. 2012. Fabrication of ultrafine edible emulsions: Comparison of high-energy and low-energy homogenization methods. *Food Hydrocolloids,* 29**,** 398-406.

CAPÍTULO 6 – CONCLUSÕES GERAIS

Microfármaco de sal de ibuprofeno sódico e microemulsão do extrato rico em δ-tocotrienol das sementes de urucum foram obtidas com sucesso neste trabalho utilizando métodos que empregam 2 tecnologias emergentes: tecnologia supercrítica e ultrassom. A primeira etapa deste trabalho foi analisar o estado da arte da formação de micro e nanopartículas e encapsulação utilizando CO_2 supercrítico, que está apresentada nos **Capítulos 1, 2 e 3**.

A pesquisa mostrou as potencialidades do emprego do CO_2 supercrítico para obtenção de partículas com as características desejadas. A técnica de maior enfoque apresentada no **Capítulo 2** foi o SFEE (Supercritical Fluid Extraction of Emulsions). A revisão da literatura mostrou que esta técnica permite a obtenção de partículas em escala nanométrica, mas o produto final obtido é uma suspensão aquosa, sendo necessário processo adicional para obtenção do produto em pó. Neste contexto, o **Capítulo 3** focou nas técnicas CAN-BD e PGSS-drying, que empregam CO_2 supercrítico para eliminação da água. A revisão mostrou o potencial da aplicação desses processos para obtenção de produtos para a indústria de alimentos, que é algo ainda pouco explorado na literatura. Adicionamente verificou-se a potencialidade de se utilizar ambos os processos para a eliminação de água de emulsões óleo em água, na qual o óleo é a fase dispersa e a água é a fase contínua, como as que foram preparadas contendo o extrato rico em δ-tocotrienol (**Capítulo 5**). O uso do CO_2 supercrítico para obtenção de micro/nanopartículas e encapsulação pode ser uma alternativa viável para as técnicas convencionais e o interesse do seu emprego para compostos bioativos vem aumentando nos últimos tempos.

Assim, a etapa seguinte foi validar a unidade SAS/SFEE, que emprega CO_2 supercrítico para formação de micro e nanopartículas e encapsulação, utilizando uma substância modelo, o sal de ibuprofeno sódico. Este trabalho foi apresentado no **Capítulo 4**. Sal de ibuprofeno sódico foi micronizado com sucesso via SAS utilizando a unidade construída pelo grupo de pesquisa do LASEFI. Com uma seleção adequada das condições operacionais foi possível obter micropartículas com diferentes morfologias, como na forma de agulha, de flocos e de folhas. A morfologia da partícula pode influir na facilidade de comprimir e na propriedade de fluidez do composto. A literatura mostra que a morfologia de folhas é a mais indicada para o processo de compressão. Desta forma, foi possível obter micropartículas de ibuprofeno sódico na forma de folhas apresentando baixo

teor de solvente residual (4,7 $mg \cdot kg^{-1}$), e alto rendimento de precipitação (70 %). O menor custo energético por unidade de produto processado (7,2 $US\$ \cdot kg^{-1}$) foi obtido aplicando a vazão de solução de 1 $mL \cdot min^{-1}$ e concentração da solução etanólica de 0,04 $g \cdot mL^{-1}$, resultando em micropartículas com morfologia predominante na forma de agulha. As partículas obtidas pelo método convencional, utilizado para comparação, apresentaram maior tamanho e maior teor de solvente residual que as obtidas na unidade SAS/SFEE.

A próxima etapa deste trabalho foi realizar ensaios experimentais para o processamento dos compostos bioativos do urucum. Os compostos bioativos de muita importância nas sementes de urucum são os δ-tocotrienóis, que foram o objetivo de estudo no **Capítulo 5**. Extrato de óleo de urucum, rico em δ-tocotrienóis, foi emulsionado com o auxílio de um biosurfactante natural extraído das sementes de ginseng brasileiro, rico em saponinas. As emulsões foram formuladas utilizando homogeneizador do tipo Dispersor de fase múltipla e ultrassom. Emulsões mais estáveis e com menores tamanhos de gotas foram obtidas com o uso do ultrassom na mesma densidade energética aplicada no dispersor de fase contínua. Foram obtidas emulsões com tamanho de gota de 0,35 μm. Os resultados mostraram que ambos os biosurfactantes empregados foram capazes de formar emulsões com relativamente pequenas gotas (< 0,83 μm) e bastante estáveis (96 a 99 %), com pouca formação de creme. O potencial zeta medido das emulsões mostrou valores negativos ao redor de -49 mV demonstrando a capacidade dos biosurfactantes em minimizar a floculação das gotas de óleo. Este estudo mostrou que biosurfactante de extrato de ginseng pode ser uma escolha atrativa para a formulação de emulsões de produtos alimentícios e bebidas.

SUGESTÕES PARA TRABALHOS FUTUROS

Em relação à micronização utilizando o processo SAS:

- ✓ Investigar outro espectro de condições operacionais para obter partículas de sal de ibuprofeno sódico com menores tamanhos e principalmente que se concentrem na faixa caracterizada como nanopartícula;
- ✓ Estudar a cristalinidade das partículas de ibuprofeno sódico produzidas por SAS e sua taxa de dissolução;
- ✓ Utilizar outros tipos de bocais de injeção, como por exemplo, um nozzle comercial, que podem influenciar na formação das partículas;
- ✓ Realizar experimentos reutilizando o dióxido de carbono, de forma a aumentar o rendimento, diminuir custos e reduzir a emissão de CO_2 para o meio ambiente;
- ✓ Implementar um sistema eficiente para o recolhimento do produto precipitado;
- ✓ Encapsular o extrato de óleo de urucum usando a técnica SAS e também SFEE utilizando diversos biopolímeros como material de parede;
- ✓ Realizar a análise econômica completa da tecnologia SAS.

Em relação à formulação das emulsões:

- ✓ Otimizar a emulsificação ultrassônica e via dispersor de fase múltipla, avaliando diferentes tempos, potência, temperatura, etc.;
- ✓ Determinar a composição dos extratos das raízes de ginseng brasileiro e avaliar possíveis efeitos dos constituintes nas propriedades surfactantes;
- ✓ Acoplar os dois homogeneizadores para melhorar a estabilidade e tamanho de gota das emulsões preparadas.

MEMÓRIA DO PERÍODO DO DOUTORADO

A doutoranda Maria Thereza de Moraes Santos Gomes, 1ª colocada no processo seletivo de doutorado do DEA/FEA/UNICAMP, realizou as atividades de pesquisa apresentadas neste projeto de pesquisa no laboratório LASEFI, com auxílio financeiro do CNPq, processo n° 140641/2011-4, com vigência de março de 2011 a fevereiro de 2015, referente ao projeto n° 870374/1997-4.

O total de 20 créditos foram cursados. As disciplinas cursadas durante o período do doutorado foram: TP199-Seminários; TP121-Tópicos em Engenharia de Alimentos (Uso do Ciclo de Aprendizagem (PDSA) para a redação de textos científicos), TP357-Microencapsulação Aplicada a Alimentos e Nutrientes e TP121-Tópicos em Engenharia de Alimentos (Estatística). A doutoranda participou do Programa de Estágio Docente grupo C - PED C com atividades de apoio parcial à docência da disciplina TA 331-A Termodinâmica, atuando como voluntária entre 08/2011 e 12/2011, 8h semanais e 0% de carga didática e como bolsista entre 03/2012 e 06/2012, 12 h semanais e 20% de carga didática.

Antes de iniciar os procedimentos experimentais do projeto de pesquisa, a aluna participou de treinamentos organizados pelos integrantes mais experientes do laboratório. Além disso, a aluna participou em 2011 do treinamento "Extração e Particulação com Fluidos Supercríticos", oferecido pelos alunos de pós-doutorado.

A doutoranda participou em 2011 na qualidade de avaliadora de trabalhos inscritos na área de Exatas no XIX Congresso Interno de Iniciação Científica da UNICAMP. Em outubro de 2012, participou como palestrante no 1° Congresso Internacional de Ciência, Tecnologia e Desenvolvimento, realizado na Universidade de Taubaté, com o tema “Uso de fluido supercrítico para a formação de micro e nanopartículas”. No 1° semestre de 2013, a doutoranda em conjunto com sua orientadora e co-orientador prestaram consultoria para a empresa Instituto Vita Nova com a realização de uma revisão da literatura para a identificação de oportunidades de aplicações de fluido supercrítico para formação de micro e nanopartículas de fármacos/drogas.

No segundo semestre de 2014, a aluna realizou o estágio de doutorado sanduíche, mediante a bolsa do Programa Institucional de bolsas de Estágio de Doutorando no Exterior

– PDSE (Processo n°. 99999.002445/2014-00). O estágio sob a co-orientação da Professora Doutora Marleny D. A. Saldaña foi realizado no período de 03 de julho a 29 de outubro de 2014, nas dependências do Department of Agricultural, Food and Nutritional Science, na University of Alberta. As propostas apresentadas no Plano de Atividades para o estágio foram previamente apreciadas e aprovadas pela Orientadora Profa. Meireles e pela co-orientadora Profa. Saldanã. O planejamento das atividades do estágio foi estruturado em: otimização das condições operacionais para a precipitação de zein utilizando a técnica de anti-solvente supercrítico (SAS), encapsulamento de diversas vitaminas utilizando o zein como material de parede pela mesma técnica SAS, caracterização das microcápsulas obtidas.

As pesquisas referentes, tanto ao projeto de Doutorado, quanto às parcerias com outros integrantes do grupo de pesquisa do LASEFI, resultaram em 2 artigos de revisão, 6 artigos experimentais, 5 capítulos de livro, 1 manuscrito (trabalho de consultoria) e 7 trabalhos publicados em anais de eventos, sendo 1 trabalho completo e 6 resumos, com participação nos eventos 9th SLACA, Campinas/SP em 2011, IUFoST, Foz do Iguaçu, em 2012 e no Workshop on supercritical fluids and energy em 2013, Campinas-SP.

Artigos completos publicados em periódicos

Silva, E.K.; **Gomes, M.T.M.S.**; Hubinger, M.D.; Cunha, R.L.; Meireles, M.A.A. Ultrasound-assisted formation of annatto seed oil emulsions stabilized by biopolymers. Food hydrocolloids, 47, p. 1-13, 2015.

Santos, D.T.; Barbosa, D.F.; Vardanega, R.; **Gomes, M.T.M.S.**; Meireles, M.A.A. Novel method to produce emulsions containing essential oils from saponin-rich pressurized aqueous plant extracts. Journal of Colloid Science and Biotechnology, in press, 2013.

Gomes, M.T.M.S.; Santos, D.T.; Meireles, M.A.A. Trends in Particle Formation of Bioactive Compounds Using Supercritical Fluids and Nanoemulsions. Food and Public Health, v. 2, p. 142-152, 2012.

Santos, D.T.; Barbosa, D.F.; Broccolo, K.; **Gomes, M.T.M.S.**; Vardanega, R.; Meireles, M.A.A. Pressurized Organic Solvent Extraction with On-line Particle Formation by Supercritical Anti Solvent Processes. Food and Public Health, v. 2, p. 231-240, 2012.

Capítulos de livro

Nogueira, G.; Rostagno, M.; **Gomes, M.T.M.S.**; Meireles, M.A.A. Fast analysis of bioactive compounds by reverse phase liquid chromatography. In: Instrumental Methods for the Analysis of Bioactive Molecules, ACS Books, 2015.

Gomes, M.T.M.S.; Santos, D.T.; Meireles, M.A.A. Micronization and encapsulation: Application of supercritical fluids in water removal. In: Conventional and advanced food processing technologies. Wiley-Blackwell, UK. 2014.

Santos, D.T.; Rodrigues, L.M.; Torres, R.A.C.; **Gomes, M.T.M.S.**; Meireles, M.A.A. Strategies for annatto seeds processing with pressurized fluids in food industries. In: Processed Foods: Quality, Safety Characteristics and Health Implications. Science Publishers, Inc. 2013.

Santos, D.T.; **Gomes, M.T.M.S.**; Vardanega R.; Rostagno, M.A.; Meireles, M.A.A. Integration of Pressurized Fluid-based Technologies for Natural Product Processing. In: Rostagno, M. A. and Prado, J. (Eds.), Natural Product Extraction: Principles and Applications. Royal Society of Chemistry, 2013.

Cavalcanti, R.N.; Forster-Carneiro, T.; **Gomes, M.T.M.S.**; Rostagno, M.A.; Prado, J.M.; Meireles, M.A.A. Uses and Applications of Extracts from Natural Sources. In: Rostagno, M. A. and Prado, J. (Eds.), Natural Product Extraction: Principles and Applications. Royal Society of Chemistry, 2013.

Trabalhos completos publicados em anais de congressos

Rodriques, L.M.; Alcazar-Alay, S.C.; **Gomes, M.T.M.S.**; Meireles, M.A.A. Pressurized liquid extraction (PLE) of bixin from defatted annatto seeds. In: III Iberoamerican Conference on Supercritical Fluids, Cartagena de Indias, p. 1-6, 2013.

Resumos publicados em anais de congress

Gomes, M.T.M.S.; Santos, D.T.; Meireles, M.A.A. A study of the particle formation of annatto extract using supercritical fluid technology. In: Workshop on supercritical fluids and energy, 2013, Campinas-SP. In.: Workshop on supercritical fluids and energy, 2013. p. 301-302.

Gomes, M.T.M.S.; Santos, D.T.; Meireles, M.A.A. Micronization of ibuprofen using a green anti-solvent by SAS. In: International Congress on "Green Extraction of Natural Products", Avignon, p. 113, 2013.

Santos, D.T.; Castillo-Torres, R.A.; Vardanega, R.; **Gomes, M.T.M.S.**; Meireles, M.A.A. Influence of Hydrostatic Pressure on Ultrasound Emulsification Using a Novel

Plant-derived Biosurfactant.. In: EFFoST Annual Meeting, 2013, Bolonha-Itália. Abstracts Book, 2013. p. 1-1.

Santos, D.T.; **Gomes, M.T.M.S.**; Meireles, M.A.A. On-line coupling of extraction and encapsulation of bioactive compounds from Brazilian sources using pressurized fluids. In: South-American Symposium on Microencapsulation, Limeira-SP, 2012.

Gomes, M.T.M.S.; Santos, D.T.; Meireles, M.A.A. Encapsulation of bixin from annatto seeds using a supercritical anti-solvent process. In: 16th World Congress of Food Science and Technology: Addressing Global Food Security and Wellness through Food Science and Technology, Paraná-Brazil, 2012.

Gomes, M.T.M.S.; Santos, D.T.; Meireles, M.A.A. Extração de bixina com líquido pressurizado: Estudo do efeito da polaridade do solvente. In: 9 SLACA - Simpósio Latino Americano de Ciências de Alimentos: Ciência de Alimentos e Qualidade de Vida: Saúde, Meio Ambiente e Sustentabilidade, Campinas-SP, 2011.

Assessoria e Consultoria

Gomes, M.T.M.S.; Santos, D.T.; Meireles, M.A.A. Recent developments in particle formation with supercritical fluids in pharmaceutics. Instituto Vita Nova, 2013.

Artigos completos em processo de submissão

Gomes, M.T.M.S.; Santos, D.T.; Petenate; A.J., Meireles, M.A.A. Experimental design for the micronization of ibuprofen sodium salt by supercritical carbon dioxide antisolvent process.

Gomes, M.T.M.S.; Silva, E.K.; Santos, D.T.; Petenate, A.J., Meireles, M.A.A. Formulating tocotrienol-rich oil as an O/W mini-emulsion by using nonpurified aqueous extract from Brazilian ginseng roots as a biosurfactant.

Silva, E.K.; **Gomes, M.T.M.S.**; Meireles, M.A.A. Ultrasound-assisted formation of emulsions stabilized by biopolymers.

Gomes, M.T.M.S.; Alvarez, V.H.; Meireles, M.A.A.; Saldaña, M.D.A. Encapsulation of vitamin complex with δ-tocopherol, riboflavin and β-carotene in zein microcapsules produced by a supercritical anti-solvent process.

APÊNDICE

Unidade de formação de partículas e encapsulação via SAS/SFEE

Os processos de formação de micropartículas via SAS e SFEE foram desenvolvidas na unidade ARADIME® (Figura A1). Essa unidade foi utilizada no estudo de precipitação do sal de ibuprofeno sódico apresentado no Capítulo 4. A unidade ARADIME® é equipada com: vaso de precipitação de volume interno de 500 mL e diâmetro interno de 6,8 cm, bomba de HPLC que foi usada para a injeção da solução etanólica de ibuprofeno, bomba pneumática para a injeção de CO_2, banho de resfriamento e jaqueta elétrica para o aquecimento do vaso de precipitação. Na sequência, estão apresentados o ibuprofeno sódico após o processamento via SAS (Figura A2) e a curva de calibração utilizada para a determinação do teor de etanol residual presentes nas partículas (Figura A3). As micrografias obtidas via MEV de todos os experimentos realizados estão apresentados na Figura A4.

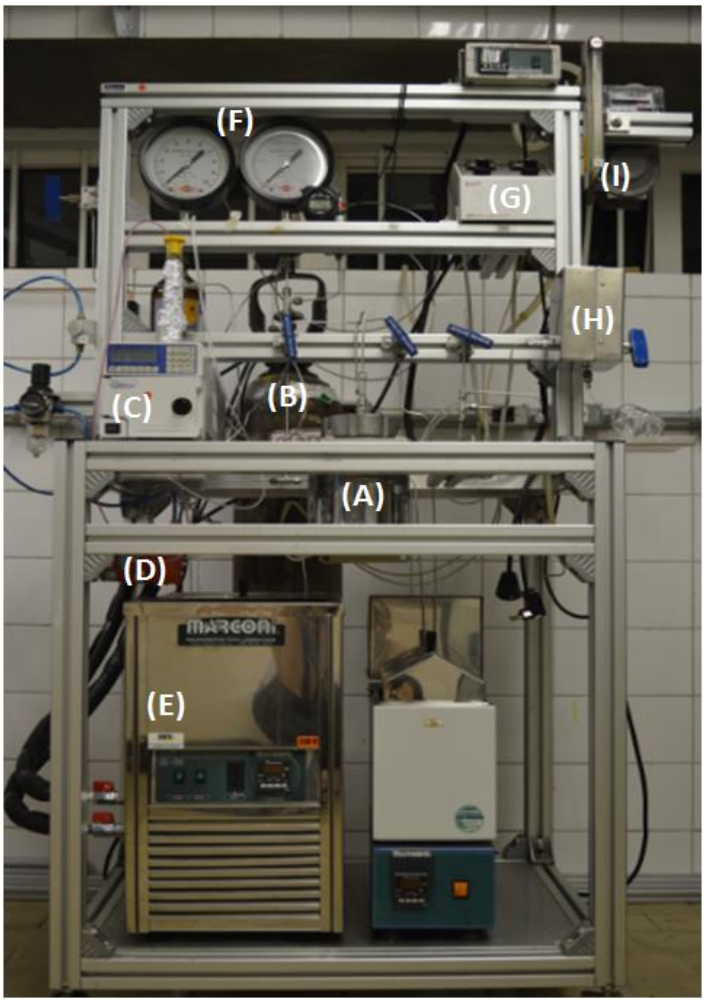

Figura A1: Visão geral da unidade ARADIME®. (A) vaso de precipitação, (B) cilindro de CO_2, (C) bomba de HPLC, (D) bomba pneumática, (E) banho de resfriamento, (F) manômetros, (G) controlador de temperatura, (H) válvula micrométrica, (I) rotâmetro e totalímetro.

Figura A2: Sal de ibuprofeno sódico micronizado via SAS.

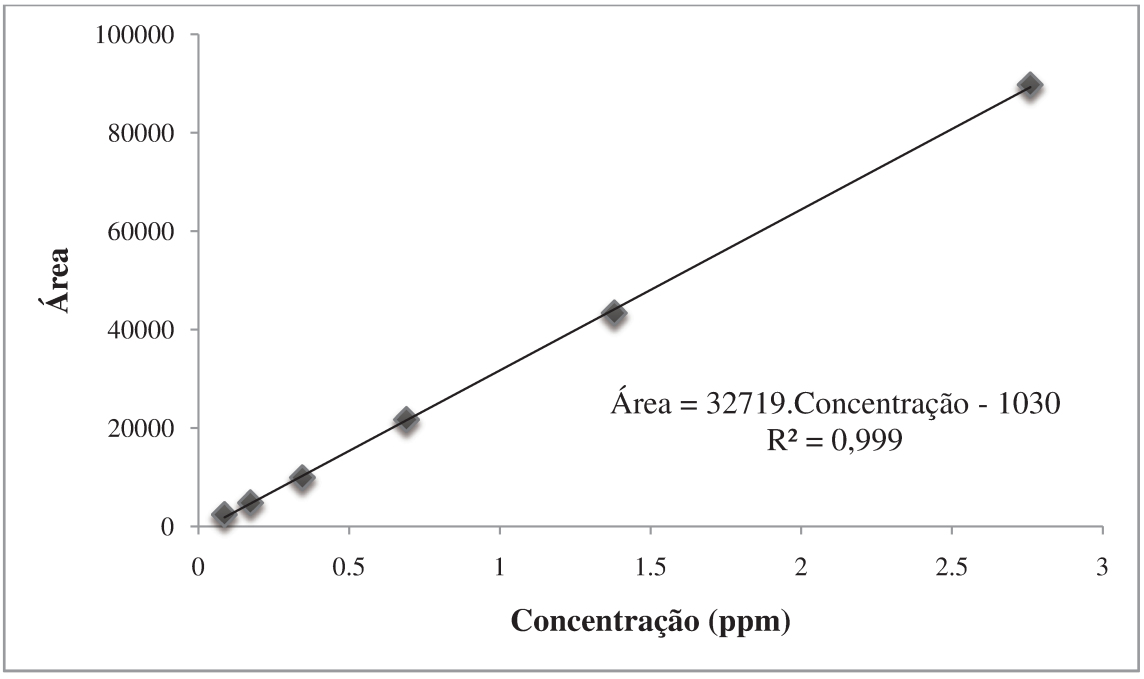

Figura A3: Curva de calibração construída com soluções padrão tolueno/etanol, contendo quantidades conhecidas de etanol.

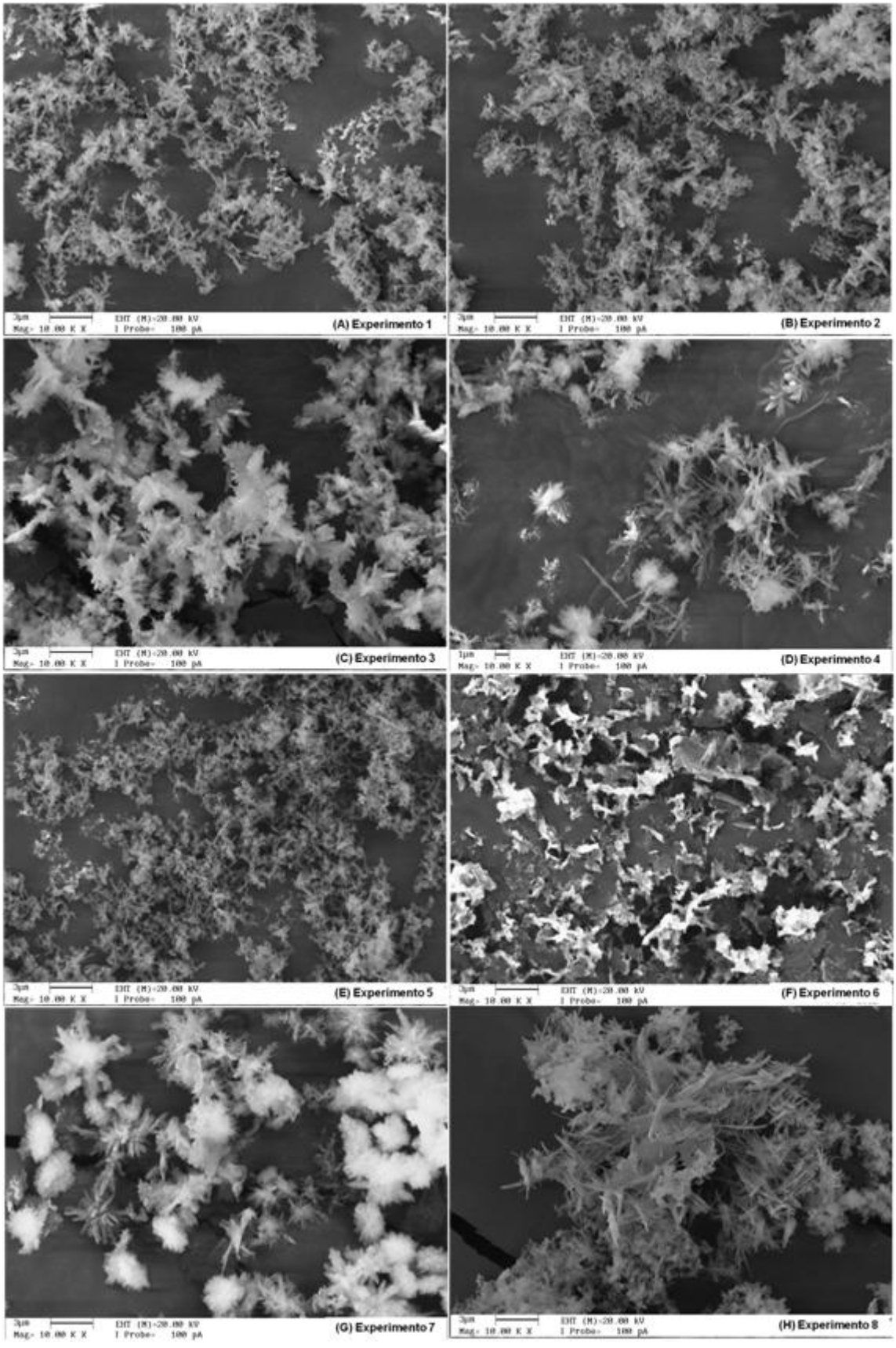
(A) Experimento 1
(B) Experimento 2
(C) Experimento 3
(D) Experimento 4
(E) Experimento 5
(F) Experimento 6
(G) Experimento 7
(H) Experimento 8

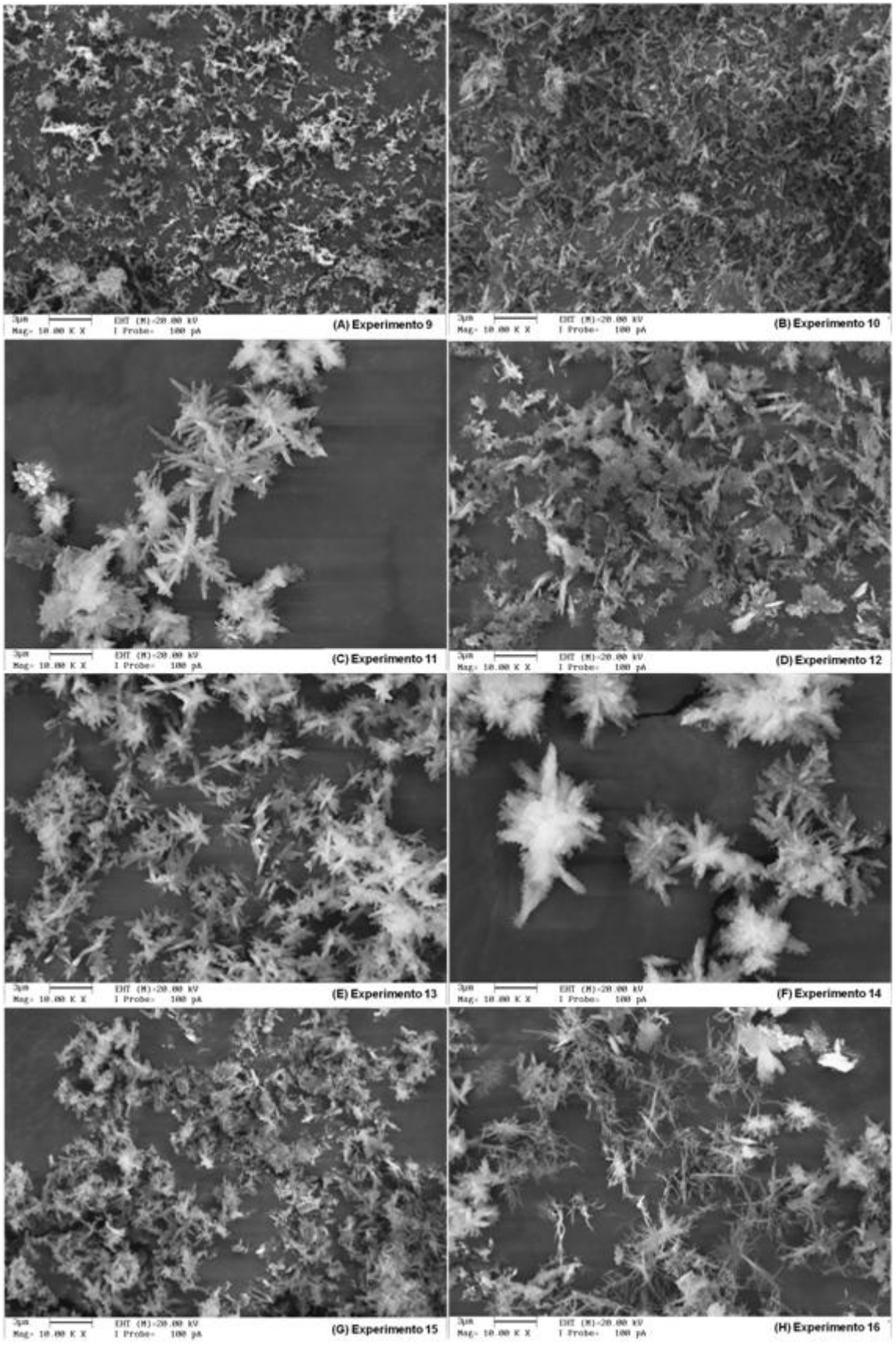
(A) Experimento 9
(B) Experimento 10
(C) Experimento 11
(D) Experimento 12
(E) Experimento 13
(F) Experimento 14
(G) Experimento 15
(H) Experimento 16

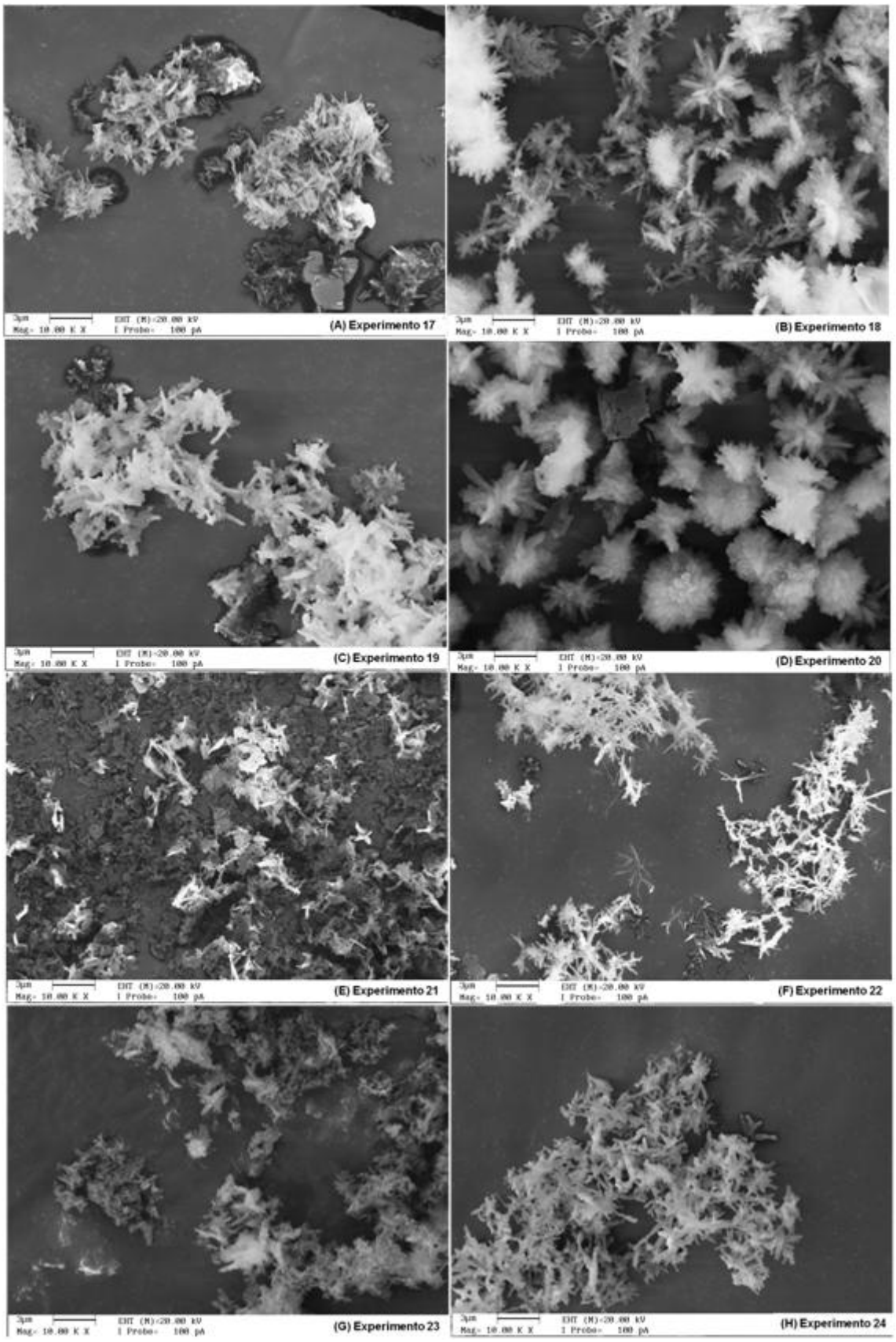
(A) Experimento 17
(B) Experimento 18
(C) Experimento 19
(D) Experimento 20
(E) Experimento 21
(F) Experimento 22
(G) Experimento 23
(H) Experimento 24

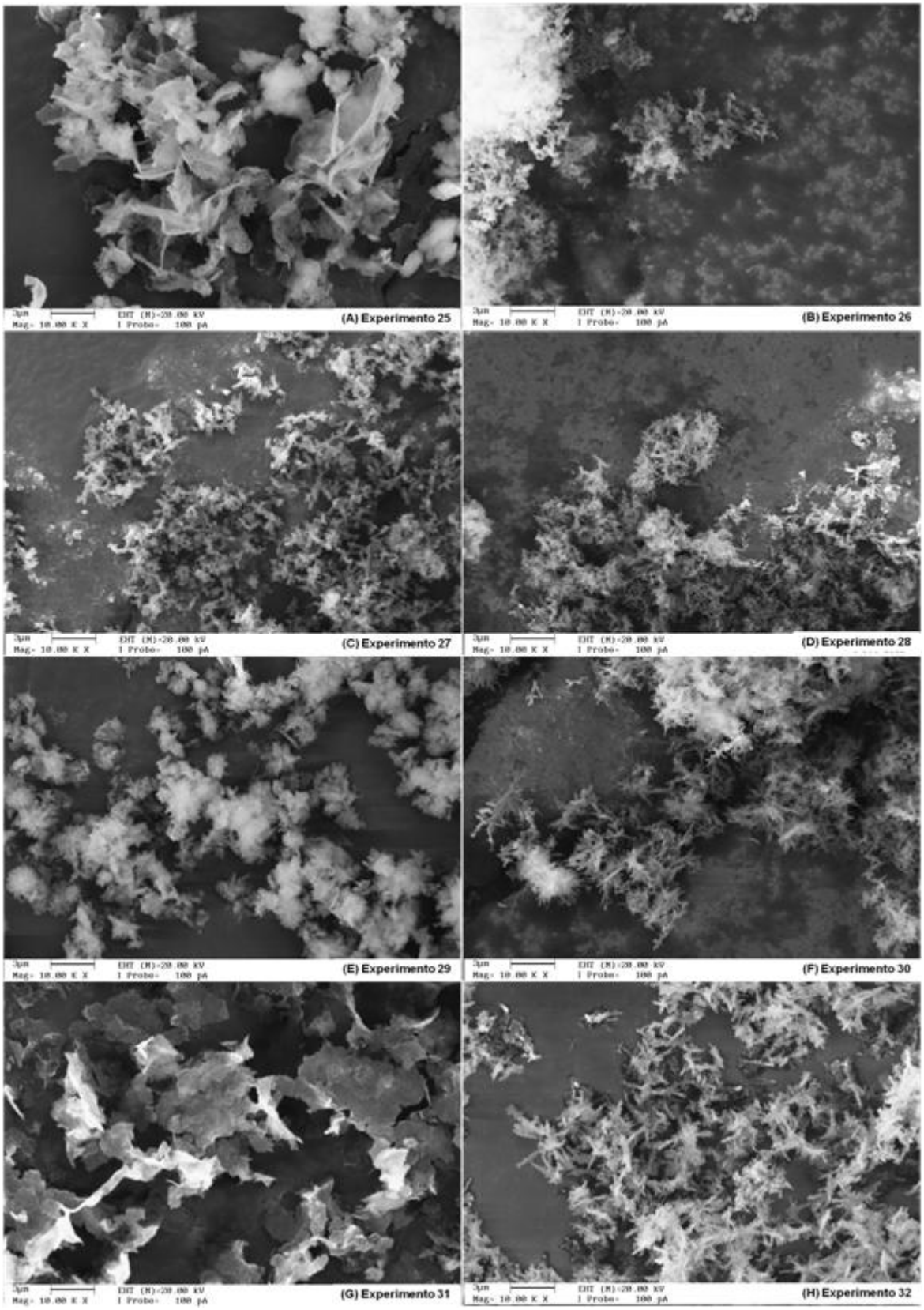

Figura A4: Micrografias MEV de todos os experimentos realizados na precipitação do sal de ibuprofeno sódico.

Unidades para a formulação das emulsões de óleo de urucum

Para o estudo e o preparo das miniemulsões contendo extrato de sementes de urucum rico em δ-tocotrienol e o biossurfactante de extrato de raiz de ginseng brasileiro rico em saponinas, que foi apresentado no Capítulo 5, dois homogeneizadores foram utilizados: o dispersor de fase múltipla e o ultrassom. A imagem destes equipamentos está apresentada nas Figuras A5 e A6. O esquema apresentado na Figura A7 esquematiza de forma simplificada o que foi realizado neste estudo. As emulsões obtidas após um dia de preparo estão mostradas na Figura A8.

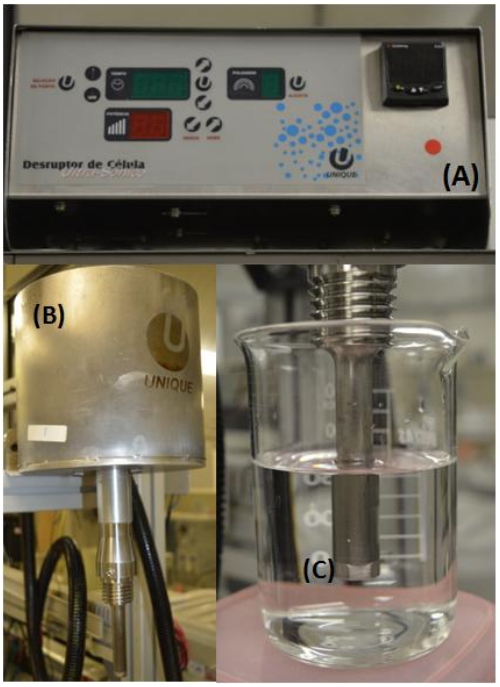

Figura A5: Equipamento de ultrassom usado para o preparo das emulsões. (A) gerador de energia, (B) transdutor e (C) sonotrodo ou probe.

O dispersor de fase múltipla usado neste trabalho é um homogeneizador do tipo rotor-estator, que permite a produção das miniemulsões forçando a pré-emulsão a passar por aberturas muito pequenas, existentes no estator, a velocidades muito elevadas. Esse sistema é composto por 3 estágios, no qual cada estágio é formado por pás (rotor) que giram dentro de um cilindro perfurado (estator). A emulsão permanece sob refluxo durante todo o processo de emulsificação.

Figura A6: Equipamento Dispersor de fase múltipla usado para o preparo das emulsões.

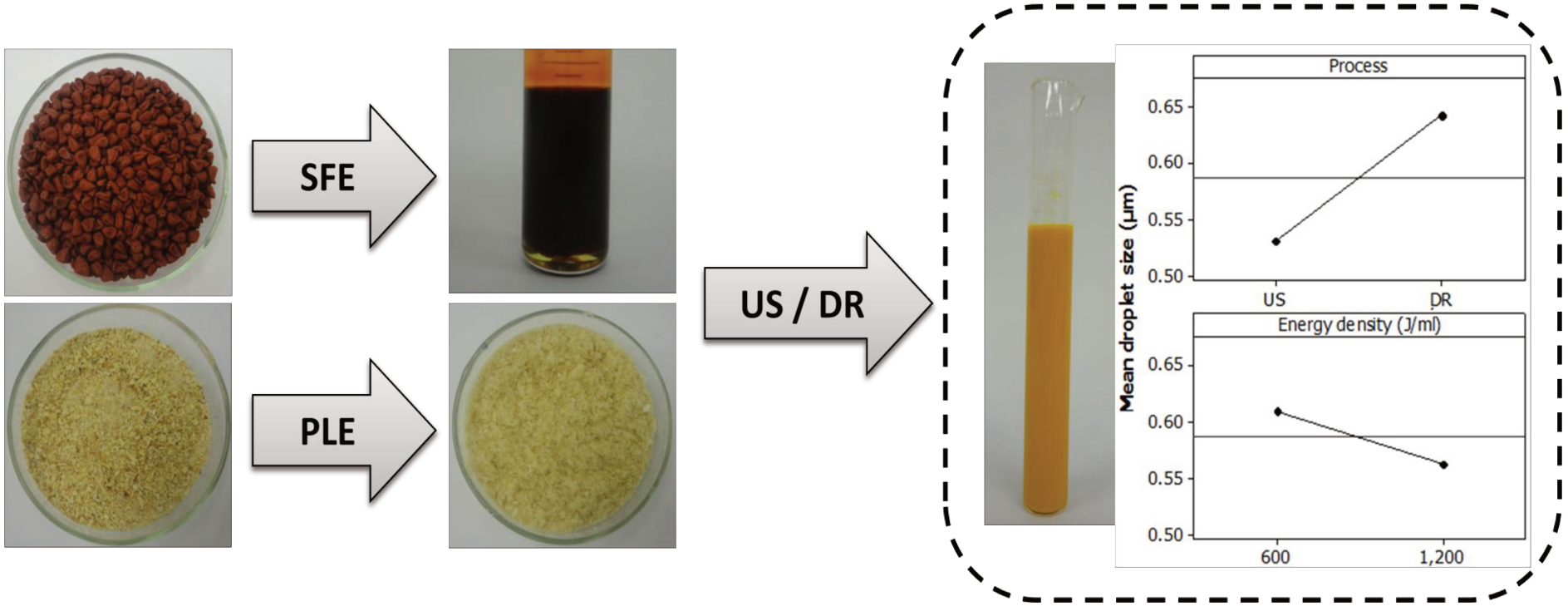

Figura A7: Esquema simplificado do processo de formulação das emulsões contendo extrato de óleo de urucum.

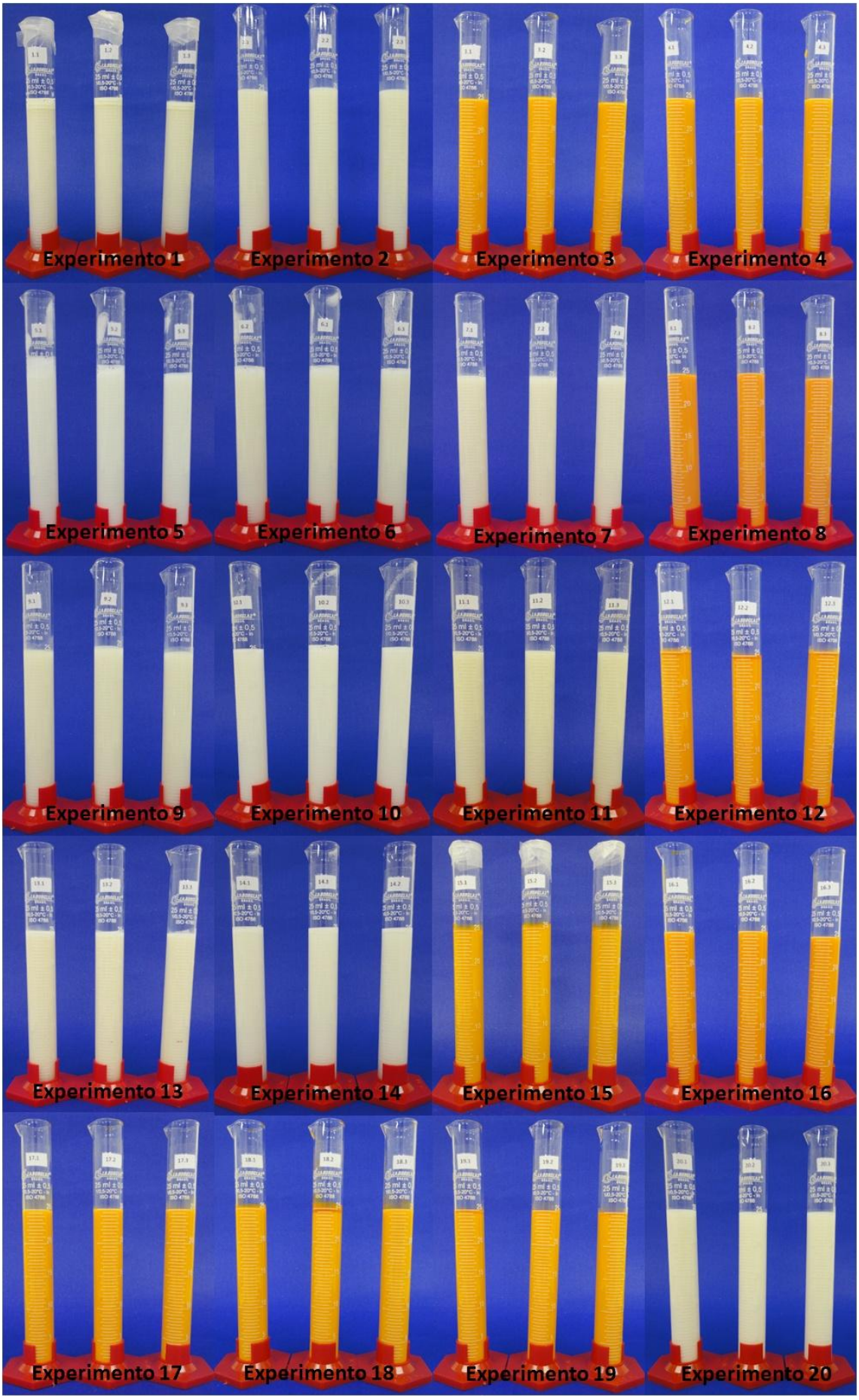
Experimento 1
Experimento 2
Experimento 3
Experimento 4
Experimento 5
Experimento 6
Experimento 7
Experimento 8
Experimento 9
Experimento 10
Experimento 11
Experimento 12
Experimento 13
Experimento 14
Experimento 15
Experimento 16
Experimento 17
Experimento 18
Experimento 19
Experimento 20

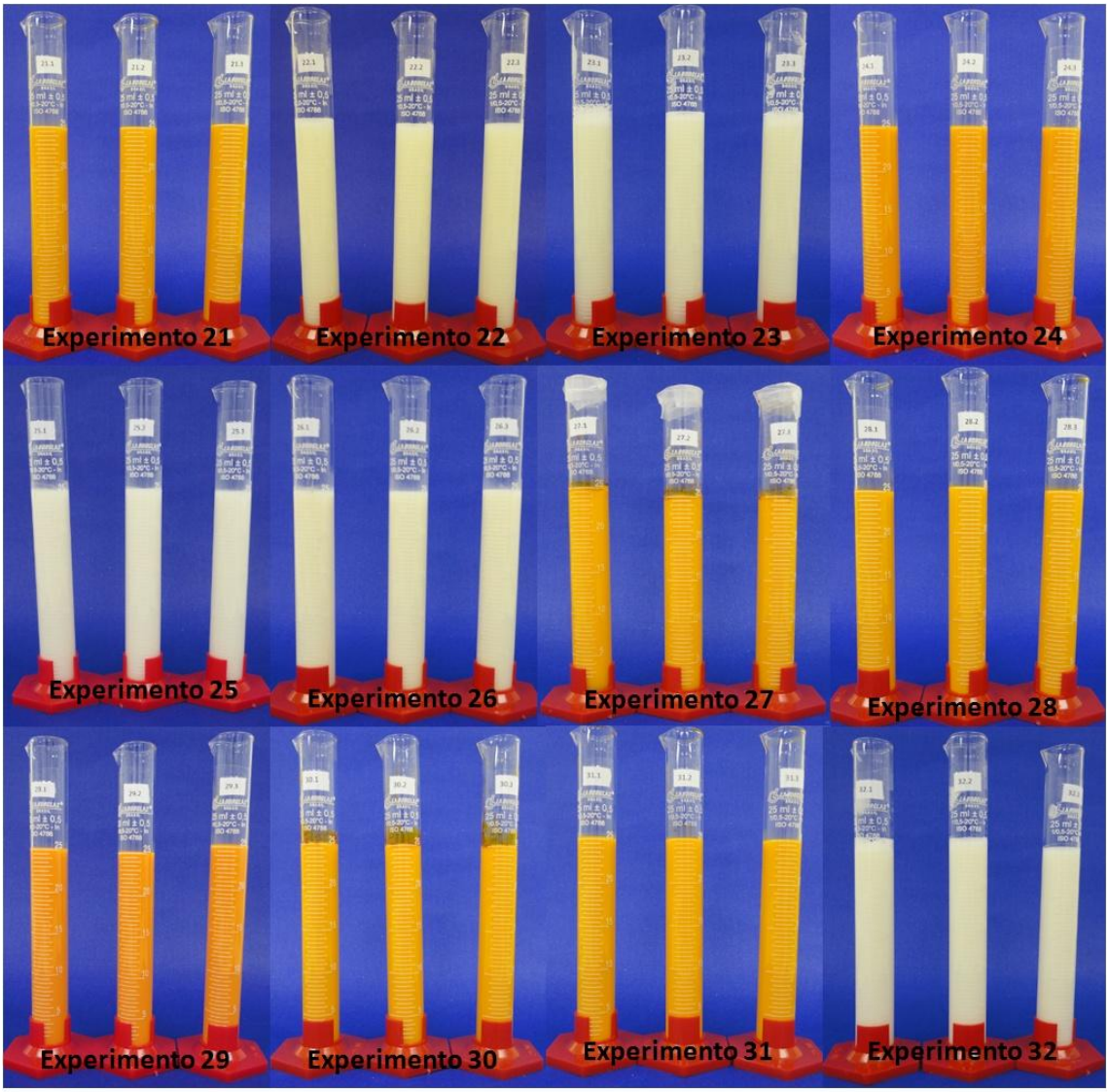

Figura A8: Emulsões obtidas nos 32 experimentos realizados.